

UNIVERSIDADE ESTADUAL DO NORTE FLUMINENSE DARCY RIBEIRO - UENF
PROGRAMA DE PÓS-GRADUAÇÃO EM BIOCÊNCIAS E BIOTECNOLOGIA

LEIDE LAURA FIGUEIREDO MACIEL

**AVALIAÇÃO DA ATIVIDADE ANTINEOPLÁSICA DE COMPOSTOS DE
COORDENAÇÃO DE PLATINA (II) E DE COBRE (II)**

CAMPOS DOS GOYTACAZES/RJ

JULHO/2019

**AVALIAÇÃO DA ATIVIDADE ANTINEOPLÁSICA DE COMPOSTOS DE
COORDENAÇÃO DE PLATINA (II) E DE COBRE (II)**

“Tese de doutorado apresentada ao Programa de Pós-Graduação em Biociências e Biotecnologia da Universidade Estadual do Norte Fluminense Darcy Ribeiro, como parte das exigências para obtenção do título de Doutor em Biociências e Biotecnologia.”

Orientador: Prof. Dr. João Carlos de Aquino Almeida

CAMPOS DOS GOYTACAZES/RJ

JULHO/2019

FICHA CATALOGRÁFICA

UENF - Bibliotecas

Elaborada com os dados fornecidos pela autora.

M152 Maciel, Leide Laura Figueiredo.

Avaliação da Atividade Antineoplásica de Compostos de Coordenação de Platina (II) e de Cobre (II) / Leide Laura Figueiredo Maciel. - Campos dos Goytacazes, RJ, 2019.

115 f. : il.

Bibliografia: 105 - 115.

Tese (Doutorado em Biociências e Biotecnologia) - Universidade Estadual do Norte Fluminense Darcy Ribeiro, Centro de Biociências e Biotecnologia, 2019.

Orientador: Joao Carlos de Aquino Almeida.

1. Compostos de platina (II). 2. Compostos de cobre (II). 3. Câncer. 4. Apoptose.
I. Universidade Estadual do Norte Fluminense Darcy Ribeiro. II. Título.

CDD - 570

**AVALIAÇÃO DA ATIVIDADE ANTINEOPLÁSICA DE COMPOSTOS DE
COORDENAÇÃO DE PLATINA (II) E DE COBRE (II)**

LEIDE LAURA FIGUEIREDO MACIEL

“Tese de doutorado apresentada ao Programa de Pós-Graduação em Biociências e Biotecnologia da Universidade Estadual do Norte Fluminense Darcy Ribeiro, como parte das exigências para obtenção do título de Doutor em Biociências e Biotecnologia.”

Aprovada em 26 de abril de 2019.

Comissão examinadora:

Prof^a. Dra. Anna Lvovna Okorokova Façanha - UENF

Prof^a. Dra. Thaís Rigueti Brasil Borges - UENF

Prof^a. Dra. Samila Ribeiro Morcelli – SEDU-ES

Prof. Dr. João Carlos de Aquino Almeida – UENF (Orientador)

AGRADECIMENTOS

- A Deus, por todo cuidado e por me dar forças e sabedoria para vencer mais uma etapa da minha vida;
- Aos meus familiares, pela torcida de sempre e incentivo diante às dificuldades;
- Ao Rangel, que esteve ao meu lado em todo o percurso desta caminhada, pelo amor, paciência e compreensão;
- Ao Professor João Carlos de Aquino Almeida pela orientação, e auxílio relevante na minha formação, mas principalmente pela amizade e por acreditar em mim. Muito obrigada;
- Ao professor Milton Masahiko Kanashiro, por todo seu apoio, disponibilidade, confiança e imensa colaboração na realização deste trabalho, bem como no tempo dispendido que teve na revisão desta tese;
- À Professora Christiane Fernandes Horn, pelo auxílio e proveitosas discussões, desde os tempos de minha graduação;
- À D. Marina, Elaine e Paula, minhas companheiras de testes biológicos, pelo auxílio, amizade e momentos de boas risadas;
- Aos colegas do laboratório de química, Érika e Rafaela pela ajuda indispensável e pela síntese dos compostos de coordenação de platina e de cobre para o desenvolvimento deste trabalho;
- Aos demais colegas de Laboratório, pela fundamental ajuda nestes anos;
- Às técnicas do LBCT, Beatriz Ribeiro e Giovana Alves, pela disponibilidade e suporte na preparação das amostras para Microscopia Eletrônica de Transmissão e Varredura;
- Às técnicas do LBR, Núbia Alencar, Rita Escocard e Juliana Azevedo, pela disponibilidade em contribuir neste trabalho;
- Às amigas Luana, Kíssila, Grazielle, Núbia e Marina pela amizade e apoio nesta caminhada;
- À comissão examinadora, que gentilmente aceitou o convite para fazer parte da banca;
- A UENF e CAPES pela estrutura e concessão de bolsa;
- Agradeço a todos aqueles que, direta e indiretamente, contribuíram para a conclusão deste trabalho.

Muito obrigada!

SUMÁRIO

LISTA DE FIGURAS E ESQUEMAS	vi
LISTA DE TABELAS	xi
LISTA DE ABREVIATURAS	xii
RESUMO	xiv
ABSTRACT	xv
1. INTRODUÇÃO	16
1.1. Epidemiologia do Câncer.....	16
1.2. Aspectos biológicos do câncer.....	18
1.3. Mecanismos de Morte celular.....	21
1.4. Tratamentos antineoplásicos.....	29
1.5. Metalofármacos.....	32
1.5.1. Compostos de coordenação de platina.....	33
1.5.2. Compostos de coordenação de cobre.....	38
2. JUSTIFICATIVA	42
3. OBJETIVO	43
3.1. Objetivos gerais.....	43
3.2. Objetivos específicos.....	43
4. PRODUÇÃO CIENTÍFICA	44
Capítulo I. Modulating the antitumoral activity by the design of new platinum(II) compounds: synthesis, characterization, DFT, ultrastructure and mechanistic studies	45
Abstract.....	45
1. Introduction.....	45
2. Experimental.....	45
2.1. Materials and methods.....	47
2.2. Synthesis.....	47
2.2.1. Synthesis of the ligands.....	47
2.2.2. Synthesis of [PtII(HL1)Cl] (1), [PtII(HL2)Cl] (2) and [PtII(HL4)Cl] (4).....	47
2.2.3. Synthesis of [PtII(HL3)Cl] (3).....	47
2.3. X-ray crystallography.....	48
2.4. DFT calculations.....	48

2.5. Antitumor activity.....	48
2.5.1. Culture of cells	48
2.5.2. Cell viability studies using the colorimetric MTT assay.....	48
2.5.3. Measurement of Annexin V and propidium iodide staining.....	48
2.5.4. Study of cell cycle arrest by flow cytometric analysis.....	48
2.5.5. Analysis of mitochondrial membrane potential ($\Delta\Psi_m$) by flow cytometry using JC-1 stain.....	49
2.5.6. Transmission electron microscopy (TEM) and scanning electron microscopy (SEM).....	49
2.5.7. Determination of caspase activities.....	49
3. Results and discussion.....	49
3.1. Syntheses and structure of platinum(II) coordination compounds.....	49
3.2. Description of crystal structure of complex (3).....	49
3.3. DFT study.....	49
3.4. Infrared.....	50
3.5. ESI(+)-MS and ESI(+)-MS/MS.....	52
3.6. Assessment of cell viability by MTT assay.....	52
3.7. Mechanistic studies of cell death.....	52
3.7.1. Measurement of apoptosis by Annexin V-FITC/PI analysis.....	53
3.7.2. Analysis of mitochondrial membrane potential ($\Delta\Psi_m$)	54
3.7.3. Cell cycle analysis by flow cytometry.....	54
3.7.4. Analysis of cell morphology by TEM and SEM.....	54
3.7.5. Determination of caspase activities.....	56
4. Conclusions.....	57
Acknowledgements.....	57
References.....	57
Capítulo II. <i>In vitro</i> and <i>in vivo</i> anti-proliferative activity and ultrastructure investigations of a copper(II) complex toward human lung cancer cell NCI- H460.....	59
Summary.....	60
Introduction.....	61

Materials and methods.....	62
Synthesis of copper(II) complex – complex (2).....	62
Cell culture.....	63
Analysis of cell viability by MTT assay.....	63
Measurement of annexin V and propidium iodide staining.....	64
Cell cycle analysis by flow cytometer.....	64
Analysis of mitochondrial membrane potential ($\Delta\Psi_m$) using JC-1 stain.....	64
Determination of caspase-12 activity.....	65
Fluorescence assay.....	65
Electron microscopy analysis.....	65
<i>In vivo</i> assessment of tumor growth inhibition.....	66
Statistical analysis.....	67
Results.....	67
Complex (2) induces cytotoxicity on neoplastic cells.....	67
Lung carcinoma cells undergo apoptosis cell death when treated with complex (2).....	68
Apoptosis induced by complex (2) on NCI-H460 involves mitochondrial dysfunction.....	71
Complex (2) induces decrease of cell microvilli, mitochondria and endoplasmic reticulum alterations on lung carcinoma cell line.....	71
NCI-H460 cell line treatment with complex (2) results in decrease of mitochondrial membrane potential and endoplasmic reticulum stress with caspase-12 release to cytoplasm.....	76
Complex (2) and cisplatin reduce tumor growth in murine model of lung cancer.....	78
Discussion.....	80
Conclusion.....	84
Ethical approval studies.....	85
References.....	85
5. DISCUSSÃO GERAL	90
6. CONCLUSÃO	103
7. PERSPECTIVAS	104
8. REFERÊNCIAS BIBLIOGRÁFICAS	105

LISTA DE FIGURAS E ESQUEMAS

INTRODUÇÃO

- Figura 1.** Os dez tipos de cânceres mais incidentes estimados para 2018/2019 por sexo, exceto pele não melanoma na população brasileira (INCA, 2018) 17
- Figura 2.** Representação dos carcinomas derivados do tecido epitelial (adaptado de ALBERTS et al., 2010).....18
- Figura 3.** Características morfológicas de apoptose, autofagia e necrose (adaptado de TAN et al., 2014).....22
- Figura 4.** Vias extrínseca e intrínseca do processo apoptótico (adaptado de TAN et al., 2014).....25
- Figura 5.** Via intrínseca de sinalização apoptótica mediada pela ativação de caspase 12 (adaptado de KAO et al., 2011).....28
- Figura 6.** Mecanismos de contribuem para a evasão da apoptose e carcinogênese (adaptado de WONG et al., 2011).....29
- Figura 7.** As três principais modalidades de tratamentos antineoplásicos (adaptado de KAJIYAMA et al., 2017).....31
- Figura 8.** Metalofármacos antineoplásicos de platina aprovados pela FDA e investigado em ensaios clínicos (ELLAHIOUI et al. 2017).....35
- Figura 9.** Principais adutos formados através da interação da cisplatina com o DNA: (a) interação entre duas fitas (1,2-interfitas); (b) interação 1,2- intrafita; (C) ligação cruzada 1,3- intrafita e (d) interação com DNA e proteína (adaptado de GONZALEZ et al., 2001).....36
- Figura 10.** Compostos metálicos submetidos à ensaios clínicos em humanos (adaptado de TAN et al., 2014; NDAGI et al., 2017).....38
- Figura 11.** Estrutura química da Casiopeína (III) Nitrato de (4,4'-dimetil-2,2'-bipiridina)(acetilacetato) cobre (II) (MARÍN-MEDINA et al., 2016).....40

CAPÍTULO I

Scheme 1. Scheme illustrating the syntheses of the platinum(II) complexes (1)–(4).....46

Figure 1. View of the ORTEP-3 projections for complex (3) and the corresponding atom labeling scheme. Ellipsoids are shown at the 40% probability level.....50

Figure 2. Comparison of the proposed structures of (a) (1), (b) (2) and (d) (4) and (c) ORTEP picture of (3) with the calculated structures for (a') (1), (b') (2) and (d') (4). For complex (3), an overlay of the calculated structure (black) with the X-ray (red) is presented in (c').....51

Figure 3. Annexin V-FITC/PI staining detected apoptosis induced by complexes (3) and (4) in U937 cells, after treatment for 24 h. A) Control. B) U937 cells after treatment at the concentration of 22 μM of complex (3). C) U937 cells after treatment at the concentration of 30 μM complex (4). The data are presented in dot blots depicting Annexin V/FITC *versus* PI staining. The percentage of cells in each quadrant is presented.....53

Figure 4. Mitochondrial transmembrane potential ($\Delta\Psi\text{m}$) assay. U937 cell line was incubated with 22 μM of complex (3) for 24 h. After being stained with JC-1, cells were analyzed by flow cytometry. Upper right quadrant - normal cells and lower right quadrant- loss of mitochondrial $\Delta\Psi\text{m}$. A) Control cells. B) Cells after treatment with complex (3).....53

Figure 5. Cell Cycle Analysis by Flow Cytometry. Leukemic cell line (U937) was stained with propidium iodide (PI) after 24 h of incubation without (control) and with complex (3). Cells with hypodiploid DNA content were measured by quantifying the sub-G1 peak in the cell cycle pattern. Each experiment per sample was determined recording 10.000 events. A) Control cells; B) cells after treatment with 22 μM of complex (3).....54

Figure 6. Transmission Electron Microscopy of human leukemia cells. (A) Control cells, (B) U937 cell strain incubated with 11 μM of complex (3) for 4 h. Altered mitochondria [M] can be seen. (C) U937 cell line incubated for 8 h. Release of

apoptotic bodies [A] can be seen at the cell periphery. Elongated endoplasmic reticulum [ER] and altered mitochondria [M] are also visible (D) U937 cell line incubated for 12 h, showing a great number of mitochondria [M] and cytoplasmic vacuoles [V].....55

Figure 7. Scanning Electron Microscopy of human leukemia cells (U937). (A) Control cells, showing microvilli [arrow] on the cell surface. (B) and (C) U937 cell line incubated with 11 μ M of complex (3) for 8 h. The release of apoptotic bodies can be seen [star]. (D) U937 cell line incubated with 11 μ M of the complex (3) for 12 h.....56

Figure 8. Caspases 3, 6, 8 and 9 activation in U937 cells after treatment with complex (3). Cells were incubated with 22 μ M of complex (3) for 3 h. Values are means \pm S. D. from two separate measurements. *P < 0.05, **P < 0.01 and ***P < 0.001 *versus* control.....56

CAPÍTULO II

Figure 1. Chemical complex (2) in solution [19].....63

Figure 2. Viability of NCI-H460 cells after treatment with complex (2) and cisplatin. The cells were treated with increasing concentrations of the complexes up to 400 μ M for 36 h of exposure. Dose-response curves were obtained by MTT assay. Each data point represents means \pm S.D. (n = 3). *P < 0.05, **P < 0.01 and ***P < 0.001 in relation to control.....68

Figure 3. Cell cycle analysis by flow cytometry of NCI-H460 cells after 24 h of incubation. Cells with hypodiploid DNA content were measured by the sub-G1 fraction in the cell cycle pattern. Each experiment per sample was determined by recording 10,000 events. (A) Control cells. (B, C) Cells treated with 1X and 2X IC₅₀ of complex (2). (D, E) Cells treated with 1X and 2X IC₅₀ of cisplatin.....69

Figure 4. The Annexin V/PI assay by flow cytometry of NCI-H460 cells after 24 h of incubation. (A) Control cells. (B, C) Cells treated with 1X and 2X IC₅₀ of complex (2). (D, E) Cells treated with 1X and 2X IC₅₀ of cisplatin. The data are presented in the

diagrams depicting annexin V/FITC vs PI staining. The percentage of cells in each quadrant is presented: necrotic cells (Q1), late apoptotic cells (Q2), living cells (Q3) and early apoptotic cells (Q4).....70

Figure 5. Morphological analysis of NCI-H460 cells double stained with Hoechst/MitoTracker examined under a fluorescence microscope after 12 h of incubation. (A) Control cells. (B) Cells treated with 2X IC₅₀ of complex (2). (C) Cells treated with 2X IC₅₀ of cisplatin. Chromatin condensation and nuclear fragmentation are indicated by the white arrow. Magnification 400x.....72

Figure 6. Morphological analysis of NCI-H460 cells treated with 2X IC₅₀ of complex (2) and cisplatin after 4, 8 and 12 h of incubation by SEM. (A, B) Control cells. (C, E, G) Cells treated with complex (2) after 4, 8 and 12 h of incubation. (D, F, H) Cells treated with cisplatin after 4, 8 and 12 h of incubation. Cells with intense membrane *blebbing* [white arrow]. The release of apoptotic bodies can be seen [star]. Numerous microvilli are shown [arrowhead] on the cell surface.....73

Figure 7. Ultrastructural analysis of NCI-H460 cells treated with 2X IC₅₀ of complex (2) and cisplatin after 4, 8 and 12 h of incubation by TEM. (A, B) Control cells. (C, E, G) Cells treated with complex (2) after 4, 8 and 12 h of incubation. (D, F, H) Cells treated with cisplatin after 4, 8 and 12 h of incubation. Microvilli [arrow] on the cell surface; [M] Mitochondria; [ER] Endoplasmic Reticulum; [V] Vacuoles and [N] Nucleus. Chromatin condensation is indicated by the star.....75

Figure 8. Mitochondrial membrane potential assay probed by JC-1 staining and flow cytometry analysis. NCI-H460 cells were incubated with complex (2) for 24 h, stained by JC-1 and analyzed by flow cytometry. (A) Control cells. (B, C) Cells treated with 1X and 2X IC₅₀ of complex (2). (D, E) Cells treated with 1X and 2X IC₅₀ of cisplatin.....77

Figure 9. The activation of caspases-12 by flow cytometry analysis in NCI-H460 cells after 18 h of incubation. (A) Control cells. (B, C) Cells treated with 1X and 2X IC₅₀ of complex (2). (D, E) Cells treated with 1X and 2X IC₅₀ of cisplatin. Results are expressed as relative fluorescent intensities (from left to right).....78

Figure 10. Evaluation of tumor growth inhibition by complex (2) in a BALB/c *nude* murine model. A) Lethal dose determination. LD₅₀ was calculated using Probit analysis. B) and C) Evaluation of tumor growth inhibition. Balb/c nude mice bearing NCI-H460 tumor nodules were treated ip with 50% of DL₅₀ of cisplatin or complex (2) in three dose with one week of intervals. D) Images of excised tumors of euthanized mice. Statistical analyses: One-way ANOVA with Tukey multiple comparison test. Significant difference was taken as *p < 0.05, **p <0.01 and ***p <0.001 comparing the treated and control groups.....79

LISTA DE TABELAS

CAPÍTULO I

Table 1. Yield, elemental analysis (C, H, N), conductivity data (in DMF) and melting point (M.P.) for compounds (1)–(4).....	47
Table 2. Crystal data and structure refinement for (3).....	48
Table 3. Selected bond and lengths (Å) and angles (°) for complex (3).....	50
Table 4. Characteristic IR bands (cm ⁻¹) of the ligands HL1-H2L4 and their respective platinum(II) complexes.....	52
Table 5. The 50% inhibitory concentration (IC ₅₀) for the platinum complexes and their respective ligands, as well as K ₂ [PtCl ₄] and cisplatin, for leukemia (THP-1 U937 and Molt-4), colon (Colo-205), lung (H460) cancer cell lines and PBMC.....	52

CAPÍTULO II

Table 1. Determination of IC ₅₀ values of copper(II) complex toward neoplastic cell lines.....	68
--	----

LISTA DE ABREVIATURAS

- APAF-1** - Apoptotic protease activating factor 1
- ATCC** - American Type Culture Collection
- Bax** - BCL2 associated X protein
- Bcl-2** - B cell lymphoma 2
- Bid** - Interacting domain death agonist
- B16-F10** - Linhagem celular murina estabelecida de melanoma metastático
- COLO 205** - Linhagem celular humana de adenocarcinoma colorretal
- DL₅₀** - Dose Letal para 50% de um grupo de animais
- DMEM/F-12** - Dulbecco's Modified Eagle's Medium: Nutrient Mixture F-12
- DMSO** - Dimetilsulfóxido
- DNA** - Ácido desoxirribonucleico
- EROs** - Espécies Reativas de Oxigênio
- FADD** - Fas-Associated Death Domain
- FDA** - Food and Drug administration
- IAP** - Inhibitor of Apoptosis Protein
- IC₅₀** - Concentração inibitória necessária para matar 50% da população celular
- INCA** - Instituto Nacional do Câncer José Alencar Gomes da Silva
- IsopOH** - Isopropanol
- JC-1** - Iodeto de 5,5',6,6'-tetracloro-1,1,3,3' tetraetilbenzimidazolil carbocianina
- MET** - Microscopia eletrônica de transmissão
- MEV** - Microscopia eletrônica de varredura
- MOLT-4** - Linhagem celular humana de leucemia linfóide aguda
- MTT** - 3-(4,5-dimetiltiazol-2-il)-2,5-difenil brometo de tretazólio
- NCI-H460** - Linhagem celular humana de adenocarcinoma de pulmão

Omi/HtrA2 - High temperature requirement protein-2

OMS - Organização Mundial de Saúde

PBMC - Células mononucleares do sangue periférico (do inglês, peripheral blood mononuclear cells)

PBS - Tampão Fosfato Salino (NaCl 0,137M; Na₂HPO₄.2H₂O, 0,008M; KCl 0,0026M; KH₂PO₄ 0,0014M, pH 7,2)

PI - Iodeto de propídio

PMM - Potencial de membrana mitocondrial

SMAC/DIABLO - Second mitochondria-derived activator of caspases/direct IAP binding protein with low pI

SKMEL - Linhagem de Melanoma Metastático Humano

THP-1 - Linhagem celular humana de leucemia monocítica aguda

TNF - Tumor necrosis fator

TRAIL - TNF-related apoptosis-inducing ligand

U937 - Linhagem celular humana de linfoma histiocítico

XIAP - X-linked Inhibitor of Apoptosis Protein

WHO - World Health Organization

$\Delta\Psi_m$ - Variação do potencial de membrana mitocondrial

RESUMO

Este trabalho teve por objetivo avaliar *in vitro* o potencial citotóxico dos novos compostos de coordenação de platina (II) (1, 2, 3 e 4), e, *in vitro* e *in vivo* investigar a eficácia inibitória do composto de cobre (II) no tratamento de lesões cancerígenas em modelos murinos. A avaliação da citotoxicidade dos compostos determinada por meio do ensaio de metabolização do MTT (brometo de 3-(4,5-17 dimetiliazol-2-il)-2,5-difeniltretazólio) demonstrou que os compostos de platina (3) e (4) foram os mais ativos contra as linhagens testadas (THP-1, U937, MOLT-4, COLO 205 e NCI-H460), sendo que a menor IC₅₀ de 6±1 µM foi observada com o composto (3) de platina frente a célula THP-1. O composto de cobre (II) diminuiu significativamente a viabilidade da linhagem de câncer de pulmão NCI-H460, com IC₅₀ de 26,5 µM comparado com 203 µM da cisplatina. O tipo de morte celular analisada através de marcação com anexina V e do ciclo celular (Sub-G1) indicou que o composto (3) promove morte por apoptose na linhagem leucêmica U937. Os dados apontaram que o composto de cobre (II) também induziu apoptose na célula NCI-H460. A análise do potencial de membrana mitocondrial (JC-1) por citometria de fluxo e a avaliação da ativação de caspases averiguada através de ensaio colorimétrico demonstrou que ambos os compostos induzem apoptose pela via intrínseca com comprometimento mitocondrial. Foi observado ainda que o composto de cobre (II) induz apoptose em células NCI-H460 com possível envolvimento do retículo endoplasmático. As análises por microscopia eletrônica de transmissão e varredura revelaram que ambos os complexos promoveram alterações ultraestruturais como *blebbing* de membrana, diminuição das microvilosidades na superfície celular, alterações nas mitocôndrias e no retículo endoplasmático. Nos ensaios *in vivo*, a toxicidade do composto de cobre (II) foi avaliada pela determinação da DL₅₀ (dose letal mediana) de 48,98 mg/Kg. No tratamento de camundongos BALB/c nude portando lesões cancerígenas de células NCI-H460, foi observado 48% de inibição tumoral quando comparado com o grupo controle. Em suma, sugere-se que os compostos de platina (3) e o de cobre (II) são promissores na busca por novos metalofármacos com atividade antineoplásica, visando uma futura aplicação clínica.

Palavras-chave: Compostos de platina (II). Compostos de cobre (II). Câncer. Apoptose

ABSTRACT

The aim of the present study was to evaluate *in vitro* cytotoxic potential of the new platinum (II) coordination compounds (1, 2, 3 and 4), and *in vitro* and *in vivo* to investigate the inhibitory efficacy of copper (II) compound in the treatment of cancerous lesions in murine models. The evaluation of the cytotoxicity of the compounds determined by the MTT metabolism test (3- (4,5-17 dimethylthiazol-2-yl) - 2,5-diphenyltetrazolium bromide) showed that the platinum (3) and (4) were the most active against the tested lines (THP-1, U937, MOLT-4, COLO 205 and NCI-H460), with the lowest IC₅₀ of $6 \pm 1 \mu\text{M}$ was observed with the platinum compound (3) the THP-1 cell. The copper (II) compound significantly decreased the viability of the NCI-H460 lung cancer line, with IC₅₀ of 26.5 μM compared to 203 μM of cisplatin. The type of cell death, analyzed by annexin V and cell cycle (Sub-G1) labeling indicated that the compound (3) promotes apoptosis death in the leukemic line U937. The data indicated that the copper (II) compound also induced apoptosis in the NCI-H460 cell. Analysis of mitochondrial membrane potential (JC-1) by flow cytometry and evaluation of caspase activation ascertained by the colorimetric assay demonstrated that both compounds induce apoptosis by the intrinsic pathway with mitochondrial impairment. It was further observed that the copper (II) compound induces apoptosis in NCI-H460 cells with endoplasmic reticulum involvement. In addition, scanning and transmission electron microscopy revealed that both complexes promoted ultrastructural alterations such as membrane *blebbing*, a decrease of microvilli on the cell surface, changes in mitochondria and endoplasmic reticulum. In the *in vivo* assays, the toxicity of the copper (II) compound was evaluated by determination of the LD₅₀ (median lethal dose) of 48.98 mg/Kg. In the treatment of BALB/c mice carrying cancerous lesions of NCI-H460 cells, 48% of tumor inhibition was observed when compared to the control group. In summary, it is suggested that the platinum (3) and copper (II) compounds are promising in the search for new metallodrugs with antineoplastic activity, aiming at a future clinical application.

Keywords: Copper (II) compound. Platinum (II) compound. Cancer. Apoptosis

1. INTRODUÇÃO

1.1. EPIDEMIOLOGIA DO CÂNCER

Em 2011, a Organização Mundial de Saúde (OMS) identificou o câncer como uma das quatro principais ameaças à saúde humana (junto às doenças cardiovasculares, doenças respiratórias crônicas e diabetes), sendo responsável por mais de 12% de todas as causas de óbitos que acometem a população mundial. Os cânceres mais diagnosticados foram de pulmão (1,8 milhão de casos), mama (1,7 milhões) e intestino grosso (1,4 milhões). Os cânceres mais letais foram o de pulmão (1,6 milhões), fígado (0,8 milhão) e estômago (0,7 milhão) (WHO, 2011; SIEGEL et al., 2014).

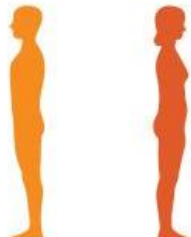
Em 2018 houve 18 milhões de novos casos de câncer e um total de 9,6 milhões de morte de pessoas em todo o mundo. Projeções recentes estimam que até o ano 2030 o câncer ocupará a principal causa de morte, sendo previstos 27 milhões de novos casos de câncer e 17 milhões de mortes ocasionadas pela doença no mundo (WHO, 2019).

O maior efeito desse aumento vai incidir principalmente nas populações de baixas e médias rendas, pois o percentual de óbito relaciona-se diretamente com os aspectos socioeconômicos e políticos, sendo a estruturação do sistema de saúde essencial para medidas preventivas, diagnóstico precoce e o tratamento eficaz da doença (BARBOSA et al., 2015; WHO, 2019).

Segundo a OMS, mais de 30% das mortes por câncer poderiam ser evitadas com medidas preventivas, incluindo a adoção de um modo de vida saudável e evitando a exposição a fatores de risco, como o uso do tabaco, o sobrepeso ou obesidade, dieta pouco saudável, falta de atividade física, o uso de bebidas alcoólicas, infecção por HPV, exposição excessiva ao sol. Dentre estes, o consumo de derivados do tabaco é o fator de risco mais importante para o desenvolvimento do câncer, causando cerca de 22% das mortes por câncer globais e cerca de 80% das mortes por câncer de pulmão (VOLTAGGIO et al., 2016; WHO, 2019).

No Brasil, as estimativas para cada ano do biênio 2018/2019 apontam a ocorrência de aproximadamente 600 mil novos casos da doença. Os tipos mais

incidentes são os cânceres de pele classificado como não melanoma para ambos os sexos, seguidos pelas neoplasias de próstata, pulmão, cólon e reto e estômago para o sexo masculino; e para o sexo feminino destacam-se os cânceres de mama, cólon e reto, colo do útero, pulmão e tireoide (figura 1) (INCA, 2018).

Localização Primária	Casos	%			Localização Primária	Casos	%
Próstata	68.220	31,7%	Homens 	Mulheres	Mama Feminina	59.700	29,5%
Traqueia, Brônquio e Pulmão	18.740	8,7%			Cólon e Reto	18.980	9,4%
Cólon e Reto	17.380	8,1%			Colo do Útero	16.370	8,1%
Estômago	13.540	6,3%			Traqueia, Brônquio e Pulmão	12.530	6,2%
Cavidade Oral	11.200	5,2%			Glândula Tireoide	8.040	4,0%
Esôfago	8.240	3,8%			Estômago	7.750	3,8%
Bexiga	6.690	3,1%			Corpo do Útero	6.600	3,3%
Laringe	6.390	3,0%			Ovário	6.150	3,0%
Leucemias	5.940	2,8%			Sistema Nervoso Central	5.510	2,7%
Sistema Nervoso Central	5.810	2,7%			Leucemias	4.860	2,4%

*Números arredondados para múltiplos de 10.

Figura 1. Os dez tipos de cânceres mais incidentes estimados para 2018/2019 por sexo, exceto pele não melanoma na população brasileira (INCA, 2018).

Os tipos mais comuns de cânceres, como os de mama e de próstata, apresentam uma boa estimativa de cura quando diagnosticados no estágio inicial. Em contrapartida, os de pulmão, estômago, fígado, esôfago, pâncreas, melanoma e leucemia apresentam elevados índices de mortalidade, o que impulsiona a pesquisa sobre esta patologia e a busca por novas estratégias terapêuticas para combatê-la (INCA, 2018).

O cenário epidemiológico atual brevemente retratado, reforça a magnitude do problema do câncer no país e no mundo. Dessa forma, é essencial a implantação de programas eficientes de prevenção e diagnóstico precoce da doença, investimento de recursos para pesquisas de novos fármacos, acesso ao tratamento especializado e de qualidade aos indivíduos acometidos, sendo estas algumas das necessidades mais relevantes para combater o câncer e melhorar os resultados terapêuticos dos pacientes (INCA, 2018).

1.2. ASPECTOS BIOLÓGICOS DO CÂNCER

Câncer, neoplasia ou tumor maligno são designações para um conjunto de mais de 200 doenças que se desenvolvem progressivamente, a partir de qualquer tecido ou órgão, caracterizadas principalmente, por uma proliferação desordenada, constituída por células transformadas, alta taxa metabólica, morfologia heterogênea, com alta capacidade de infiltração e disseminação (KUMAR et al., 2014).

Por outro lado, os tumores benignos são formados por células bem diferenciadas, com crescimento lento e ordenado, não apresentando características invasivas e podem ser removidos eficazmente por excisão cirúrgica. Já os tumores malignos não reconhecem limites anatômicos, possuem elevada capacidade de invasão, cujas células têm a capacidade de infiltrarem-se nos tecidos normais adjacentes ou originam tumores secundários em outros tecidos distantes do foco primário, migrando através dos sistemas circulatório e linfático. Este processo de disseminação sistêmica de células cancerígenas é denominado metástase, tal fato compromete o funcionamento geral do organismo (figura 2) (ALBERTS et al., 2010).

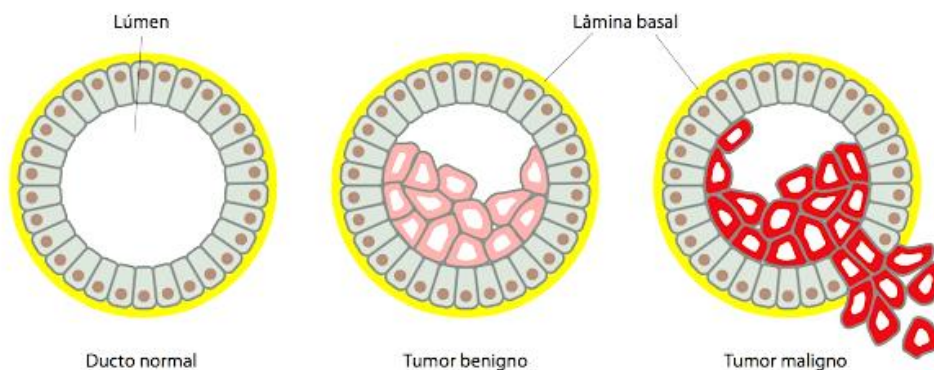


Figura 2. Representação dos carcinomas derivados do tecido epitelial (adaptado de ALBERTS et al., 2010).

Devido a grande heterogeneidade tumoral, os vários tipos de cânceres são classificados de acordo com o tecido e tipo de célula dos quais se originam. Cânceres originados a partir do tecido epitelial de revestimento, como pele e mucosa são denominados carcinomas. No entanto, se o tumor for derivado do epitélio glandular, receberá o prefixo adenocarcinoma. Tumores oriundos de tecidos conjuntivos (mesenquimais) são denominados sarcomas. Cânceres que não se

encaixam nessas categorias incluem os vários tipos de leucemia, derivados de células hematopoiéticas, e cânceres derivados de células do sistema nervoso. Aproximadamente 90% dos cânceres humanos são carcinomas, talvez porque a maioria das células em proliferação no corpo se encontra no epitélio, ou porque os tecidos epiteliais são mais expostos a várias formas de danos físicos e químicos que favorecem o desenvolvimento de neoplasias (KUMAR et al., 2014).

A origem da célula cancerosa é consequência de desordem genética causada por mutações em genes celulares que controlam o crescimento e a proliferação, conhecidos como proto-oncogenes, supressores de tumor e genes de estabilidade. O equilíbrio entre a atuação destes genes garante o perfeito funcionamento do ciclo celular. As mutações podem estar associadas a fatores hereditários ou ser produzidas por agentes químicos, físicos e biológicos, os chamados carcinógenos (SIEBER et al., 2003; VOGELSTEIN e KINZLER, 2004).

A Organização Mundial de Saúde (OMS) relacionou cerca de 100 fatores ambientais como carcinogênicos, cuja exposição frequente a essas substâncias genotóxicas podem induzir lesões no DNA. Entre os fatores físicos, a exposição à radiação ultravioleta está associada, por exemplo, ao desenvolvimento de câncer de pele. Hidrocarbonetos aromáticos e tabaco representam importantes fatores químicos de risco para o desenvolvimento de câncer de pulmão. Alguns tipos de vírus, bactérias e parasitos associados a infecções crônicas também estão presentes no processo de desenvolvimento do câncer, com destaque para o papilomavírus humano (HPV), a *Helicobacter pylori*, os vírus das hepatites B e C, agentes infecciosos que podem causar câncer cervical, gástrico e hepatocarcinoma, respectivamente. Além dos fatores ambientais citados acima, que são responsáveis por 90% dos carcinomas, fatores genéticos ou hereditários estão associados a 10% dos cânceres em humanos (BARBOSA et al., 2015; INCA, 2018; WHO, 2019).

Os proto-oncogenes incluem genes que regulam de forma direta a proliferação celular e são responsáveis por codificar proteínas que diminuem a velocidade de crescimento celular, reparam o DNA e atuam como reguladores do ciclo celular, uma vez que estão associados ao reconhecimento e transdução dos sinais de divisão celular. Os proto-oncogenes quando sofrem alterações estruturais, provenientes do processo de translocação entre cromossomos, amplificação de

sequência ou mutações em pares de bases, passam a ser denotados como oncogenes, estando agora constitutivamente ativos. Desta forma, as proteínas traduzidas a partir desses genes, atuam de forma desordenada o que contribui para a transformação das células normais em células malignas (CROCE, 2008).

Os genes supressores de tumor estão associados às vias de inibição do ciclo celular e metástase, reparo do DNA e ao processo de morte celular programada. Um exemplo é a regulação negativa da proteína p53, codificada pelo gene Tp53, sua inativação tem sido associada à maioria dos tumores malignos. A p53 atua através de vários mecanismos no controle do ciclo celular, uma vez que ela pode induzir a codificação de proteínas de reparo do DNA, interromper o crescimento celular no ponto de verificação G1/S, além de induzir apoptose se o dano no DNA se mostrar irreversível, sendo esta uma das ações mais importantes do organismo para a proteção contra o câncer. Quando a estrutura desses genes é perturbada, através do processo de inserção, deleção, mutação pontual ou silenciamento, a célula perde o controle da divisão celular, pois as mutações inibem a atuação dessas proteínas, contribuindo assim para o crescimento e desenvolvimento tumoral (ALBERTS et al., 2010; GUDISEVA et al., 2017).

Além das alterações nos genes supressores de tumor e nos proto-oncogenes, há um conjunto de genes de reparo de DNA que não atua diretamente sobre o ciclo celular. Porém, seus produtos proteicos estão envolvidos no processo de manutenção da estabilidade genômica. Quando suas sequências são alteradas eleva-se a taxa de mutação, aumentando o potencial descontrole do ciclo celular e a progressão do câncer (VOGELSTEIN e KINZLER, 2004). Ainda, a superexpressão de genes relacionados à manutenção da integridade genômica tem destacado a importância da instabilidade cromossômica tanto no desenvolvimento de resistência intrínseca quanto na resistência adquirida a medicamentos quimioterápicos (SWANTON et al., 2009).

No entanto, mais recentemente tem-se evidenciado o papel regulatório importante dos MicroRNAs (miRNAs), que são propostos como uma família de pequenas moléculas endógenas não-codificantes, capazes de gerenciar e controlar a expressão gênica no nível pós-transcricional. Eles contribuem em vários mecanismos fisiológicos fundamentais, incluindo ciclo celular e proliferação,

sobrevivência celular e apoptose, diferenciação e desenvolvimento, bem como apresentam um papel essencial na patogênese de diferentes doenças humanas, como o início e progressão do câncer, regulando a expressão de múltiplos genes-alvo, associados a processos moleculares de migração, invasão e metástase (IORIO e CROCE, 2009; KHORDADMEHR et al., 2019).

Vários mecanismos podem levar a alterações na expressão de miRNAs, incluindo alterações genômicas como amplificações e deleções, mutações, polimorfismos, alterações epigenéticas e alterações na maquinaria de biogênese de miRNAs. Essas alterações são responsáveis pela desregulação dos níveis de expressão de miRNAs. O silenciamento ou a superexpressão de miRNAs específicos parecem ser fenômenos essenciais na iniciação da carcinogênese. Notavelmente, a descoberta dos miRNAs como importantes moduladores da expressão gênica e envolvidos em doenças crônico-degenerativas como o câncer tem sugerido que estas moléculas podem constituir biomarcadores clinicamente aplicáveis, e poderosa ferramenta de diagnóstico e prognóstico, bem como apresentarem utilidade como promissoras moléculas terapêuticas para a detecção de células tumorais (IORIO e CROCE, 2012; GROSSI et al., 2017).

Assim, o acúmulo das múltiplas alterações genéticas resulta no fenótipo das células cancerosas, permitindo uma elevada capacidade proliferativa, devido à baixa sensibilidade aos inibidores de crescimento, evasão do processo de morte celular programada, angiogênese sustentada, ou seja, induzir a vascularização do tumor e, por conseguinte o fornecimento de oxigênio e nutrientes, invasão e metástase. Dessa forma, as células transformadas adquirem habilidade de atingir a circulação sanguínea e linfática e se estabelecem em tecidos distintos daquele de origem, dando início a novos tumores, assegurando a manutenção e a propagação do fenótipo alterado (HANAHAN e WEINBERG, 2011; GUDISEVA et al., 2017).

1.3. MECANISMOS DE MORTE CELULAR

A morte celular é uma resposta fundamental na formação do organismo vivo durante o desenvolvimento e na manutenção da homeostase. Além disso, a

regulação da morte celular desempenha um papel central sobre o metabolismo, em respostas a danos ao DNA e no desenvolvimento de células de defesa, sendo o desequilíbrio deste processo correlacionado com várias doenças, incluindo o câncer (OKADA e MAK, 2004; PEIXOTO et al., 2017).

Em geral, os principais mecanismos de morte celular são classificados em apoptose, morte celular autofágica e necrose. Estes eventos de morte celular são os mecanismos melhor compreendidos. As diferenças dessas formas de morte estão relacionadas a alterações morfológicas e bioquímicas das células, sendo apresentados resumidamente na figura 3 (GALLUZZI et al., 2012; TAN et al., 2014).

No entanto, existem pelo menos outros 10 tipos diferentes de morte celular que podem ocorrer em situações mais específicas ou em resposta a algumas condições patológicas, a exemplos: a catástrofe mitótica, piroptose e cornificação (GALLUZZI et al., 2012; PEIXOTO et al., 2017). Recentemente foi descoberta uma nova forma de morte celular, a ferroptose, que é desencadeada por sobrecarga de ferro, sendo considerada um contribuinte para morte celular associada a doenças como diabetes, câncer, neurodegeneração, tuberculose e insuficiência renal. No entanto, pouca informação está disponível até o momento sobre estes eventos e, apesar de muitos esforços na área, ainda alguns autores divergem quanto a esta classificação (GALLUZZI et al., 2015; CAO e DIXON, 2016).

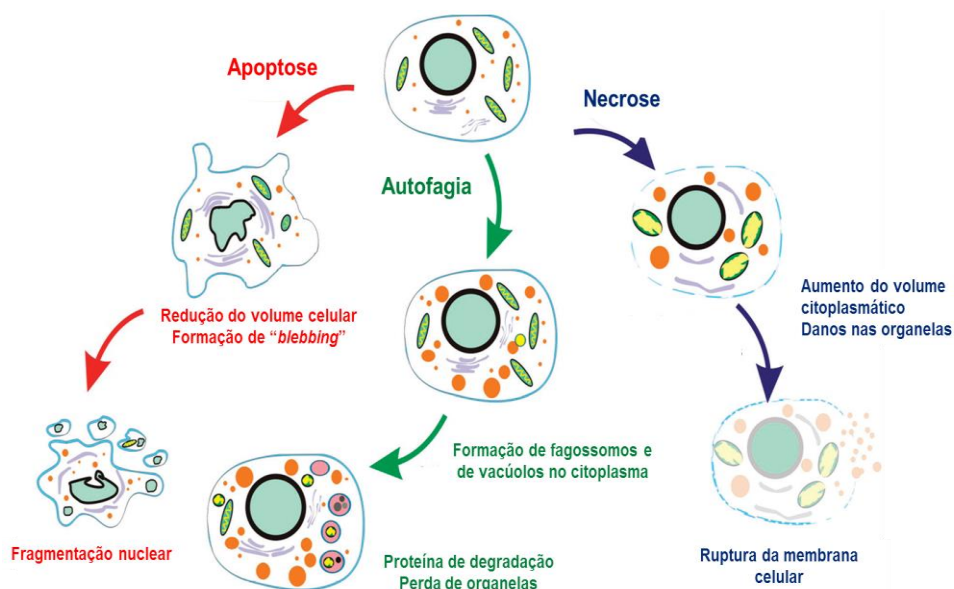


Figura 3. Características morfológicas de apoptose, autofagia e necrose (adaptado de TAN et al., 2014).

Necrose é caracterizada principalmente por induzir rápida perda do potencial de membrana, ocasionando aumento do volume celular, desorganização do citoplasma e posterior ruptura de sua membrana plasmática (ZIEGLER e GROSCURTH, 2004; PEIXOTO et al., 2017). Durante este processo, o conteúdo intracelular rico em hidrolases e metabolitos é liberado, desencadeando o processo de inflamação e interferindo na fisiologia das células vizinhas (GOLSTEIN e KROEMER, 2007). Embora, o termo “necroptose” tem sido mais recentemente utilizado como um sinônimo de necrose regulada que depende da atividade da proteína quinase e da interação com receptor-1 (RIPK1) (TAN et al., 2014).

Em geral, a necrose é considerada um processo de morte celular parcialmente controlado, sem gastos energéticos durante a execução, que resulta em perda progressiva da estrutura e da função celular após uma lesão severa ou condições adversas. As principais causas que desencadeiam esse processo são fatores químicos como a administração de drogas; agentes físicos, por exemplo, a temperatura e a radiação; e biológicos como os patógenos, a hipóxia, as reações imunológicas, os distúrbios genéticos, bioquímicos e nutricionais (KANDUC et al., 2002; PORTUGAL et al., 2009).

Autofagia refere-se a um evento proteolítico intracelular, conservado evolutivamente que ocorre em todas as células eucarióticas, sendo fundamental para o funcionamento do organismo, pois compreende um processo catabólico que promove a degradação e reciclagem de componentes citoplasmáticos desnecessários, controlando os potenciais danos que essas macromoléculas e estruturas celulares poderiam ocasionar. Entretanto, quando sustentada por longos períodos, a autofagia pode contribuir para a morte celular, especialmente quando moduladores essenciais pró-apoptóticos como BAX e BAK e ativação de caspases estejam ausentes (LEVINE e KROEMER, 2008; CHEN et al., 2014).

O processo de autofagia é conduzido em resposta a sinais de estresse celular, ocorrendo a inibição da atividade do complexo quinase mTOR (*Mammalian Target of Rapamycin*) e regulada por uma ação ordenada de proteínas relacionadas à autofagia (ATG) (JOHANSEN e LAMARK, 2011). Durante este evento, os materiais citoplasmáticos indesejados são inicialmente capturados em vesículas de dupla membrana, conhecidas como autofagossomos. As membranas desta estrutura

se alongam e se fundem com os lisossomos, formando os autolisossomos, aonde os substratos são degradados pela ação das hidrolases ácidas lisossomais para posterior reciclagem (GLICK et al., 2010; TAN et al., 2014). Para que as células possam manter o equilíbrio homeostático, é necessário que se tenha um balanço entre a biossíntese e a degradação de componentes celulares. Desta forma, falhas na via autofágica estão correlacionadas com a ocorrência de diversas patologias, como infecções, doenças neurodegenerativas, cardiovasculares e neoplasias (LEVINE e KROEMER, 2008; JIANG e MIZUSHIMA, 2014).

Diante deste papel dual, há um grande interesse em modular a via autofágica como tentativa de melhorar o prognóstico de pacientes com câncer. A administração de agentes indutores ou inibidores da autofagia em combinação com fármacos antineoplásicos pode ser uma alternativa promissora para a obtenção de melhores respostas ao tratamento quimioterápico (JIANG e MIZUSHIMA, 2014).

Já a morte celular programada do tipo apoptose é um processo ativo, altamente seletivo e regulado, exercendo um papel central para vários processos biológicos, tanto em condições fisiológicas como em condições patológicas, ocorrendo nas mais diversas situações, como por exemplo, na organogênese e hematopoiese, na reposição fisiológica de certos tecidos maduros, na atrofia dos órgãos, na resposta inflamatória e na eliminação de células após dano celular por agentes genotóxicos. Diversos são os fatores que podem desencadear tal mecanismo, entre eles: ligação de moléculas a receptores de membrana, agentes quimioterápicos, radiação ionizante, danos no DNA, choque térmico, privação de fatores de crescimento, baixa quantidade de nutrientes e níveis aumentados de espécies reativas de oxigênio (EROs) (WONG, 2011; TAN et al., 2014).

Para sua execução, o processo de apoptose fundamenta-se em uma cascata bioquímica dependente de energia, mediada por caspases, dividida em duas vias principais denotadas como intrínseca e extrínseca (figura 4). As caspases correspondem a uma família de proteases sintetizadas na célula como precursores inativos, denominadas de pró-caspases (zimogênio), que após sofrerem clivagem proteolítica promovem a iniciação e regulação do "suicídio celular". Caspases ativadas são as responsáveis por clivarem inúmeras proteínas vitais, alterando tanto a estrutura nuclear quanto o citoesqueleto. (ELMORE, 2007; TAN et al., 2014).

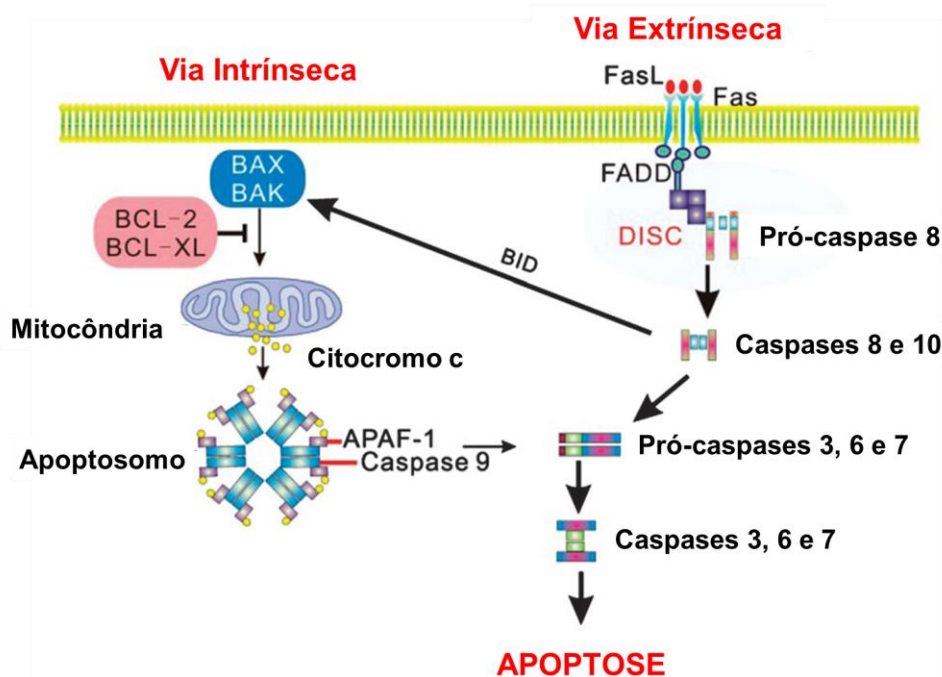


Figura 4. Vias extrínseca e intrínseca do processo apoptótico (adaptado de TAN et al., 2014).

A via intrínseca (ou mitocondrial) é ativada através de estímulos internos como o aumento da concentração de Ca^{2+} citosólico, ausência de fatores de crescimento, danos ao DNA, bloqueadores de componentes do citoesqueleto, drogas quimioterapêuticas, estresse oxidativo, dentre outros fatores que alteram a fisiologia celular. Esta via é modulada por uma família de proteínas pró e anti-apoptóticas de morte celular, que participam ativamente da regulação da apoptose, a família Bcl-2. A família Bcl-2 é dividida em dois grupos de proteínas, as anti-apoptóticas (tendo como principais componentes Bcl-2- o primeiro membro descrito e que deu origem ao nome da família de proteínas, além de Bcl-XL, Bcl-W, Bfl-1 e Mcl-1) e as pró-apoptóticas (por exemplo, Bax, Bak, Bad, Bcl-Xs, Bid, Bik, Bim, Bcl-2L1) (BORNBERG, 2003; WONG, 2011).

Em resposta aos estímulos de estresse celular, ocorre o desbalanço entre as proteínas anti e pró-apoptóticas, as pró-apoptóticas levam a formação de poros (cujos principais componentes são as proteínas Bax e Bak) na membrana da mitocôndria, levando a alteração do potencial da membrana mitocondrial, bem como a permeabilização desta organela, com consequente liberação de moléculas para o citoplasma da célula, como o citocromo c e de endonucleases oriundas do espaço

mitocondrial, que mais tarde clivam o DNA, além da produção substancial de EROs (BORNER, 2003). O citocromo c no citoplasma interage com um complexo de ativação de caspases composto por Apaf1, formando uma estrutura denominada como apoptosoma, que apresenta um domínio de recrutamento de caspase, que possibilita a interação do complexo com a pró-caspase-9, que na presença de ATP, assume sua conformação ativa, denominada de caspase 9, que por sua vez, ativa as pró-caspases 3, 6 e 7, responsáveis por executar o processo apoptótico (ELMORE, 2007). Juntamente com citocromo c, as proteínas SMAC/DIABLO e Omi/HtrA2 localizadas nas mitocôndrias também são liberadas no citoplasma. Quando liberadas, essas duas proteínas se ligam a uma proteína inibidora de caspases conhecida como XIAP, essa ligação ajuda a ativar os mecanismos de apoptose por neutralizar a função inibitória da mesma (WONG, 2011).

Por outro lado, a via extrínseca (ou via de receptores de morte) é desencadeada em resposta a fatores externos, através de receptores de membrana relacionados com o processo de apoptose pertencentes à superfamília de fatores de necrose tumoral (TNF) que incluem os receptores TNFR, os receptores ativados por ligante Fas como, por exemplo, o CD95 e TRAIL-R como os receptores DR4 e DR5, que são denominados como receptores de morte, localizados na superfície celular. Após a ligação dos receptores, a sinalização a seguir é mediada pela porção citoplasmática desses receptores que contém uma sequência de 65 aminoácidos chamada “domínio de morte”. Quando os receptores de morte celular reconhecem um ligante específico, os seus domínios de morte interagem com a proteína adaptadora FADD (Fas-associated death domain protein), que possibilita o recrutamento de pró-caspases 8 e 10, formando o complexo de sinalização indutor de morte (DISC). Com clivagem desse complexo as caspases 8 e 10 assumem sua conformação ativa, amplificando a cascata apoptótica que por sua vez, ativa as caspases executoras 3, 6 e 7, que são comuns em ambas as vias (GARCÍA et al., 2012; HONG et al., 2015).

Entretanto, em algumas ocasiões de estresse celular pode ser desencadeada a sinalização de morte apoptótica via retículo endoplasmático (KAO et al., 2011; WONG, 2011; HUANG et al., 2017). Acredita-se que a caspase 12 possa mediar a apoptose que é especificamente ativada pelo estresse do retículo

endoplasmático (RE), incluindo a alteração na homeostase de cálcio do RE, hipóxia, excesso de ROS e o acúmulo de proteínas mal enoveladas nesta organela, dessa forma, o cálcio citoplasmático é rapidamente absorvido pelas mitocôndrias, resultando em inchaço mitocondrial e perda do potencial de membrana mitocondrial, sendo este evento considerado um fator limitante para ativar a via intrínseca apoptótica (HUANG et al., 2017). O estresse do RE aumenta a expressão de fatores pró-apoptóticos e leva, portanto, a ativação e translocação de caspase 12 do RE para o citosol e, juntamente com o acúmulo de EROs, facilita a liberação do citocromo c da mitocôndria, seguido da ativação da cascata de caspases 9 e 3, culminando na apoptose (figura 5) (KAO et al., 2011; AL-BAHLANI et al., 2017).

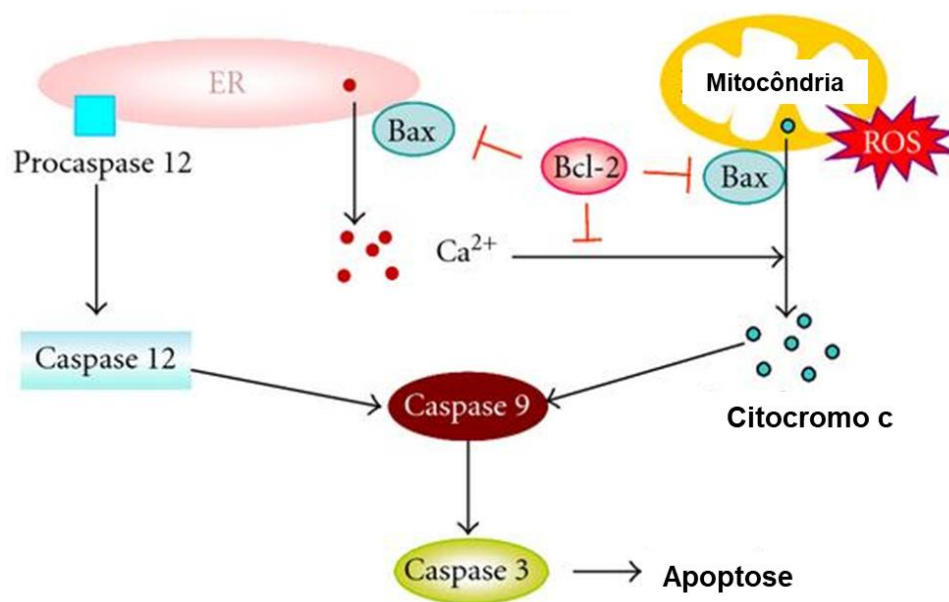


Figura 5. Via intrínseca de sinalização apoptótica mediada pela ativação de caspase 12 (adaptado de KAO et al., 2011).

Apesar destas vias serem conduzidas por componentes bioquímicos distintos, elas eventualmente levam a uma via comum ou à fase de execução da apoptose, contribuindo para as alterações morfológicas típicas do processo apoptótico (WONG, 2011). Tais características incluem o comprometimento da estrutura do citoesqueleto, alteração do volume celular (picnose) e retração de filopódios, modifica a assimetria dos fosfolípidios e a estrutura física da membrana plasmática levando a exposição da fosfatidilserina e a formação de *blebbing* de membrana, promove a fragmentação característica do DNA através da atividade de endonucleases liberadas, ocasionando a condensação da cromatina nas porções

adjacentes à membrana nuclear e finalmente a formação de corpos apoptóticos, resultando em fagocitose sem a liberação de componentes celulares pró-inflamatórios (KROEMER et al., 2009; WONG, 2011; TAN et al., 2014).

Diariamente, mais de 30 milhões de células somáticas sofrem morte celular e são repostas em um organismo saudável, e a apoptose é responsável por aproximadamente 90% destas mortes, eliminando células velhas, com funcionalidade diminuída ou com algum dano potencialmente prejudicial à homeostase do organismo, entre as quais estão as células iniciadoras de tumores (Elmore, 2007).

Neste contexto, tais achados evidenciam que a evasão da morte celular é uma das principais alterações genéticas durante as quais uma célula normal é transformada em uma maligna, uma vez que, a redução da apoptose ou sua resistência desempenha um papel vital na carcinogênese. Há muitas maneiras pelas quais uma célula maligna pode adquirir redução ou resistência à apoptose. Geralmente, os mecanismos podem ser divididos em: 1) desequilíbrio entre proteínas pró-apoptóticas e anti-apoptóticas, 2) redução da função de caspases e 3) sinalização de receptores de morte prejudicados (WONG, 2011). A figura 6 resume os mecanismos que contribuem para este processo.

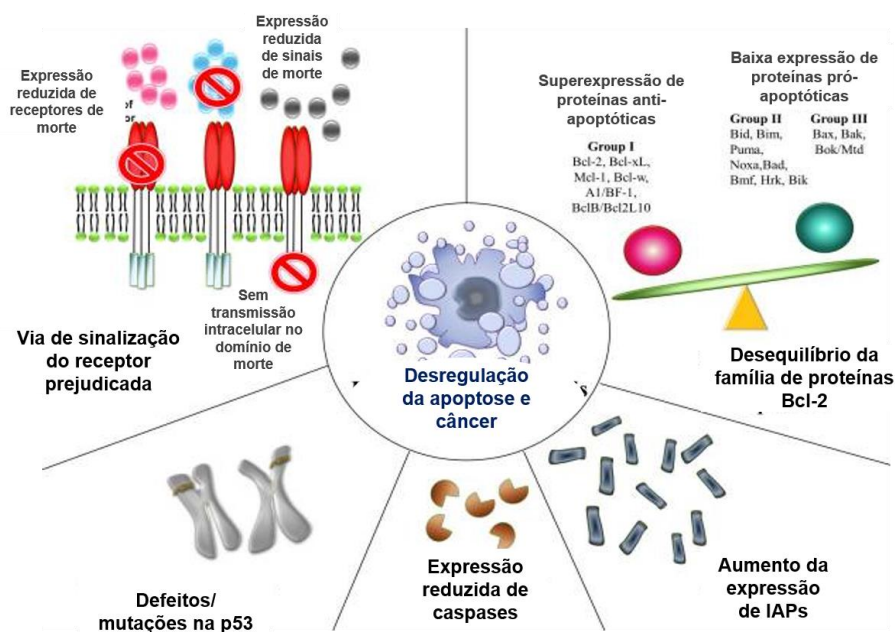


Figura 6. Mecanismos que contribuem para a evasão da apoptose e carcinogênese (adaptado de WONG, 2011).

A apoptose na prática clínica desempenha um importante papel como estratégia terapêutica, uma vez que inúmeros fármacos de origem natural ou sintética com diferentes mecanismos de ação induzem morte celular por esta via. Com o desenvolvimento de compostos promissores, particularmente se tratando dos complexos metálicos, a indução deste tipo de morte celular tem sido considerada como uma via principal pela qual estes complexos citotóxicos combatem as neoplasias (TAN et al., 2014; MEDICI et al., 2015).

Portanto, o estudo dos mecanismos moleculares e das vias apoptóticas de morte celular é essencial e pode ajudar no desenvolvimento de novas drogas ou para a compreensão dos mecanismos de resistência à quimioterapia para o tratamento do câncer e outras condições patológicas (WONG, 2011).

1.4. TRATAMENTOS ANTINEOPLÁSICOS

A quimioterapia, radioterapia e a cirurgia são os três tratamentos mais frequentemente adotados na terapia oncológica, podendo ser realizado individualmente ou em combinação com outros métodos (figura 7) (KAJIYAMA et al., 2017). Existem ainda diferentes técnicas empregadas em tipos específicos de câncer, como a hormonioterapia, imunoterapia, transplante de células tronco, terapia fotodinâmica, entre outras. A escolha do método a ser utilizado depende do estadiamento da doença e da ocorrência ou não de metástase (AMERICAN CANCER SOCIETY, 2019).

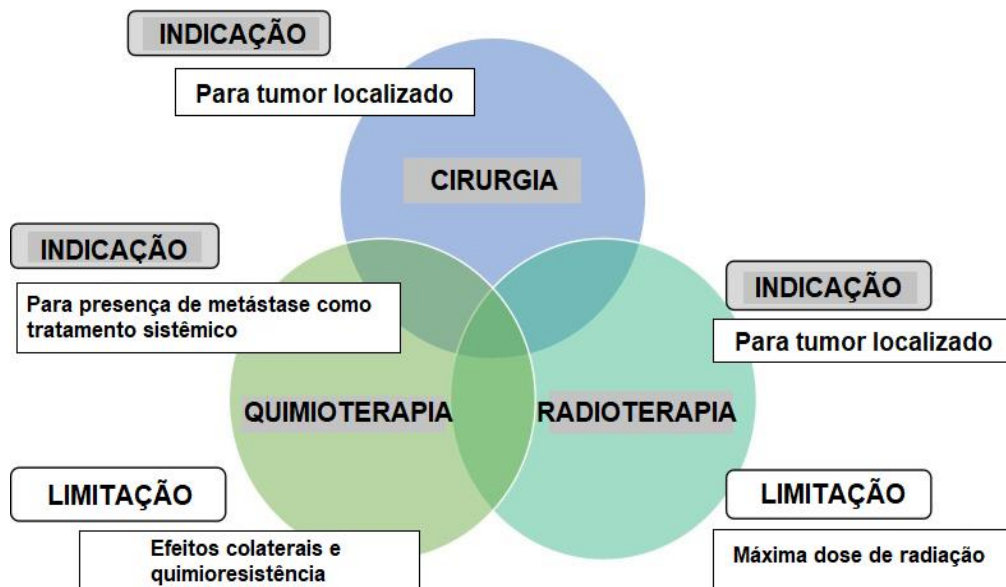


Figura 7. As três principais modalidades de tratamentos antineoplásicos (adaptado de KAJIYAMA et al., 2017).

A quimioterapia consiste na administração de fármacos que inibem o processo de divisão celular seguido da indução do processo de morte celular. A radioterapia é fundamentada na interação entre ondas eletromagnéticas como os raios gama e partículas carregadas, visando à extensiva perturbação estrutural da molécula de DNA e conseqüentemente inviabilizando a divisão e sobrevivência das células neoplásicas. Já a técnica cirúrgica consiste na retirada de toda massa tumoral, é indicada nos casos iniciais da maioria dos tumores primários (GUICHARD et al., 2017; INCA 2019).

A quimioterapia é possivelmente a terapia oncológica que pode ser mais explorada, uma vez que podem ser testadas a capacidade de indução de morte celular de inúmeros compostos químicos (ESPINOSA e RAPOSO, 2010). Um terço dos pacientes alcança a cura através de medidas locais (cirurgia ou radioterapia), que são eficazes quando o tumor ainda não metastatizou. Todavia, na maioria dos casos, a neoplasia caracteriza-se pelo desenvolvimento precoce de micrometástases, indicando a necessidade de uma abordagem sistêmica, que pode ser efetuada com a quimioterapia ou sua combinação com outros métodos, sendo que a última possibilidade visa aumentar a eficiência terapêutica, alcançando maior resposta por dose administrada, atenuando o desenvolvimento de resistência aos

medicamentos, além da atuação sinérgica nas células que se apresentam em diferentes estágios do ciclo celular (DASARI et al., 2014; GUICHARD et al., 2017).

Um dos primeiros quimioterápicos foi desenvolvido a partir do gás mostarda, utilizado durante a primeira guerra mundial como arma química. Foi observado que soldados expostos a este agente desenvolveram supressão medular e linfóide, posteriormente, a administração desta droga destinou-se ao tratamento de linfomas. A partir da publicação, em 1946 (DIXON e NEEDHAM, 1946), dos estudos clínicos realizados com o gás mostarda (mostarda nitrogenada), houve um impacto singular na estratégia de desenvolvimento de novos fármacos antineoplásicos e antibacterianos dentre outros, sendo que medicamentos utilizados atualmente no tratamento de inúmeras doenças, foram desenvolvidos durante esse período (GUICHARD et al., 2017).

Na década de 70 a quimioterapia antineoplásica foi fortemente impulsionada pela introdução da cisplatina *cis*-[Pt(NH₃)₂Cl₂] (ROSENBERG e VANCAMP, 1970), um poderoso agente antitumoral que teve sua atividade descoberta acidentalmente e é amplamente utilizado até os dias de hoje. A cisplatina é clinicamente comprovada para combater numerosos tipos de cânceres humanos, o que mudou muito as perspectivas para pacientes com tumores de ovário, testículo, bexiga, esôfago, cabeça e pescoço entre outros, sendo uma das drogas antineoplásicas de maior sucesso (DASARI et al., 2014; MEDICI et al., 2015).

Os quimioterápicos mais empregados no tratamento do câncer são categorizados de acordo com o perfil de atuação, incluindo os antimetabólitos, alquilantes e inibidores mitóticos. Os fármacos que compõem a classe dos antimetabólitos, como o metotrexato e a gemcitabina inibem a biossíntese dos componentes essenciais para a composição de ácidos nucleicos, a atuação das drogas alquilantes, como os complexos de platina e mostardas nitrogenadas baseia-se na interação direta com estrutura do DNA afetando o ciclo celular, já os inibidores mitóticos, como os alcaloides da vinca e taxanos atuam sobre proteínas do citoesqueleto comprometendo a metáfase, impedindo o processo de divisão celular (GUICHARD et al., 2017).

Entretanto, em contraste com a eficácia clínica da maioria dos agentes quimioterápicos, sua atividade farmacológica é limitada pelos severos efeitos

colaterais como náuseas, degeneração da mucosa do trato digestivo, quedas de cabelo e maior susceptibilidade às infecções, bem como o problema de resistência (ALMEIDA et al., 2005; FLOREA e BÜSSELBERG, 2011). Dessa forma, o desenvolvimento de novas abordagens quimioterápicas faz-se necessário e permanecem como um dos grandes desafios voltados para este fim.

1.5. METALOFÁRMACOS

Compostos inorgânicos têm sido descritos na medicina há muitos séculos, o cobre, por exemplo, foi usado na antiguidade para esterilização de água, compostos de arsênico foram relatados com forma de tratamento para sífilis e a prata, reconhecida por suas propriedades antimicrobianas, empregada no tratamento de feridas, queimaduras e úlceras (SCHWIETERT e MCCUE, 1999; MEDICI et al., 2015).

Atualmente, vários compostos à base de metais são utilizados na clínica, dentre os quais podemos destacar os complexos de gadolínio (III) utilizados como agentes de contraste em ressonância magnética, os do tecnécio-99, usados na obtenção de imagens cardiovasculares, compostos de ouro, ferro e bismuto que atuam no tratamento da artrite reumatóide, hipertensão e úlceras pépticas, respectivamente (BARRY e SADLER, 2013; MEDICI et al., 2015).

No entanto, o marco que consolidou esses compostos na história da medicina baseada em metais, começou há mais de 50 anos com a descoberta acidental da cisplatina, quando Rosenberg e colaboradores na década de 60 analisavam os efeitos do campo elétrico dos metais no processo de proliferação celular e perceberam que os produtos da hidrólise de platina tinham atuação inibitória em cultura de bactéria *Escherichia coli* (ROSENBERG et al., 1965). Dentre os compostos liberados pelos eletrodos de platina, foi identificado que o composto *cis*-diaminodicloroplatina (II) (cisplatina) seria o agente responsável pela atividade antimicrobiana observada e surgiu o interesse na investigação deste complexo como agente antitumoral. Este fato impulsionou a busca de outros compostos desta natureza no tratamento do câncer e outras patologias (ROSENBERG et al., 1965; ROSENBERG e VANCAMP, 1970; KOSTOVA, 2006; DASARI et al., 2014).

1.5.1. COMPOSTOS DE COORDENAÇÃO DE PLATINA

No início da década de 70, a eficácia antineoplásica do composto de coordenação contendo platina *cis*-diaminodicloroplatina (II) *cis*-[Pt(NH₃)₂Cl₂], também conhecido como cisplatina foi relatada no tratamento de tumores do tipo sarcoma 180 e leucemias L1210, usadas como modelos em testes farmacológicos de murinos, sendo posteriormente utilizada no tratamento sistêmico de pacientes terminais e, mais tarde, em portadores de tumores de ovário e testículo. Este foi o primeiro complexo baseado em platina aprovado pela FDA (Food and Drug Administration) para uso clínico em humanos em 1978 (ROSENBERG e VANCAMP, 1970; DASARI et al., 2014; DILRUBA e KALAYDA, 2016).

Desde o advento da cisplatina, muitos derivados deste composto foram sintetizados e suas atividades citotóxicas testadas. Na década de 90, foram aprovados para amplo uso os fármacos de segunda e terceira geração derivados de platina, a carboplatina (*cis*-diamino(2-ciclobutanodicarboxilato)platina(II)) e a oxaliplatina (trans-diaminociclohexaneoxalatoplatina(II)), respectivamente (PASETTO et al., 2006; NEVES e VARGAS, 2011). A carboplatina apresenta menor grau de citotoxicidade que a cisplatina e redução dos efeitos colaterais gerados em resposta ao tratamento, o que aumenta a dose da droga tolerada pelo organismo, facilitando seu uso clínico associado com outros quimioterápicos (WHEATE et al., 2010). Já a oxaliplatina tem sua atuação farmacológica reconhecida sobre vários tipos de tumores resistentes às gerações anteriores dos derivados de platina, principalmente de câncer colorretal. Além disso, seus metabolitos ativos se acumulam pouco no plasma, implicando em ausência de nefrotoxicidade (PASETTO et al., 2006).

Ademais, outros fármacos baseados em platina foram aprovados para uso clínico: a nedaplatina, a lobaplatina e a heptaplatina, porém sua comercialização é restrita ao Japão, China e Coréia, respectivamente (WHEATE et al., 2010). A figura 8 apresenta as estruturas da cisplatina e de alguns de seus análogos que foram aprovados ou estão em fase de ensaios clínicos como agentes antineoplásicos (ELLAHIOUI et al., 2017).

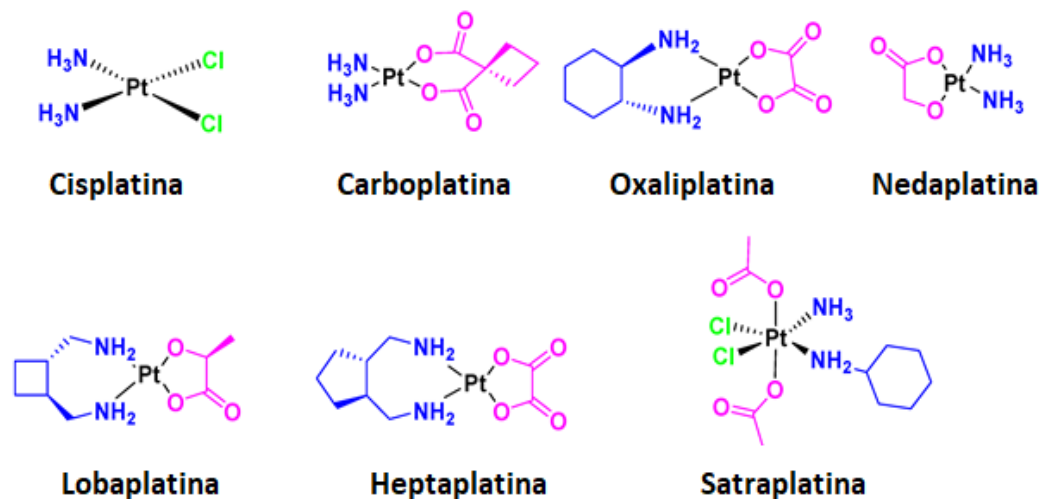


Figura 8. Metalofármacos antineoplásicos de platina aprovados pela FDA e investigado em ensaios clínicos (ELLAHIOUI et al. 2017).

O mecanismo de ação da cisplatina, assim como de seus derivados está relacionado primariamente à sua habilidade de se ligar covalentemente ao DNA através de interação interfitas, intrafitas ou com proteínas citoplasmáticas formando adutos na dupla hélice do DNA (figura 9). A formação de adutos com a cisplatina provocam graves danos estruturais à molécula, causando desenovelamento e torção da sua estrutura, e como consequência, uma cascata de reação é desencadeada, bloqueando a transcrição e replicação do DNA, que por sua vez, induzem à morte celular (GONZALEZ et al., 2001; FLOREA e BÜSSELBERG, 2011). Além disso, a cisplatina pode induzir a formação de EROs, interferir na homeostase de cálcio, e levar à morte celular por ativação simultânea das vias de sinalização, levando a apoptose por via intrínseca e/ou extrínseca (FLOREA e BÜSSELBERG, 2011).

Apesar de apresentar atuação farmacológica promissora sendo altamente eficaz no tratamento de diversos tipos de cânceres, o uso da cisplatina e seus análogos apresentam duas grandes limitações, os inúmeros efeitos colaterais e a possibilidade de resistência intrínseca ou a adquirida em resposta ao tratamento. Em geral os principais efeitos adversos relacionados com as drogas de primeira geração incluem nefrotoxicidade, hepatotoxicidade, cardiotoxicidade e ototoxicidade, e observa-se a correlação entre a mielossupressão e neuropatia na administração das drogas da segunda e terceira geração, respectivamente (WHEATE et al., 2010; BRABEC et al., 2017). Vários mecanismos estão envolvidos no processo de

resistência à cisplatina e incluem aumento do efluxo, inativação e alterações no alvo da droga, mecanismos de reparo do DNA (reparo de adutos), e evasão das vias apoptóticas (FLOREA e BÜSSELBERG, 2011; DILRUBA e KALAYDA, 2016).

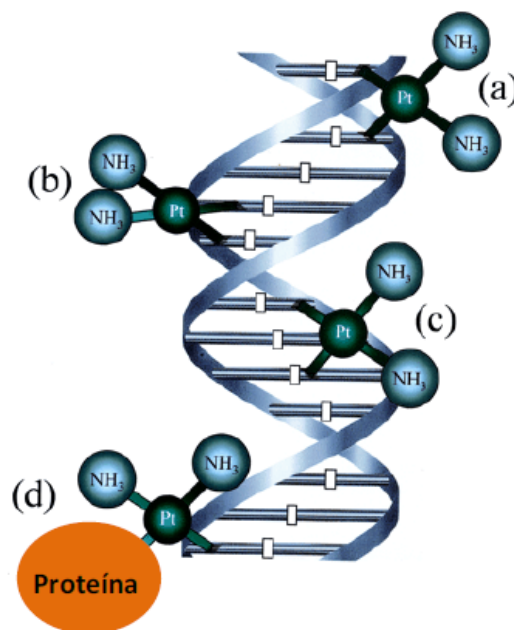


Figura 9. Principais adutos formados através da interação da cisplatina com o DNA: (a) interação entre duas fitas (1,2-interfitas); (b) interação 1,2- intrafita; (C) ligação cruzada 1,3- intrafita e (d) interação com DNA e proteína (adaptado de GONZALEZ et al., 2001).

Dessa forma, na tentativa de minimizar tais efeitos secundários gerados ao tratamento, a quimioterapia combinada visa aumentar a eficiência terapêutica, utilizando medicamentos com diferentes mecanismos que são apontados como uma estratégia promissora para combater as neoplasias (CHOU, 2006; DILRUBA e KALAYDA, 2016). Nos casos de câncer de ovário, por exemplo, a estratégia de primeira linha de tratamento é a associação entre a cisplatina e o paclitaxel (CAI et al., 2015). Segundo Dasari e Tchounwou (2014) a cisplatina associada com o paclitaxel, a doxorubicina e a gencitabina, mostra-se como uma estratégia eficiente para o tratamento de neoplasias que acometem o estômago, a glândula salivar e a vesícula biliar, respectivamente. A oxaliplatina em combinação com 5-fluorouracil e folinato, é utilizada como um tratamento eficiente nos casos de câncer colorretal metastático refratário à cisplatina (DILRUBA e KALAYDA, 2016).

Embasado neste êxito clínico da cisplatina e seus análogos, vários estudos visam analisar o perfil citotóxico de novos metalofármacos baseados em platina,

bem como sua associação com fármacos já comercializados. Souza e colaboradores (2013) relataram a alta citotoxicidade de dois complexos de platina (II) em células de câncer de ovário A2780cisR resistentes à cisplatina e em células de câncer de mama MCF-7. Estes complexos apresentaram baixa toxicidade contra células renais normais LLC-PK1. Recentemente, Chen e colaboradores (2018) analisaram a atuação antineoplásica de cinco novos complexos de platina (IV) combinados com lonidamina em linhagem de carcinoma de próstata LNCaP. O complexo mais citotóxico induziu a morte celular apoptótica pela via mitocondrial e desencadeou o acúmulo de EROs. A satraplatina, uma promissora droga de platina, ativa por via oral e que atualmente encontra-se em ensaios clínicos de fase III, quando associada ao docetaxel ou com a prednisolona, tem apresentado resultados promissores para o tratamento do câncer de próstata, de pulmão de células não pequenas e outros tumores sólidos avançados (DILRUBA e KALAYDA, 2016; NDAGI et al., 2017).

O cenário brevemente relatado aponta que os compostos de platina, sozinhos ou ministrado em conjunto com outros fármacos, são usados para tratar de 40 a 80% dos pacientes com câncer, o que comprova a importância destes compostos para o tratamento desta doença e intensifica a busca por novos complexos de coordenação de platina, com destaque para a oumaplatina, aroplatina, enoplatina, zeniplatina, sebriplatina, miboplatina, picoplatina, satraplatina, lipoplatina e iproplatina que são objetos de extensiva pesquisa na terapia oncológica, sendo que vários desses complexos encontram-se em fase de teste clínico (NEVES e VARGAS, 2011; DILRUBA e KALAYDA, 2016; NDAGI et al., 2017).

Embora a administração desses fármacos esteja correlacionada com efeitos colaterais e com os mecanismos de resistência, o êxito terapêutico dos compostos metálicos impulsionam novas pesquisas com substâncias desta natureza que, assim como a cisplatina e seus análogos, sejam capazes de interagir com o DNA, ou de forma diferenciada, cujo mecanismo de ação envolva outros alvos moleculares, como o RNA, proteínas e enzimas que induzam a morte celular, e que poderiam potencialmente superar os obstáculos das drogas clínicas atuais, incluindo a toxicidade sistêmica, resistência, seletividade e outras deficiências farmacológicas (LAINÉ e PASSIRANI, 2012; MUHAMMAD e GUO, 2014).

A descoberta do potencial terapêutico de complexos com outros centros metálicos além dos prósperos compostos baseados em platina, contendo ferro (Fe),

paládio (Pd), cobalto (Co), ouro (Au) e zinco (Zn) ganham destaque por apresentarem atuação antiproliferativa promissora e estão atraindo crescente interesse na medicina clínica moderna, principalmente porque os metais exibem características únicas, como atividade redox, modos de coordenação variáveis e reatividade em relação ao substrato alvo (HORN et al., 2013; FISCHER-FODOR et al., 2014; FERNANDES et al., 2015; MORCELLI et al., 2016; KHAN et al., 2018; ELIE et al., 2019; MOREIRA et al., 2019). Além disso, existem compostos de rutênio (NAMI-A e KP1019), gálio (Ga-maltolato e KP46), titânio (titanoceno) e de cobre (Cu-ATSM), que vem demonstrando importantes resultados frente a inúmeras linhagens neoplásicas *in vitro* e *in vivo*, incluindo tumores metastático de pulmão, colorretal avançado, linfoma, melanoma, próstata e câncer cervical, respectivamente, sendo que alguns deles encontram-se atualmente em fase de ensaios clínicos, conforme apresentado na figura 10 (TAN et al., 2014; NDAGI et al., 2017).

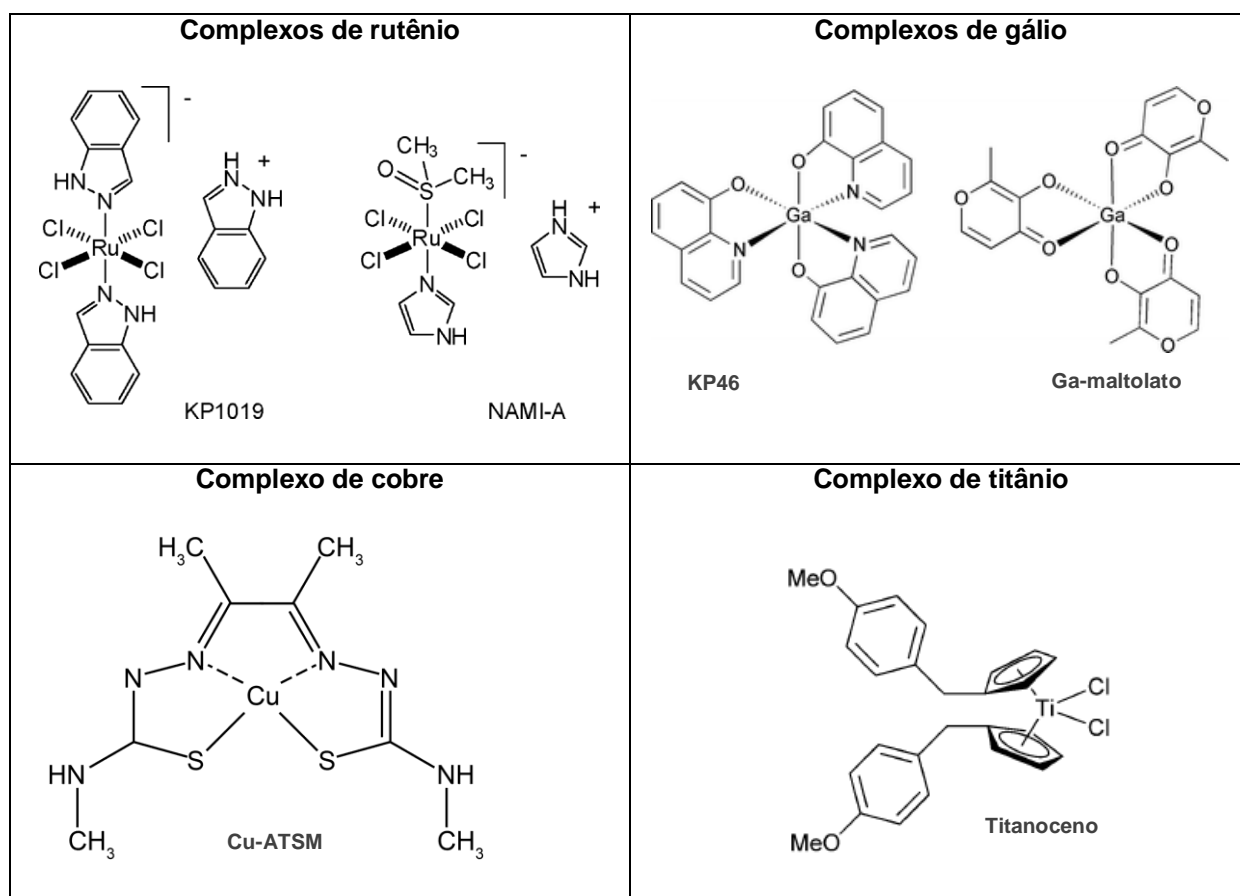


Figura 10. Compostos metálicos submetidos a ensaios clínicos em humanos (adaptado de TAN et al., 2014; NDAGI et al., 2017).

1.5.2. COMPOSTOS DE COORDENAÇÃO DE COBRE

Um metal que merece atenção especial no estudo da sua atuação terapêutica é o cobre. Este metal é considerado um dos elementos traços mais importantes para o funcionamento celular, sendo o terceiro mais abundante no corpo humano. O íon está associado a vários processos bioquímicos, envolvidos na estrutura e função de um grande número de metaloproteínas, participando assim de diferentes vias metabólicas, envolvendo o processo de detoxificação, diferenciação de tecidos, respiração mitocondrial, síntese de hormônios, coagulação, e muitos outros processos, sendo indispensável para a homeostase do organismo (TAN et al., 2014; BHATTACHARJEE et al., 2017).

O cobre Cu^{2+} ao ser absorvido é direcionado para o fígado, onde é estocado e redirecionado para a corrente sanguínea através da ceruloplasmina e da albumina, com posterior transporte para o meio intracelular com auxílio da proteína transportadora de cobre (CTR1). O cobre é assim distribuído para diferentes compartimentos intracelulares em resposta a demanda metabólica, atuando em seguida por meio de processos redox (DENOYER et al., 2015). No entanto, esse padrão de regulação sistêmica de Cu^{2+} não se observa em tecidos tumorais, sendo relatadas concentrações mais elevadas do íon em células cancerígenas, devido a possível atuação do metal no processo de angiogênese e metástase. Acredita-se que complexos bioativos com este metal, poderiam induzir maior resposta citotóxica para as células neoplásicas em relação às células não tumorais, devido ao seu intenso metabolismo celular e a alta demanda de ATP requeridos pelo transporte de nutrientes, este fato poderia inibir o processo de proliferação celular (DENOYER et al., 2015; BHATTACHARJEE et al., 2017).

Neste sentido, em função da característica endógena do íon, a atividade antitumoral dos complexos de cobre tem gerado grande interesse na busca por novos agentes quimioterápicos que seja menos agressivo ao organismo que os metais não essenciais. Este fato é apoiado por um número considerável de trabalhos que buscam determinar o mecanismo de ação contra diferentes linhagens incluindo, leucemia (BORGES et al., 2016; FERNANDES et al., 2015; XU et al., 2017), carcinoma de mama (DHIVYA et al., 2015; KHAN et al., 2018), câncer de estômago

(YANG et al., 2018), carcinoma pulmonar (LIU et al., 2016; MACIEL et al., 2019) e carcinoma de próstata (XIE et al., 2018).

A síntese, caracterização e atividade citotóxica de inúmeros complexos derivados do íon cobre já foram relatadas e reflete-se em várias revisões na última década (MARZANO et al., 2009; SANTINI et al., 2014; DENOYER et al., 2015; BENTOUHAMI et al., 2017; DENOYER et al., 2018). Dentre os complexos testados, os que contêm tiosemicarbazonas, dissulfiram, clioquinol e hidrazonas têm se mostrado promissores, sendo ativos contra uma ampla gama de tipos de neoplasias, visto que a coordenação do cobre com estas moléculas bioativas pode potencializar as propriedades biológicas dos ligantes (DENOYER et al., 2015; MEDICI et al., 2015). Apesar dos compostos serem estruturalmente distintos, os mecanismos de atuação propostos compartilham aspectos comuns como a interação com o DNA, o bloqueio do ciclo celular, a inibição de proteassoma, estresse de retículo endoplasmático e a geração de EROs, conduzindo às células tumorais a morte por apoptose (MA et al., 2012; DENOYER et al., 2015).

Embora a comercialização de medicamentos derivados deste metal ainda não tenha tido aprovação para tratamento de pacientes oncológicos, membros das classes de complexos de cobre denotados como Casiopeínas ganham destaque em pesquisas médicas neste campo, apresentando resultados antineoplásicos promissores tanto *in vitro* como *in vivo*, estando a Casiopeína (III) Nitrato de (4,4'-dimetil-2,2'-bipiridina)(acetilacetonato) cobre (II) em fase de teste clínico (figura 11) (SANTINI et al., 2014; SERMENT-GUERRERO et al., 2017).

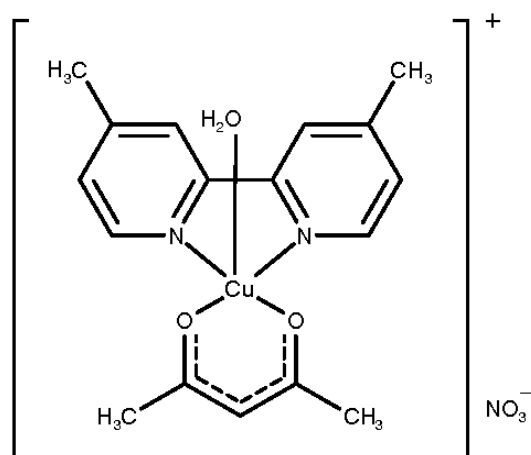


Figura 11. Estrutura química da Casiopeína (III) Nitrato de (4,4'-dimetil-2,2'-bipiridina)(acetilacetonato) cobre (II) (MARÍN-MEDINA et al., 2016).

Paralelamente aos estudos referentes à atividade anticâncer, aplicações e desenvolvimentos de novos compostos de coordenação de cobre também têm demonstrado relevante ação anti-inflamatória (BOULSOURANI et al., 2017), antibacteriana (DJOKO et al., 2014), antiparasitária (PORTES et al., 2017), no tratamento da doença de Alzheimer, de Parkinson e da esclerose lateral amiotrófica (DENOYER et al., 2018).

Com base na potencial atuação dos metalofármacos o grupo de pesquisa em Química Bioinorgânica em parceria com Laboratório de Biologia do Reconhecer (LBR) da Universidade Estadual do Norte Fluminense Darcy Ribeiro, tem realizado a síntese e investigado o potencial citotóxico de diferentes compostos de coordenação. A atividade farmacológica de alguns desses complexos já foram ou estão sendo publicados, incluído os complexos de cobre (BORGES et al., 2016; FERNANDES et al., 2015; MACIEL et al., 2019), ferro (HORN et al., 2013), cobalto (MORCELLI et al., 2016) e platina (MOREIRA et al., 2019). Além disso, estudo com complexos de cobre vem sendo relatado em vários trabalhos do grupo ou estão em andamento no laboratório, como mostrado a seguir.

Bull (2008) avaliou o potencial citotóxico de dois complexos de cobre, um com ligante contendo uma piridina e o outro apresentando uma piridina e um grupamento fenol em sua estrutura frente a linhagens leucêmicas U937 e THP-1 e verificou que os complexos de coordenação obtidos a partir dos dois ligantes apresentaram maior atividade biológica do que os seus respectivos ligantes isolados. Em seu trabalho, Lopes (2012) sintetizou oito complexos de coordenação de cobre e avaliou a atividade biológica sobre as linhagens leucêmicas U937 e THP-1. Dentre os compostos testados, o composto $[Cu(L1)Cl]Cl \cdot 2H_2O$ ($Cu\alpha$) foi o que apresentou melhor resultado, exibindo a concentração inibitória de 50% (IC_{50}) de 13,85 μM para as células U937 e 11,06 μM para as células THP1, sendo este composto mais ativo que a cisplatina. Além disso, o composto apresentou baixa citotoxicidade sobre células normais do sangue periférico (PBMC). Posteriormente, Borges (2013) verificou atividade antineoplásica de compostos de coordenação de cobre (II) contendo ligantes N,O-doadores e a unidade naftoil, frente as linhagens humanas leucêmicas U937 e THP-1, linhagem de melanoma murino B16F10 e melanoma humano SK-MEL5. Os resultados demonstraram que o composto inibe o

crescimento de células neoplásicas *in vitro* por induzir morte celular por apoptose e que ambas as vias (extrínseca e intrínseca) foram ativadas. Subsequente Freitas (2014) avaliou os efeitos antitumorais do complexo (Cuα) *in vivo*, em camundongos Balb/c e C57BL/6, verificando a dose letal mediana e a inibição do desenvolvimento de lesões subcutâneas. O complexo demonstrou notável potencial inibitório no tratamento de lesões de células B16-F10 (melanoma metastático murino), NCI-H460 (carcinoma de pulmão humano), SK-MEL-5 (melanoma metastático humano), apresentando redução de aproximadamente 12, 47 e 41% do volume tumoral respectivamente, valores significativamente menores do que os tumores do grupo controle. Bull (2016) investigou a atividade citotóxica de compostos de coordenação de gálio e cobre frente a linhagens neoplásicas de leucemia THP-1, U937, MOLT-4, carcinoma pulmonar NCI-H460 e colorretal COLO 205. Os resultados apontaram que os complexos de cobre foram os mais ativos, apresentando maior atividade biológica contra as linhagens U937 e NCI-H460 e induzindo morte celular por apoptose. Os mesmos ligantes também foram testados com o gálio, no entanto, apresentando atividade citotóxica inferior, confirmando que a atividade do ligante orgânico é dependente do íon metálico ao qual ele está coordenado.

Recentemente Guimarães (2019) verificou a combinação do complexo de cobre [Cu(L1)Cl]Cl.2H₂O com a cisplatina em linhagens de câncer de pulmão (NCI-H460), mama (MDA-MB-231), próstata (PC-3) e pâncreas (BXP-3). Os testes iniciais foram animadores, com destaque para seu efeito sobre a linhagem MDA-MB-231, onde o composto de cobre e a cisplatina isolados exibiram a IC₅₀ de 20,26 μM e 80,58 μM, respectivamente. Quando as células MDA-MB-231 foram tratadas em associação com ambas as drogas, observou-se ainda um efeito citotóxico superior quando comparado ao uso isolado de cada agente, exibindo perfil de atuação sinérgico e reduzindo em aproximadamente 50% da dose de ambos os compostos.

Os estudos relatados comprovam a importância dos compostos contendo metais e seu crescente desenvolvimento, estimulando a busca por novos compostos desta natureza que sejam mais eficientes, menos tóxicos e com potenciais aplicações terapêuticas futuras em câncer e outras áreas da medicina, sendo por isso escolhido como o objeto principal de investigação de nosso grupo de trabalho.

2. JUSTIFICATIVA

O câncer é um dos mais graves problemas de saúde pública, devido a elevada incidência e taxa de óbito por esta doença, sendo uma das principais causas de morte mais recorrente da população mundial.

A quimioterapia continua sendo a principal forma de tratamento para a maioria dos casos de câncer, onde aliada a outros métodos, como a cirurgia e a radioterapia, alcança bons resultados de cura. No entanto, o maior obstáculo dos fármacos antineoplásicos, são os diversos efeitos colaterais gerados ao tratamento, incluindo quedas de cabelo, náuseas, degeneração da mucosa do trato digestivo, nefrotoxicidade e hepatotoxicidade, além disso, o mecanismo de resistência dos tumores às principais drogas eleva o insucesso terapêutico e o número de mortes (MUHAMMAD e GUO, 2014).

Desde o êxito do uso clínico da cisplatina, metalofármaco amplamente utilizado no tratamento de vários tumores, como os cânceres de ovário, testículo, bexiga, esôfago, cabeça e pescoço, inúmeras pesquisas com outros complexos metálicos impulsionam os avanços na Química Bioinorgânica medicinal na tentativa de se obter novos agentes antitumorais mais potentes, seletivos e menos tóxicos, permanecendo como uma das metas mais urgentes no sentido de melhorar a sobrevivência dos pacientes (DASARI et al., 2014).

Neste contexto, o grupo de pesquisa em Química Bioinorgânica em parceria com o Laboratório de Biologia do Reconhecer, ambos da Universidade Estadual do Norte Fluminense Darcy Ribeiro vem produzindo compostos metálicos de cobre, ferro, zinco, cobalto, gálio e platina com resultados preliminares promissores, exibindo atividade antineoplásica tanto *in vitro* como também *in vivo* (FERNANDES et al., 2015; MORCELLI et al., 2016; MOREIRA et al., 2019).

Sendo assim, visando a obtenção de novos metalofármacos como estratégia terapêutica, os compostos de platina (II) (Patente 06/12/16-BR1020160285801) e o de cobre (II) (Patente 23/05/12-PI 1020140173397-8), foram previamente selecionados devido ao seu alto potencial citotóxico, dessa forma, torna-se relevante um estudo mais detalhado da sua ação, para melhor elucidar seus efeitos antineoplásicos, em busca de alternativas aos tratamentos já existentes.

3. OBJETIVO

3.1. Objetivo Geral

Avaliar o potencial antineoplásico de quatro compostos de coordenação de platina (II) e um de cobre (II), frente a linhagens de células leucêmicas U937 e de carcinoma pulmonar NCI-H460, respectivamente, bem como o mecanismo de indução de morte celular dos mesmos e comparar seu efeito inibitório com a cisplatina.

3.2. Objetivos Específicos

- Avaliar a atividade citotóxica dos compostos de platina (II) e de cobre (II) nas células neoplásicas humanas (THP-1, U937, MOLT-4, COLO 205 e NCI-H460), através de teste *in vitro* por meio de ensaio de viabilidade celular baseado na metabolização do MTT;
- Investigar o tipo de indução de morte celular e das vias apoptóticas ocasionados pelos compostos de platina (II) e de cobre (II) contra células leucêmicas U937 e carcinoma pulmonar NCI-H460, respectivamente, através da análise do ciclo celular (Sub-G1), do potencial de membrana mitocondrial (JC-1), marcação com anexina e iodeto de propídeo, avaliados por citometria de fluxo, e a atividade de caspases averiguadas por meio de ensaio colorimétrico.
- Verificar alterações morfológicas e ultraestruturais nas células leucêmicas U937 e carcinoma pulmonar NCI-H460, após tratamento com os compostos de platina (II) e de cobre (II) por microscopia de fluorescência e microscopia eletrônica de varredura e de transmissão;
- Determinar a DL_{50} (dose letal mediana) do composto de cobre (II) em camundongos BALB/c nude;
- Avaliar o potencial antitumoral do composto de cobre (II) *in vivo* em modelo murino de câncer de células de carcinoma pulmonar NCI-H460.

4. PRODUÇÃO CIENTÍFICA

- **CAPÍTULO I** – Modulating the antitumoral activity by the design of new platinum(II) compounds: synthesis, characterization, DFT, ultrastructure and mechanistic studies

AUTORES – Rafaela Oliveira Moreira, Samila R. Morcelli, Milton Masahiko Kanashiro, Leide Laura Figueiredo Maciel, Jackson Resende, João Carlos de Aquino Almeida, Lawrence Gahan, Adolfo Horn Jr, Christiane Fernandes Horn

SITUAÇÃO – Publicado no *Journal of Inorganic Biochemistry*, v. 194, p. 200-213, 2019. DOI: 10.1016/J.JINORGBIO.2018.12.016.

- **CAPÍTULO II** – *In vitro* and *in vivo* anti-proliferative activity and ultrastructure investigations of a copper(II) complex toward human lung cancer cell NCI-H460

AUTORES – Leide Laura Figueiredo Maciel, Willian Rodrigues de Freitas, Erika Soares Bull, Christiane Fernandes Horn, Milton Masahiko Kanashiro, Adolfo Horn Jr, João Carlos de Aquino Almeida

SITUAÇÃO – Manuscrito submetido para a Revista *Investigational New Drugs*.



Modulating the antitumoral activity by the design of new platinum(II) compounds: Synthesis, characterization, DFT, ultrastructure and mechanistic studies

Rafaela O. Moreira^a, Samila R. Morcelli^a, Milton M. Kanashiro^b, Jackson A.L.C. Resende^{c,d},
Leide L.F. Maciel^{b,e}, João Carlos de A. Almeida^e, Lawrence R. Gahan^f, Adolfo Horn Jr.^a,
Christiane Fernandes^{a,*}

^a Laboratório de Ciências Químicas, Universidade Estadual do Norte Fluminense Darcy Ribeiro, 28013-602 Campos dos Goytacazes, RJ, Brazil

^b Laboratório de Biologia do Reconhecer, Universidade Estadual do Norte Fluminense Darcy Ribeiro, 28013-602 Campos dos Goytacazes, RJ, Brazil

^c Laboratório de Difração de Raios X, Universidade Federal Fluminense, 24020-150 Niterói, RJ, Brazil

^d Instituto de Ciências Exatas e da Terra, Campus Universitário do Araguaia, Universidade Federal do Mato Grosso, 78600-000 Barra do Garças, MT, Brazil

^e Laboratório de Fisiologia e Bioquímica de Microorganismos, Universidade Estadual do Norte Fluminense Darcy Ribeiro, 28013-602 Campos dos Goytacazes, RJ, Brazil

^f School of Chemistry and Molecular Biosciences, The University of Queensland, Brisbane, QLD 4072, Australia

ABSTRACT

The synthesis, physico-chemical characterization, Density functional theory (DFT) calculation and cytotoxicity against five human tumoral cell lines (THP-1, U937, Molt-4, Colo205 and H460) of four new platinum(II) coordination compounds are reported, *i.e.* [Pt(HL1)Cl]·H₂O (1), [Pt(HL2)Cl]·H₂O (2), [Pt(HL3)Cl]·H₂O (3) and [Pt(HL4)Cl]·H₂O (4). The ligands contain N2O donor sets. Furthermore, H2L3 and H2L4 present α and β -naphthyl groups respectively, which are absent in HL1 and H2L2. X-ray diffraction studies were performed for complex (3), indicating the formation of a mononuclear platinum(II) complex. Complexes (3) and (4), which contain α and β -naphthyl groups respectively, have presented lower IC₅₀ (inhibitory concentration) values than those exhibited by complexes (1) and (2). The mechanism of cell death promoted by complexes (3) and (4) was investigated, suggesting that, toward U937 cell line, the α isomer promotes death by apoptosis and the β isomer by necrosis. Transmission and scanning electron microscopy investigations are in agreement with the loss of mitochondrial membrane potential ($\Delta\Psi_m$) observed by JC-1 mitochondrial potential sensor and indicate that the activity of complex (3) against U937 cell line is mediated by an apoptotic mechanism associated with mitochondrial dysfunction. A quantification of caspases 3, 6, 8 and 9 indicated that both the intrinsic and extrinsic pathways are involved in the apoptotic *stimuli*. Based on DFT calculations all the Pt(II) complexes present the same coordination environment for the metal centre, indicating that the higher cytotoxic activities exhibited by complexes (3) and (4) are related to the presence of the α and β -naphthyl groups in the ligand structure.

1. Introduction

The development of new platinum antitumor drugs has been motivated by the usefulness of cisplatin and derivatives in chemotherapy and the resistance of many tumors to these compounds [1]. The four main steps in the mechanism of action of cisplatin are: cellular uptake, aquation/activation, DNA platination and cellular processing of Pt-DNA lesions, leading to cell survival or apoptosis [2]. Numerous studies show that cisplatin forms in DNA ~90% intrastrand cross-links (CLs) between neighboring purine bases (1,2-GG or 1,2-AG intrastrand CLs) and remaining lesions are intrastrand CLs between purine bases separated by a third base, interstrand CLs and monofunctional adducts [3]. The interaction of cisplatin with DNA causes significant distortion of helical structure and results in inhibition of DNA replication and transcription, driving the cell to die by apoptosis [4]. Cisplatin is the first generation

of platinum-based drugs (PBDs) used as anticancer agents, inducing dose-limiting toxicity on the cells. Due to the severe side effects (neurotoxicity, ototoxicity, nausea and vomiting) and to overcome the resistance observed in some cancers, Carboplatin and Oxaliplatin were developed [5]. Recently, Gao and co-workers have reviewed the recent progress in research of platinum complexes as well as their biological activities and insights into the development and design of new platinum drugs [6].

In 2013, Souza and co-workers reported the high cytotoxicity in cisplatin resistant A2780cisR tumor cells (ovarian) as well as in breast cancer MCF-7, and reduced toxicity against LLC-PK1 cells (normal renal cells), of two novel platinum(II) complexes. These complexes, which present thiosemicarbazone in their structures exhibit high anti-proliferative activity and very low nephrotoxicity, suggesting they are very specific on cancer cells. However, no mechanism of action was

* Corresponding author.

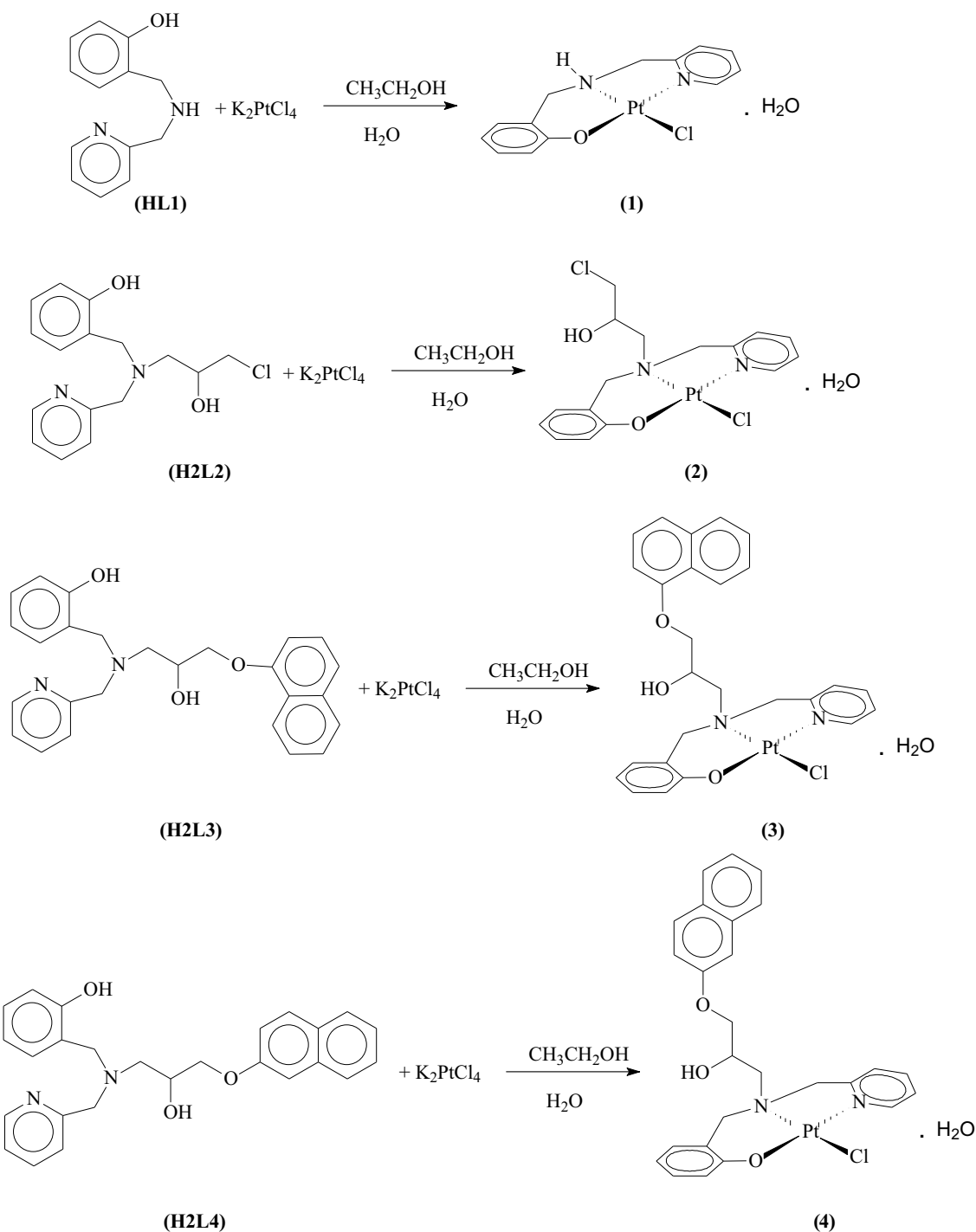
E-mail address: chris@pq.cnpq.br (C. Fernandes).

<https://doi.org/10.1016/j.jinorgbio.2018.12.016>

Received 16 June 2018; Received in revised form 22 December 2018; Accepted 24 December 2018

Available online 30 January 2019

0162-0134/ © 2019 Elsevier Inc. All rights reserved.



Scheme 1. Scheme illustrating the syntheses of the platinum(II) complexes (1)–(4).

proposed by the authors [7]. In 2016, Keppler and co-workers reported the investigation of cell ultrastructure and drug distribution in samples (murine tumor and kidney) obtained from mice treated with therapeutically relevant doses of two platinum(IV)-based anticancer compounds. These studies revealed cytoplasmic sulfur-rich organelles accumulating platinum in both kidney and malignant cells, showing high sensitivity [8]. Recently, Gou and co-workers have reported the cytotoxicity of new five platinum(IV) prodrugs conjugated with the potentiator Lonidamine (LND), which increases the response of human tumor cells to platinum(II) drugs in preclinical studies. LND works on the mitochondria, provoking disruption of the mitochondria transmembrane potential *via* a direct effect on the mitochondrial

permeability transition pore (mPTP). The most cytotoxic complex triggered cancer cell death *via* an apoptotic pathway and effectively induced apoptosis in LNCaP cells, which is closely associated with mitochondrial function disruption and reactive oxygen species accumulation [9].

We have been investigating the coordination behavior of ligands HL1 and H2L2 (Scheme 1) with several transition metals, aiming to develop synthetic models for metalloenzymes and as metallo-drugs. In 2015 we described the synthesis and antitoxoplasma activity of a Zn(II) complex, containing the ligand HL1 and sulfadiazine, the current medicine to treat the infection caused by *T. gondii* [10]. In 2016, we reported the synthesis, X-ray crystal structure and *in vitro* and *in vivo*

studies of the antineoplastic activity of the complex $[\text{Cu}(\text{HL1})\text{Cl}_2]$ against human leukemia THP-1 and murine melanoma B16-F10 cell lines. This complex presents LD_{50} (lethal dose) of $24 \text{ mg}\cdot\text{kg}^{-1}$ and showed a 92% inhibition of tumor growth in BALB/c nude bearing THP-1 tumor [11]. In 2018, we reported the antitumoral activity of a copper(II) complex $[\text{Cu}(\text{HBPA})(\text{L1})\text{Cl}]\cdot 3\text{H}_2\text{O}$ which was obtained through the reaction between the ligand stilbene-quinone (HL1) and the complex $[\text{Cu}(\text{HBPA})\text{Cl}_2]$. Results from MTT assay [MTT = (3-(4,5-dimethylthiazol-2-yl)-2,5-diphenyl tetrazolium bromide)] revealed that this new complex is more active against sarcoma cell lines (MES-SA/Dx5 and MES-SA) than both the free ligand HL1 and complex $[\text{Cu}(\text{HL1})\text{Cl}_2]$, reducing cell viability to $< 50 \mu\text{M}$ [12]. With regard to ligand H2L2, its coordination behavior has been studied with iron(III), copper(II), zinc(II) and nickel(II) ions [13–18]. In order to improve the biological activities presented by these coordination compounds, two new ligands H2L3 and H2L4, whose structures may be considered as derived from HL1 and H2L2 were developed. The attachment of naphthyl groups was successful and copper(II), cobalt(II) and iron(III) complexes were obtained and reported previously [19–21]. Copper(II) complexes were obtained as dinuclear in the solid state but form mononuclear species in solution [19]. The complex containing the ligand H2L3 (α isomer) exhibits higher activity than *cis*-platin against U937 and LD_{50} of $55 \text{ mg}\cdot\text{kg}^{-1}$. Mechanistic investigations for this complex suggests that the apoptosis signal starts from an extrinsic pathway involving the activation of caspases 4 and 8. This signal is amplified by mitochondria with the concomitant release of cytochrome *a* and the activation of caspase 9 [19]. The synthesis, physico-chemical characterization and cytotoxicity toward five human tumoral cell lines (THP-1, U937, Molt-4, Colo205 and H460) of cobalt(II) complexes, obtained with the ligands H2L2, H2L3 and H2L4 were reported in 2016 [20]. Complexes containing the ligands H2L3 and H2L4 have presented IC_{50} values lower than those exhibited by complex containing the ligand H2L2. The complex containing the ligand H2L4 has presented IC_{50} values lower than *cis*-platin toward Colo205 and H460. Mechanistic investigation suggests that the cytotoxic activity of this complex against U937 cell line is mediated by an apoptotic pathway, associated with mitochondrial dysfunction [20]. Dinuclear iron(III) complexes, which presented moderate antitumoral activity, were obtained with ligands H2L3 and H2L4 [21]. Therefore, based on our results, we can state that the antitumoral activity of complexes containing the same ligands show dependence on the metal nature, nuclearity and the isomerism. In this sense, looking to develop new coordination compounds with increased antitumoral activity, we report herein the synthesis, characterization and antitumoral activity of four new platinum(II) complexes containing the ligands HL1, H2L2, H2L3 and H2L4: $[\text{Pt}(\text{HL1})\text{Cl}]\cdot\text{H}_2\text{O}$ (1), $[\text{Pt}(\text{HL2})\text{Cl}]\cdot\text{H}_2\text{O}$ (2) $[\text{Pt}(\text{HL3})\text{Cl}]\cdot\text{H}_2\text{O}$ (3) and $[\text{Pt}(\text{HL4})\text{Cl}]\cdot\text{H}_2\text{O}$ (4) (HL1: N-(2-hydroxybenzyl)-N-(2-pyridylmethyl)amine; H2L2: N-(2-hydroxybenzyl)-N-(2-pyridylmethyl)[(3-chloro)(2-hydroxy)]-propylamine; H2L3: 1-[2-hydroxybenzyl(2-pyridylmethyl)amino]-3-(1-naphthoxy)-2-propanol and (H2L4): 1-[2-hydroxybenzyl (2-pyridylmethyl)amino]-3-(2-naphthoxy)-2-propanol). The interaction with complex (3) with U937 cells was monitored *via* annexin staining, mitochondrial membrane potential ($\Delta\Psi\text{m}$) analysis, cell cycle analysis, transmission electron microscopy (TEM), scanning electron microscopy (SEM) and quantification of caspases 3, 6, 8 and 9. Compared with the respective cobalt(III) complex previously reported by us [20], complex (3) is much

more active confirming the relevance of the platinum on the biological activity.

2. Experimental

2.1. Materials and methods

The ligands and their respective platinum(II) complexes were synthesized using analytical grade reagents. UV–Vis, electrochemical and ESI(+)-MS investigations were carried out employing spectroscopic, HPLC or MS quality solvents. All chemicals and reagents were purchased from Aldrich and used as such. ^1H and ^{13}C NMR spectra were recorded with a JEOL eclipse 400+ spectrometer. Chemical shifts (δ) are given in ppm, and the spectra were recorded in appropriate, deuterated solvents, as indicated. TMS (0 ppm) was employed as standard. The elemental analysis (CHN) for the complexes was performed with a Perkin Elmer 2400 CHN analyzer. Infrared spectra were recorded with a Shimadzu FT-IR 8300 spectrophotometer. The solid sample was prepared in a KBr pellet and spectra were recorded over the frequency range of $400\text{--}4000 \text{ cm}^{-1}$. UV–Vis spectra for all the ligands and copper complexes were recorded in methanol with a UV–Vis Varian, Cary 50 Bio. Full scan mass spectra (MS mode) were obtained with a MicroTOF LC Bruker Daltonics spectrometer equipped with an electrospray source operating in positive ion mode. Samples were dissolved in a MeOH/ H_2O (50/50) solution and were injected in the apparatus by direct infusion. The determination of melting points was made in the Microquímica MQAPF-301 apparatus. The electrical conductivity of solution of each complex ($1 \times 10^{-3} \text{ mol}\cdot\text{L}^{-1}$), in DMF, was measured with a Biocrystal conductometer.

2.2. Synthesis

2.2.1. Synthesis of the ligands

The ligands N-(2-hydroxybenzyl)-N-(2-pyridylmethyl)amine (HL1), N-(2-hydroxybenzyl)-N-(2-pyridylmethyl)[(3-chloro)(2-hydroxy)]-propylamine (H2L2), 1-[2-hydroxybenzyl(2-pyridylmethyl)amino]-3-(1-naphthoxy)-2-propanol (H2L3) and 1-[2-hydroxybenzyl (2-pyridylmethyl)amino]-3-(2-naphthoxy)-2-propanol (H2L4) were synthesized as described in the literature (HL1: [22], H2L2: [23], H2L3 and H2L4: [19]).

2.2.2. Synthesis of $[\text{Pt}^{\text{II}}(\text{HL1})\text{Cl}]$ (1), $[\text{Pt}^{\text{II}}(\text{HL2})\text{Cl}]$ (2) and $[\text{Pt}^{\text{II}}(\text{HL4})\text{Cl}]$ (4)

The cited compounds (Scheme 1) were prepared in reactions between the ligands (HL1, 1 mmol, 214 mg; H2L2, 1 mmol, 307 mg; H2L4, 1 mmol, 414 mg) and $\text{K}_2[\text{PtCl}_4]$ (1 mmol, 415 mg), in ethanol, with constant stirring at room temperature for 2 days. Thereafter, 50 mL of water was added to the solution, which was stirred for another day. After allowing the solution to stand for a few days, a light yellow (complex (1)), a light grey (complex (2)) and a beige solid (complex (4)) were filtered off, washed with cold propan-2-ol and dried in a desiccator. Table 1 shows some data concerning the synthesis and characterization of complexes (1)–(4).

2.2.3. Synthesis of $[\text{Pt}^{\text{II}}(\text{HL3})\text{Cl}]$ (3)

Complex (3) (Scheme 1) was prepared in a reaction between the

Table 1

Yield, elemental analysis (C, H, N), conductivity data (in DMF) and melting point (M.P.) for compounds (1)–(4).

Complex	Composition	Yield (%) / mass (mg)	%C (Found/Calcd)	%H (Found/Calcd)	%N (Found/Calcd)	Λ_{M} ($\text{cm}^2\Omega^{-1} \text{ mol}^{-1}$)	M. P. ($^{\circ}\text{C}$)
(1)	$\text{C}_{13}\text{H}_{15}\text{ClN}_2\text{O}_2\text{Pt}$	62/290	33.47/33.81	3.11/3.27	5.86/6.07	17	295
(2)	$\text{C}_{16}\text{H}_{21}\text{Cl}_2\text{N}_2\text{O}_3\text{Pt}$	32/180	35.98/35.83	3.48/3.38	5.03/5.22	12	265
(3)	$\text{C}_{26}\text{H}_{27}\text{ClN}_2\text{O}_4\text{Pt}$	23/150	46.89/47.17	4.05/4.11	3.97/4.23	18	245
(4)	$\text{C}_{26}\text{H}_{27}\text{ClN}_2\text{O}_4\text{Pt}$	44/290	47.13/47.17	3.98/4.11	4.10/4.23	20	190

ligand H₂L3 (1 mmol, 414 mg) and K₂[PtCl₄] (1 mmol, 415 mg), in ethanol/water 1:1, with constant stirring at room temperature for 24 h. Thereafter, the solution was filtered, rendering a brown solid (small amount) and 50 mL of propan-2-ol was added to the filtrate. After allowing the solution to stand for 6 days light yellow crystals were collected, washed with cold propan-2-ol and dried in a desiccator. Table 1 shows data concerning the synthesis and characterization of complex (3).

2.3. X-ray crystallography

X-ray diffraction data was carried out with a Bruker D8-Venture diffractometer equipped with the detector Photon 100 CMOS using microfocus MoK α ($\lambda = 0,71,073 \text{ \AA}$) X-ray radiation at 150 K. The collect, reduce and integrate data were performed utilizing APEX3 software [24]. Absorption correction was performed by a numerical method implemented in SADABS [25]. The structure was solved by intrinsic phasing [26] and refined by full-matrix least squares on F² with SHELX package [27]. The positions of hydrogen atoms were generated geometrically and refined according to a riding model. All non-hydrogen atoms were refined anisotropically. Selected crystallographic data are summarized in Table 2.

2.4. DFT calculations

Density functional theory calculations were performed in Gaussian 09 [28]. The B3LYP functional was used in conjunction with a mixed basis set consisting of LANL2DZ on platinum and 6-31G(d) on other atoms [29–33]. Solvation in water was modelled with the SMD implicit solvent model [34]. The least squares fit for (3) comparing the calculated and observed X-ray structures were performed using Mercury 3.8. and are shown in Fig. 2 [35]. A conformation search for complexes (3) and (4) was undertaken with Avogrado (V 1.2.0) using the UFF force-field [36,37]. The Cartesian coordinates for the optimized geometries are listed in the Supplementary material, together with the following energies (in Hartree): B3LYP solution-phase electronic energy (E), and B3LYP solution-phase Gibbs free energy at 298.15 K and 1 M (G) and the results of the conformational search.

Table 2
Crystal data and structure refinement for (3).

Empirical formula	C ₂₆ H ₂₅ ClN ₂ O ₃ Pt
Formula weight	644.02
Temperature/K	150.0
Crystal system	Orthorhombic
Space group	P ₂ ₁ 2 ₁ 2 ₁
a/Å	10.5397(19)
b/Å	12.745(2)
c/Å	16.770(3)
α /°	90
β /°	90
γ /°	90
Volume/Å ³	2252.8(7)
Z	4
$\rho_{\text{calc}}/\text{cm}^{-3}$	1.899
μ/mm^{-1}	6.380
F(000)	1256.0
Crystal size/mm ³	0.316 × 0.105 × 0.094
Radiation	MoK α ($\lambda = 0.71073$)
2 θ range for data collection/°	4.014 to 51.374
Index ranges	−12 ≤ h ≤ 12, −15 ≤ k ≤ 15, −20 ≤ l ≤ 20
Reflections collected	35,933
Independent reflections	4288 [R _{int} = 0.0480, R _{sigma} = 0.0291]
Data/restraints/parameters	4288/0/299
Goodness-of-fit on F ²	1.111
Final R indexes [I ≥ 2 σ (I)]	R ₁ = 0.0198, wR ₂ = 0.0389
Final R indexes [all data]	R ₁ = 0.0237, wR ₂ = 0.0405
Largest diff. peak/hole/e Å ^{−3}	1.52/−0.63
Flack parameter	−0.009(4)

2.5. Antitumor activity

2.5.1. Culture of cells

Human leukemia cell lines THP-1 (acute monocytic leukemia cell line) and U937 (histiocytic lymphoma cell line), Molt-4 (acute lymphoblastic), Colo205 (human colon adenocarcinoma) and H460 (lung carcinoma) were cultured routinely in DMEM-F12 medium (Dulbecco's Modified Eagle Medium) (Gibco, BRL) supplemented with 10% fetal calf serum and gentamicin (20 $\mu\text{g}\cdot\text{mL}^{-1}$, Gibco, BRL) at 37 °C in a humidified atmosphere containing 5% CO₂ in air. Culture media were changed every 2–3 days. Blood samples were collected from healthy donors in Sodium Heparin glass tubes "Vacutainer™" (Becton Dickinson) and the PBMC (peripheral blood mononuclear cells) isolated over Ficoll-Paque™ Plus (1.08 $\text{g}\cdot\text{mL}^{-1}$) in a 50 mL conical tube (2:1 - blood:ficoll). Twenty milliliters of fresh heparinized blood sample were diluted in phosphate buffer saline (PBS), gently laid over 10 mL of Ficoll and centrifugated at 500 × g for 20 min at 25 °C. PBMC were collected from the interface of spun blood samples and were washed three times with PBS by centrifugation at 500 × g for 10 min at 4 °C. The supernatant was discarded and the cells were suspended in DMEM-F12 medium (Gibco, BRL). Trypan blue solution 0.4% (Sigma, Germany) was used to count the cells into an appropriate concentration and the viability of cells was checked; the required range of cells' viability is 95–99%.

2.5.2. Cell viability studies using the colorimetric MTT assay

The viability of the cells lines incubated with the platinum(II) complexes was evaluated by a MTT assay, as described by Mosman [38]. Tumoral and normal cells (THP-1, U937, Molt-4, Colo205, H460 and PBMC, respectively) were plated in 96-well plates at densities of 1 × 10⁶ cells·mL^{−1}, and different concentrations of the Pt(II) coordination complexes (100, 50, 25, 12.5 and 6.5 μM) were added to the culture and maintained for 36 h at 37 °C. Previously, stock solutions of the platinum(II) complexes and ligands were prepared in DMSO (dimethyl sulfoxide) (2 × 10^{−2} M). Stock solutions of metallic salt and cisplatin were prepared in deionized water. In order to reach the desired concentrations, the stock solutions were diluted in DMEM-F12 medium (Gibco, BRL). Twenty microliters of 3-(4,5-dimethyl-2-thiazyl)-2,5-diphenyl-2H-tetrazolium bromide (MTT) stock solution (5 mg mL^{−1}) were added into each well, containing 100 μL of complex, and the cells were incubated at 37 °C for 4 h. The formazan crystals were dissolved in acidic isopropanol and their absorbance was determined at 570 nm using a microplate reader (Thermo Labsystems Multiskan, 352 model). Each concentration was tested in three independent experiments run in triplicate. IC₅₀ values were obtained from dose-response curves using GraphPad Prism 5.0 for Windows. Cisplatin (Sigma) was used as a positive control.

2.5.3. Measurement of Annexin V and propidium iodide staining

U937 were cultured at 1 × 10⁶ cells·mL^{−1} in 24 multiwell plates and treated with 22 μM of complex (3) for 24 h. Apoptosis was detected by using Annexin V-FITC Apoptosis Detection Kit. Briefly, after incubation, cells were washed twice with phosphate buffered saline (PBS) and incubated in 500 μL of binding buffer (100 mM HEPES/NaOH, pH 7.5, 1.4 M NaCl and 25 mM CaCl₂). To each sample, 5 μL of Annexin V-FITC and 10 μL of PI were added. Samples were incubated at room temperature for 10 min protected from light. Cell fluorescence was determined immediately with a flow cytometer (FACS Calibur-BD Sciences). The result was determined by recording 10,000 events per sample.

2.5.4. Study of cell cycle arrest by flow cytometric analysis

Cells were plated at 1 × 10⁶ cells·mL^{−1} in 24 multiwell plates and treated with complex (3) (22 μM) for 24 h in DMEM-F12 medium (Gibco, BRL). The incubated cells were then fixed in 70% ethanol at 4 °C for 30 min. Cells were stained with propidium iodide (PI) for 2 h in

darkness. The DNA content was measured by flow cytometer (FACS Calibur-BD Sciences) and cell cycle distribution was analyzed by WinMDI version 2.9 software. The proportions of cells in G₀/G₁, S, and G₂/M phases were represented as DNA histograms. Apoptotic cells with hypodiploid DNA content were measured by quantifying the sub-G₁ peak in the cell cycle pattern. The result was determined by recording 10,000 events per sample.

2.5.5. Analysis of mitochondrial membrane potential ($\Delta\Psi_m$) by flow cytometry using JC-1 stain

U937 cells were seeded at 1×10^6 cells mL⁻¹ in 24-well plate and treated with complex (3) (22 μ M) for 24 h in DMEM-F12 medium (Gibco, BRL). After the elapsed time, the cell suspension was transferred to a sterile tube and pelleted (400 \times g, for 7 min, at room temperature). Cells were stained with JC-1 dye (25 μ g mL⁻¹) and incubate at 37 °C in a 5% CO₂ incubator for 15 min. The cells were washed twice with fresh medium and analyzed immediately by flow cytometry. JC-1 (5,5',6,6'-tetrachloro-1,1',3,3' tetraethylbenzimidazolylcarbocyanine iodide) exists as a monomer in the cytosol (green) and also accumulates as aggregates in the mitochondria which stain red. In contrast, in apoptotic and necrotic cells, JC-1 exists in monomeric form and stains the cytosol green. Mitochondria containing red JC-1 aggregates in healthy cells are detectable in FL2 channel and express intact mitochondrial membrane potential ($\Delta\Psi_m$), whereas green JC-1 monomers in apoptotic cells are detectable in FITC channel (FL1) and express loss of ($\Delta\Psi_m$). The Mitochondria transmembrane potential ($\Delta\Psi_m$) was measured by flow cytometer (FACS Calibur) and was analyzed by WinMDI version 2.9 software.

2.5.6. Transmission electron microscopy (TEM) and scanning electron microscopy (SEM)

For TEM analysis, U937 cells were incubated with complex (3) at a concentration of 11 μ M and after 4, 8 and 12 h of incubation the cell suspension was centrifuged at 100 \times g for 10 min, washed three times with phosphate-buffered saline (PBS; pH 7.2) and fixed by 2 h in 2.5% Glutaraldehyde, in 0.1 M sodium cacodylate buffer, post-fixed for 20 min in 1:1 solution osmium tetroxide (1%) and potassium ferricyanide (0.8%). For transmission electron microscopy, cells were dehydrated sequentially in a graded series of acetone (50–100%), and embedded in Epoxy resin (Poly/Bed® 812). Resin-embedded cells were placed in a silicon mold form well at 60 °C for 48 h for polymerization. The obtained blocks were sectioned and ultrathin sections (70 nm thick) were taken using an ultra microtome Reichert Ultracut S, collected on copper grids (400 mesh), stained with uranyl acetate and lead citrate, and observed in a Transmission Electron Microscope, TEM-900 (Zeiss, Germany). For SEM analysis, the cells were incubated with platinum complex in the concentration of 11 μ M for 8 and 12 h. Fixed cells were dropped onto poly-L-lysine (Sigma®) precoated coverslips, post-fixed for 30 min. in 1:1 solution osmium tetroxide (1%) and potassium ferricyanide (0.8%), dehydrated sequentially in a graded series of alcohol (50–100%), and critical-point dried (Bal-Tec CPD 030 Critical Point Dryer) with CO₂. The samples were mounted on a stub of metal with adhesive, coated with 40–60 nm of metal such as Gold/Palladium (Sputter Coater SDC 050) and viewed in a Scanning Electron Microscope (JSM 6610 LV).

2.5.7. Determination of caspase activities

Caspases 3, 6, 8 and 9 activities were determined using the substrates VDVAD-pNA or DEVD-pNA (caspase 3 substrate), VEID-pNA (caspase 6 substrate), IETD-pNA (caspase 8 substrate), and LEHD-pNA (caspase 9 substrate) following the protocols of the Caspase Activity Assay kit from Invitrogen™ (ApoTarget™ caspase colorimetric protease assay kit). U937 cells ($3\text{--}5 \times 10^6$ mL⁻¹) were incubated with 22 μ M of complex (3) for 3 h and centrifuged at 400 \times g for 10 min. The supernatant was removed, and the pellet was suspended in 0.1 mL of lysis buffer and incubated on ice for 10 min followed by centrifugation at

10,000 \times g for 1 min. Protein concentrations were determined and cytosol extracts were diluted to a concentration of 50–200 μ g protein per 50 μ L cell lysis buffer (1–4 mg mL⁻¹). Aliquots (50 μ L) of the supernatant were removed and placed in a 96-well microplate containing reaction buffer (Invitrogen™). 5 μ L of each substrate was added, and the microplate was incubated at 37 °C for 12 h. Activity was monitored as the cleavage and release of free pNA and quantified at 450 nm using a Microplate spectrophotometer (Epoch™, BioTek® Instruments, Inc.). Caspase activation of treated cells was compared with an uninduced control sample for the determination of the increase in caspase activity.

3. Results and discussion

3.1. Syntheses and structure of platinum(II) coordination compounds

The ligands H2L3 and H2L4 were designed to increase the anti-tumor activity of coordination compounds by adding naphthyl groups to the structure of the ligand HL1. This strategy proved to be successful previously where an increase in the antitumor activities for the analogous copper(II) and cobalt(III) complexes were reported [19,20]. As platinum(II) is an ion related to cisplatin, we decided to synthesize new platinum(II) compounds, containing the ligands HL1-H2L4, in order to investigate the effect of the naphthyl groups on the antitumoral activity of these compounds. The reactions between the ligands HL1-H2L4 and the platinum(II) salt K₂[PtCl₄] resulted in pale colored compounds with average yield of 35%. The interaction between the ligand H2L3 and the Pt(II) salt appeared to be the most efficient. Table 1 shows that all the complexes were obtained in high purity and the conductivity suggested that they are neutral species. All four complexes are stable in air and soluble in polar solvents such as DMF, DMSO and slightly soluble in CH₃CN, ethanol, MeOH and chloroform.

3.2. Description of crystal structure of complex (3)

The compound (3) crystallizes in a non-centrosymmetric space group with one mononuclear platinum(II) complex per asymmetric unit. The Flack parameter was refined [−0.009(4)] indicating the occurrence of enantiopure crystal [39]. A perspective view of the molecule is displayed in Fig. 1. The relevant bond lengths and angles for complex (3) are listed in Table 3. In complex (3) the platinum(II) centre is coordinated by a σ -N₂OCl donor set provide by the ligand H2L3 via one amine nitrogen atom (N2), one pyridine nitrogen atom (N1), one phenolic oxygen atom (O1) and one chloro ligand (Cl1), resulting in a tetracoordinated platinum(II) complex. The geometry for Pt(II) complex is described as distorted square-planar. The presence of the deprotonated phenol group (O1) coordinated to the Pt(II) centre indicates greater Lewis acidity of the Pt(II) centre in complex (3) when compared with the previously reported copper(II) complexes containing the same ligand, in which the phenol group is protonated [19]. Similarly, in the Co(II) complex previously reported, containing the same ligand, the phenolic oxygen is deprotonated [20]. The H2L3-metal bond lengths are slightly longer in the platinum compound than in cobalt and copper complexes, as an effect of the ionic radius presented by the metal ions.

3.3. DFT study

While the X-ray structure for (3) is known the structures of the other three complexes were not available. In order to gain further understanding of the probable structures of (1), (2) and (4) DFT calculations were employed using the known X-ray structural parameters for (3). An implicit solvent (water) model was included in order to mimic the medium employed in the biological studies. An initial trial showed that the methodology was able to reproduce the structural parameters around the square planar platinum(II) centre (Fig. 2) and orientation of the side-chain in (3); structural overlays (least squares fits) for this complex comparing the experimental (solid-state) and simulated (in

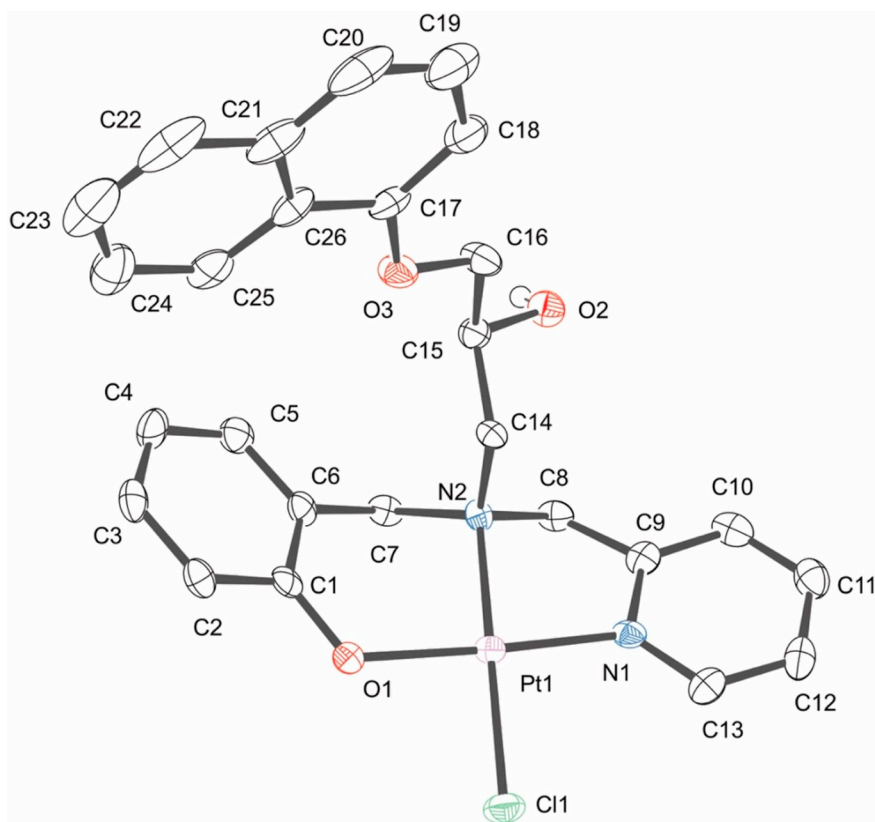


Fig. 1. View of the ORTEP-3 projections for complex (3) and the corresponding atom labeling scheme. Ellipsoids are shown at the 40% probability level.

Table 3

Selected bond and lengths (Å) and angles (°) for complex (3).

Pt1	Cl1	2.2909(15)	
Pt1	O1	2.007(4)	
Pt1	N2	2.055(5)	
Pt1	N1	2.002(5)	
O1	Pt1	Cl1	85.69(12)
O1	Pt1	N2	95.13(17)
N2	Pt1	Cl1	177.47(14)
N1	Pt1	Cl1	96.27(13)
N1	Pt1	O1	176.58(17)
N1	Pt1	N2	83.03(18)

water) structures are shown in Fig. 2. Based on the ability of the calculations to reproduce the structure of (3), the structures of complexes (1), (2) and (4) were calculated, again assuming the implicit solvent (water) model. For each of the complexes (1), (2) and (4) the known structure of (3) was modified using Avogadro [36] to accommodate the different side chains and the resulting Cartesian coordinates employed as input for the DFT calculations. The resulting structures are shown in Fig. 2. These calculations are not expected to represent the only possible structure of complexes (1), (2) and (4) in the biological medium. While the metal centre and tridentate ligand would be relatively rigid, the side chain is expected to have many possible conformations. The decision to focus only on a single conformation in the DFT study was made in order to examine how closely the DFT calculations were able to reproduce the structure of the complex in the region of the platinum centre. For complex (3), where the X-ray structure is available, the direct comparison shows that the calculations do show a close agreement between the X-ray crystal and DFT calculated structures. Therefore, the calculations are expected to reliably characterize the ML₄ centre of the other complexes. In terms of the enhanced antitumoral activity exhibited by complexes (3) and (4), the orientations of the α

and β naphthyl groups are clearly of most interest. Several orientations of these naphthyl groups are possible and in order to probe this further, conformational studies were undertaken with complexes (3) and (4). For each complex a UFF conformer search revealed 26 low energy conformers [36,37]. The five or six lowest energy conformers are given in the Supplementary material. For (3) the spread of energies calculated for the five lowest energy conformers was 2.6 kcal/mol; all five of these would therefore be expected to be present at room temperature. One of these conformers corresponded to the conformer utilized in the DFT calculation (*i.e.* the one in the X-ray structure). For (4) the energy of the six most stable conformers differed by < 1.6 kcal/mol, the first five being practically identical in energy. The orientation of the naphthyl group in conformer 6 was equivalent to the structure utilized in the DFT calculation above. The calculations support the idea that the side chains of these complexes are flexible and multiple orientations of the α and β naphthyl groups are possible.

3.4. Infrared

Table 4 presents the characteristic IR bands of HL1-H2L4 ligands and their respective Pt(II) complexes. The IR spectra of complexes (1)–(4) were analyzed in comparison with those of their free ligands. For all the complexes, the main bands showed small shifts when compared to the respective free ligands (Table 4). The bands related to ν_{C-H} and $\nu_{C=N}$ exhibited downward (lower energy) after coordination to platinum(II) salt. The phenol group is deprotonated and it is coordinated to the platinum(II) centre as phenolate, as indicating by the absence of the bands at 1380, 1374, 1364 and at 1364 cm^{-1} , present in the ligands HL1-H2L4, respectively, attributed to δ_{OH} [20].

Based on the output from the DFT the calculated vibrational frequencies have been compared with the known infrared data for the four complexes. The resultant spectra are shown in the Supplementary material (Figs. S1–S4). The agreement between the calculated and

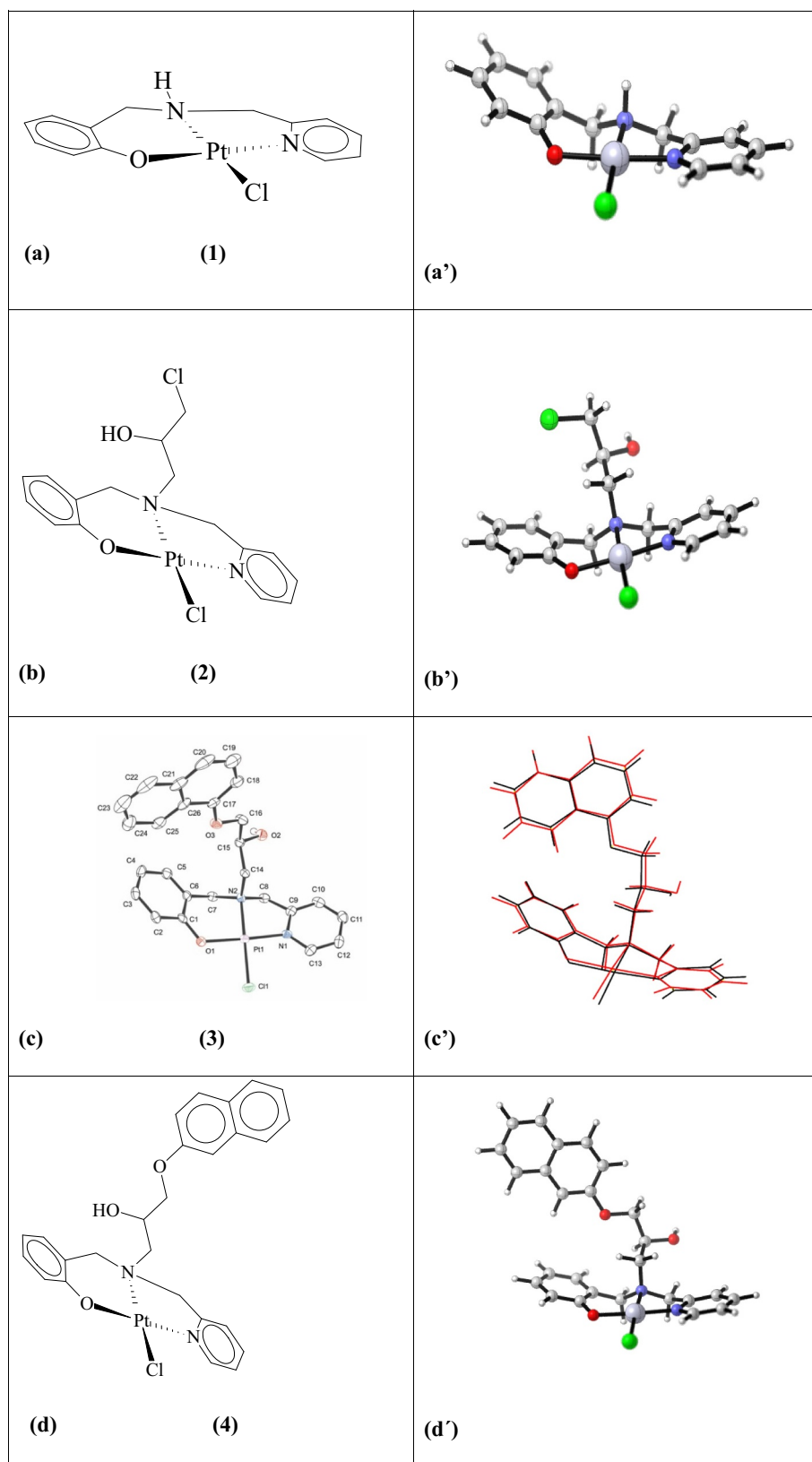


Fig. 2. Comparison of the proposed structures of (a) (1), (b) (2) and (d) (4) and (c) ORTEP picture of (3) with the calculated structures for (a') (1), (b') (2) and (d') (4). For complex (3), an overlay of the calculated structure (black) with the X-ray (red) is presented in (c').

Table 4
Characteristic IR bands (cm^{-1}) of the ligands HL1–H2L4 and their respective platinum(II) complexes.

Assignment	(1)	(2)	(3)	(4)
$\nu_{\text{C-H aromatic}}$	3088 (3032)	3088 (3053)	3069 (3053)	3073 (3053)
$\nu_{\text{C=N}}$	1595 (1595)	1599 (1581)	1598 (1569)	1599 (1569)
$\nu_{\text{C=C}}$	1450 (1438)	1452 (1458)	1445 (1449)	1448 (1449)
$\delta_{\text{(pyridine ring)}}$	767 (754)	769 (756)	762 (769)	758 (769)
$\delta_{\text{(OH-phenol)}}$	– (1380)	– (1374)	– (1364)	– (1364)

Data in parenthesis are related to the respective ligand.

experimental spectra is remarkably good, although further comparative structural information, other than the presence of the expected functional groups, would be speculative.

3.5. ESI(+)-MS and ESI(+)-MS/MS

ESI(+)-MS and ESI(+)-MS/MS of complexes (1)–(4) present a characteristic set of isologue ions due mainly to the presence of metal and Cl atoms. For complex (1), the ESI(+)-MS data indicate the presence of peaks with m/z 426, 445, 516, 622, 659 and 851, revealing the presence of five mononuclear cations and one binuclear cation (m/z 851). The peaks with m/z 426, 445, 622, 659 and 851 are ascribed to the species $[\text{Pt(II)(L1)(H}_2\text{O)}]^+$, $[\text{Pt(II)(HL1)(Cl)}]^+$, $[\text{Pt(II)(L1)(HL1)}]^+$, $[\text{Pt(II)(HL1)}_2(\text{Cl})]^+$ and $[(\text{OH})\text{Pt(II)(}\mu\text{-L1)}_2\text{Pt(II)(H}_2\text{O)}]^+$. The peak with m/z 516 contains a fragmented ligand HL1 coordinated to the Pt(II) centre. For complex (2), the ESI(+)-MS data indicate the presence of peaks with m/z 501, 537, 549, 575 and 1037, revealing the presence of five mononuclear complexes and one binuclear complex in (m/z 1037). The peaks with m/z 501, 537, 549 and 575 are ascribed to the species $[\text{Pt(II)(L2)}]^+$, $[\text{Pt(II)(HL2)(Cl)}]^+$, $[\text{Pt(II)(HL2)(H}_2\text{O)(formaldehyde)}]^+$, $[\text{Pt(II)(KL2)(Cl)}]^+$ and $[(\text{L2})\text{Pt(II)(}\mu\text{-Cl)Pt(II)(L2)}]^+$. These proposals are based on MS/MS data, which indicate that the species with m/z 1037 yields the cation with m/z 501, by the loss of a neutral molecule of 536 Da, described as a neutral complex $[\text{Pt(II)(L2)(Cl)}]$. For complex (3), the ESI(+)-MS data indicate the presence of peaks with m/z 542, 608, 1158 and 1251, revealing the presence of two mononuclear and two binuclear complexes (m/z 1251 and 1158). The peaks with m/z 608 and 1251 are ascribed to the species $[\text{Pt(II)(HL3)}]^+$ and $[(\text{HL3})\text{Pt(II)(}\mu\text{-Cl)Pt(II)(HL3)}]^+$. The peaks with m/z 542 and 1158 contain fragmented ligand coordinated to the Pt(II) centre. These proposals are based on MS/MS data, which indicate that the species with m/z 1251 yields the cation with m/z 1158, by the loss of a neutral molecule of 93 Da. The species with m/z 1251 also yields the cation with m/z 608 $[\text{Pt(II)(HL3)}]^+$, by the loss of a neutral molecule of 643 Da, ascribed as $[\text{Pt(II)(HL3)Cl}]$. For complex (4), the ESI(+)-MS data indicate the presence of peaks with m/z 415, 608, 916, 1022 and 1059, revealing the presence of four mononuclear species (m/z 608–1059). The peak with m/z 415 is ascribed to the protonated ligand $[\text{H3L4}]^+$. The peaks with m/z 608, 1022 and 1059 are ascribed to the species $[\text{Pt(II)(HL4)}]^+$, $[\text{Pt(II)(H2L4)(HL4)}]^+$ and $[\text{Pt(II)(H2L4)(Cl)}]^+$. The peak with m/z 916 contains fragmented ligand coordinated to the Pt(II) centre. These proposals are based on MS/MS data, which indicate that the species with m/z 1022 yields the cation with m/z 415, by the loss of a neutral molecule of 607 Da, ascribed as $[\text{Pt(II)(L4)}]$. Figs. S5–S8 shows the proposals for the main peaks presented in the ESI(+)-MS spectrum of complexes (1)–(4).

3.6. Assessment of cell viability by MTT assay

The cytotoxicity against cancer cell lines (Colo-205, H460, THP-1, U937 and Molt-4) were determined by means of the colorimetric MTT assay and the IC_{50} values were calculated in order to identify the more cytotoxic compounds and then to carry out studies related with the cell death mechanism. For a comparison of cytotoxicity, the compounds

Table 5

The 50% inhibitory concentration (IC_{50}) for the platinum complexes and their respective ligands, as well as $\text{K}_2[\text{PtCl}_4]$ and cisplatin, for leukemia (THP-1 U937 and Molt-4), colon (Colo-205), lung (H460) cancer cell lines and PBMC.

Compound	IC_{50} (μM)					
	Colo-205	H460	U937	THP-1	Molt-4	PBMC
HL1	> 100	> 100	> 100 ^a	> 100 ^a	> 100 ^a	–
H2L2	> 100	> 100	> 100	> 100	> 100	–
H2L3	> 100	> 100	28 ± 2	68 ± 2	43 ± 1	> 100
H2L4	> 100	> 100	> 100	> 100	> 100	> 100
$\text{K}_2[\text{PtCl}_4]$	> 100	> 100	> 100	> 100	> 100	–
(1)	> 100	> 100	72 ± 2	> 100	> 100	–
(2)	> 100	> 100	> 100	> 100	> 100	–
(3)	30 ± 2	51 ± 1	11 ± 1	6 ± 1	9 ± 1	22 ± 1
(4)	38 ± 2	78 ± 1	15 ± 2	20 ± 1	11 ± 2	42 ± 1
Cisplatin	41 ± 2	> 100	8 ± 1 ^a	10 ± 1 ^a	6 ± 1 ^a	44 ± 2

^a [40].

were also tested against peripheral blood mononuclear cells (PBMCs). Cisplatin, the prototype of many metal-based drugs, was also evaluated and included in some experiments as positive control for cell death. As presented in Table 5 the IC_{50} values were evaluated from the concentration dependence of viable cells 36 h after exposure to the platinum(II) compounds. As controls, we also tested the cytotoxic effects of the salt ($\text{K}_2[\text{PtCl}_4]$) and the ligands HL1–H2L4. Table 5 shows that, in general, complexes (3) and (4) are the most cytotoxic compound for all of the cell lines investigated, showing the effect of the presence of the naphthyl groups. Comparing the IC_{50} values for complex (3), (4) and their respective ligands (H2L3 and H2L4, respectively), complex (3) is slightly more cytotoxic than complex (4) against Colo-205, U937 and Molt-4. It is worth noting that complex (3) is more active than complex (4) against the H460 cell line ($\text{IC}_{50} = 51 \pm 1$ and $78 \pm 1 \mu\text{M}$, respectively) and THP-1 (6 ± 1 and $20 \pm 1 \mu\text{M}$, respectively). It is important to note that for the H460 cell line (lung cancer), cisplatin is not active, resulting in $\text{IC}_{50} > 100 \mu\text{M}$. Complexes (3) presents IC_{50} values lower than cisplatin toward Colo205 (30 and 41 μM , respectively), H460 (51 and $> 100 \mu\text{M}$, respectively), THP-1 (6 and 10 μM , respectively) and comparable to cisplatin toward U937 (11 and 8 μM , respectively) and Molt-4 (9 and 6 μM , respectively) cell lines. The greater cytotoxicity of complex (3) could be related to the ligand, since H2L3 is the most active ligand of this investigation, presenting IC_{50} values of 28 ± 1 , 68 ± 1 and $43 \pm 1 \mu\text{M}$ against U937, THP-1 and Molt-4 cells line, respectively. The low IC_{50} values indicate greater susceptibility of the leukemia cell lines U937, THP-1 and Molt-4 toward complexes (3) and (4) than to cell lines Colo-205 and H460, since leukemia cell lines are more sensitive than Colo-205 and H460. Similar results were obtained for cisplatin. Complexes (3) and (4), which contain naphthyl groups in their structures, presented IC_{50} values of 22 ± 1 and $42 \pm 1 \mu\text{M}$ against PBMC. The value obtained for complex (2) is comparable to that determined for cisplatin ($44 \pm 1 \mu\text{mol L}^{-1}$). Complexes (3) and (4), which contain naphthyl in their structures, presented IC_{50} values of 22 ± 1 and $42 \pm 1 \mu\text{M}$, respectively, against PBMC. Complex (4) exhibits a IC_{50} value comparable to cisplatin ($44 \pm 1 \mu\text{M}$) against PBMC, suggesting that complex (4) is a promising complex, since presents lower IC_{50} value than cisplatin toward H460 (78 ± 1 and $> 100 \mu\text{M}$) and comparable IC_{50} values toward Colo-205, U937, THP-1, Molt-4 and PBMC.

3.7. Mechanistic studies of cell death

Based on the cytotoxicity assessment presented in Table 5 complexes (3) and (4) were selected to investigate the mechanism by which they induce cell death in cancer cells. Therefore, we decided to investigate the mechanism by which complexes (3) and (4) induce cell death in the U937 cell line, in order to examine the effect of the

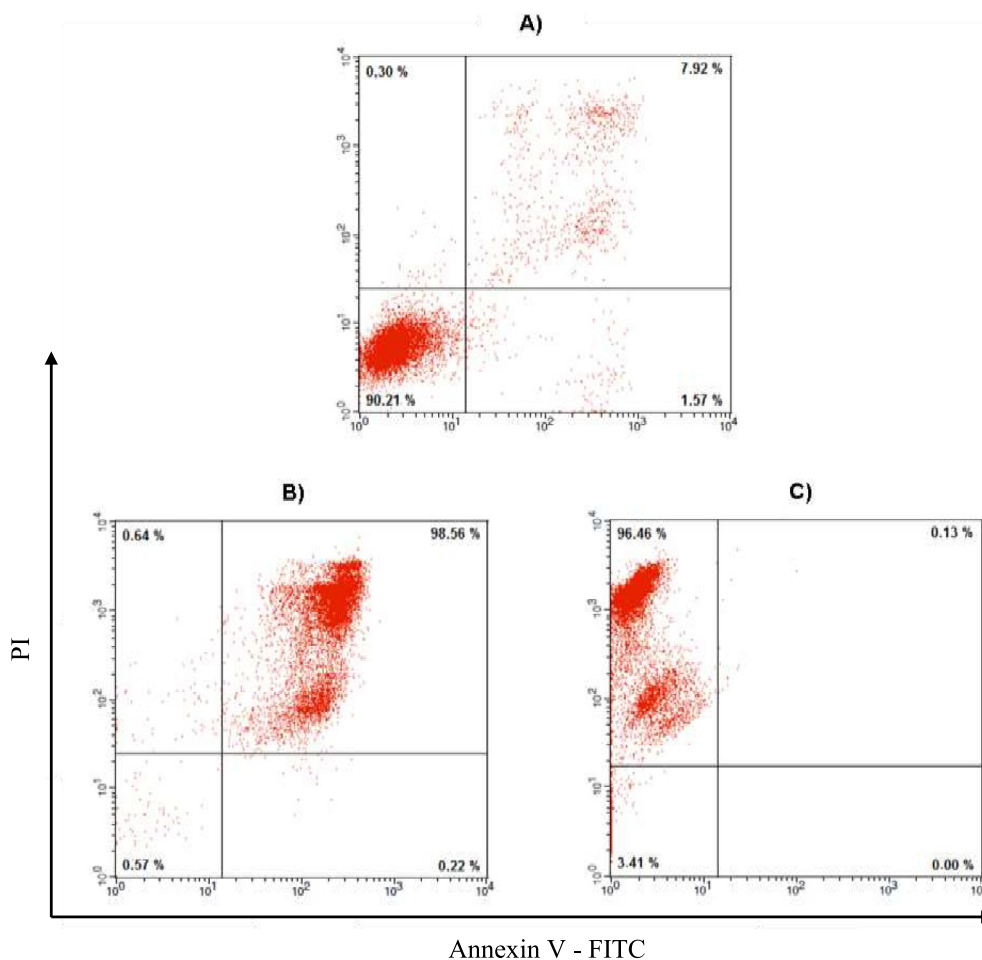


Fig. 3. Annexin V-FITC/PI staining detected apoptosis induced by complexes (3) and (4) in U937 cells, after treatment for 24 h. A) Control. B) U937 cells after treatment at the concentration of 22 μM of complex (3). C) U937 cells after treatment at the concentration of 30 μM complex (4). The data are presented in dot blots depicting Annexin V/FITC versus PI staining. The percentage of cells in each quadrant is presented.

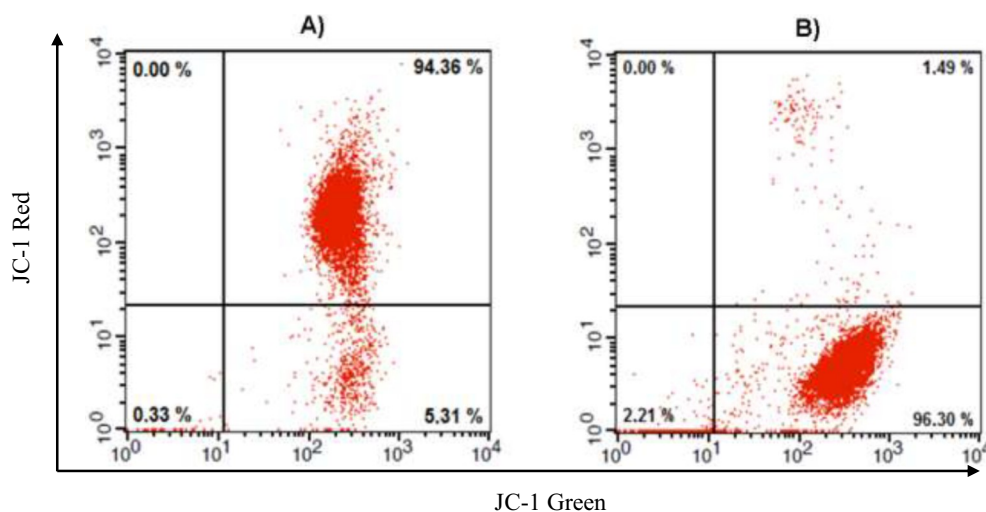


Fig. 4. Mitochondrial transmembrane potential ($\Delta\Psi\text{m}$) assay. U937 cell line was incubated with 22 μM of complex (3) for 24 h. After being stained with JC-1, cells were analyzed by flow cytometry. Upper right quadrant - normal cells and lower right quadrant- loss of mitochondrial $\Delta\Psi\text{m}$. A) Control cells. B) Cells after treatment with complex (3).

isomerism on the biological activity and compare these findings with those previously reported for Cu(II) and Co(II) complexes, containing the same ligands [19,20]. The first investigation was carried out by the measurement of apoptosis by Annexin V-FITC/PI analysis. Complex (3) showed high apoptosis rate (96%), the same value for cisplatin. However, complex (4) showed high necrosis rate (96%), after 24 h of treatment. Based on the results, the function of complex (3) in apoptosis

was further investigated by analysis of mitochondrial membrane potential ($\Delta\Psi\text{m}$), flow cytometric analysis of cell cycle arrest, transmission electron microscopy (TEM) and scanning electron microscopy (SEM).

3.7.1. Measurement of apoptosis by Annexin V-FITC/PI analysis

In order to confirm and quantify the extent of apoptosis, a double-

labeling technique using Annexin V-FITC and propidium iodide (PI) was utilized. In the flow cytometer dot plot cytogram analysis (Fig. 3) the lower left quadrant (negative for Annexin V and PI) is regarded as the population of live cells (normal), the one in the lower right quadrant (positive for Annexin V and negative for PI) illustrates the cell population at the early apoptosis stage, while the upper right quadrant (positive for Annexin V and PI) and the upper left quadrant (negative for Annexin V and positive for PI) represents the cell population at the late apoptosis stage and the necrotic cell population, respectively. Fig. 3 shows that after 24 h of treatment with 22 μM of complexes (3), 30 μM of complex (4) and the control. For the control (Fig. 3A), 90.21% of U937 are ascribed as normal cells and 7.92% were in upper right quadrant (late apoptotic stage). For the treatment with complex (3), (Fig. 3B) 98.56% were in upper right quadrant (late apoptotic stage) while for complex (4) (Fig. 3C) 96.46% were in the upper left quadrant, suggesting death by necrosis. As a positive control, U937 cells were incubated with 50 μM cisplatin and 29.8% of apoptotic cells were observed, suggesting that complex (3) was more effective than cisplatin (Fig. S9). So, based on these results, we decided to continue our investigation about the mechanism associated with the inhibition of U937 cell lines only promoted by complex (3), since this complex effectively induces apoptosis in these cells.

3.7.2. Analysis of mitochondrial membrane potential ($\Delta\Psi\text{m}$)

As shown in Fig. 4, control cells of U937 show a strong red fluorescence (94.36%) after staining with JC-1. Following treatment of U937 cells with complex (3), for 24 h, the red fluorescence decreased to 1.49% (Fig. 4B). The lower right quadrant represents the cells with the loss of mitochondria $\Delta\Psi\text{m}$ indicating mitochondrial damage. The negative control and the treatment with complex (3) show 5.31 and 96.30% of cells in these quadrants, respectively. Positive control, treatment of U937 cell with cisplatin result in 88.04% of cell $\Delta\Psi\text{m}$ loss (Fig. S9). Our result shows that the treatment with complex (3) generates damage on mitochondria and suggests the involvement of intrinsic pathway of apoptosis.

These results are in good agreement with those obtained from MTT assay (Table 5) and indicate that the cytotoxicity of complex (3) against U937 cell line is mediated *via* apoptosis, which is directly related to mitochondrial dysfunction. The loss of mitochondrial potential is believed to occur through the formation of pores in the mitochondria.

3.7.3. Cell cycle analysis by flow cytometry

The relative cellular DNA content and distribution during the cell cycle was determined by flow cytometry (Fig. 5). In this study, U937 cells were incubated with complex (3) by 24 h and the results

demonstrate the population of U937 cells in each phase of the cell cycle. The G1 phase, also called growth phase as it ensures that the cell is primed for DNA synthesis, plays a crucial role in cell cycle progression. As shown in Fig. 5, the population of U937 cells in the G1 phase changed from 44.64 in the control to 7.38% after treatment with complex (3). It is also worthwhile noting that the population of cells in the sub-G1, increased significantly upon the treatment with complex (3), resulting in change from 7.38 to 61.38%. Cisplatin positive control, U937 cell sub-G1 population increases from 0.26 to 89.52% after drug administration (Fig. S9). The increase of cell sub-G1 population corresponds to cell whose DNA has been cleaved by cellular nucleases that were activated by the apoptotic machinery. Thus, our results clearly show that complex (3) induces cell death by apoptosis. Furthermore, these results are in agreement with previous studies carried out with copper(II) and cobalt(II) complexes, obtained with the same ligand. These complexes promoted a decrease from 60% to 17% and from 60% to 20%, respectively, for copper(II) and cobalt(II) complexes, in the population of U937 cells in the G1 phase, after treatment with these complexes. The population of cells in the sub-G1, for treatment with these complexes increases significantly resulting in change from 0.2 (control) to 48% and from 7.73% to 83.56% after treatment with copper(II) and cobalt(II) complexes respectively.

3.7.4. Analysis of cell morphology by transmission electron microscopy (TEM) and scanning electron microscopy (SEM)

The cytotoxic effect of complex (3) (11 μM and time intervals of 4, 8 and 12 h) on the surface and the ultrastructural features on U937 cells was investigated by TEM and SEM. Representative images are presented in Figs. 6 and 7, respectively. U937 cells from the control group present a homogenous cytoplasm, with few and small regular mitochondria (M). Some endoplasmic reticulum (ER) profiles as seen, indicating good cell status (Fig. 6A).

Transmission electron micrographs show that complex (3) causes changes in U937 cells by a time-dependent process, which presents apoptotic morphological patterns and initially targets the mitochondria. Fig. 6B shows the alterations after 4 h, Fig. 6C after 8 h and Fig. 6D after 12 h of treatment, respectively. As depicted in Fig. 6B, a significant increase in the number and size of the mitochondria is observed. Complex (3) induces alterations in the mitochondria, which present more rarefied mitochondrial matrix and changes in the arrangement of the mitochondrial ridges. After 8 h of treatment (Fig. 6C), the formation and releasing of elements like apoptotic bodies (A) can be clearly seen. Some of these apoptotic bodies present endoplasmic reticulum profiles and vacuoles. More elongated endoplasmic reticulum profiles (ER) and mitochondria (M) are seen in the cytoplasm. After 12 h of treatment

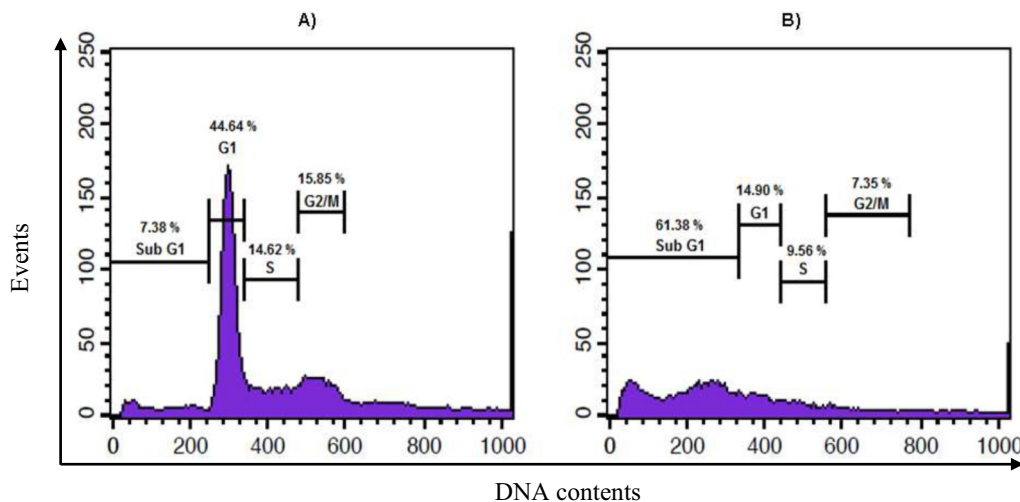


Fig. 5. Cell Cycle Analysis by Flow Cytometry. Leukemic cell line (U937) was stained with propidium iodide (PI) after 24 h of incubation without (control) and with complex (3). Cells with hypodiploid DNA content were measured by quantifying the sub-G1 peak in the cell cycle pattern. Each experiment per sample was determined recording 10,000 events. A) Control cells; B) cells after treatment with 22 μM of complex (3).

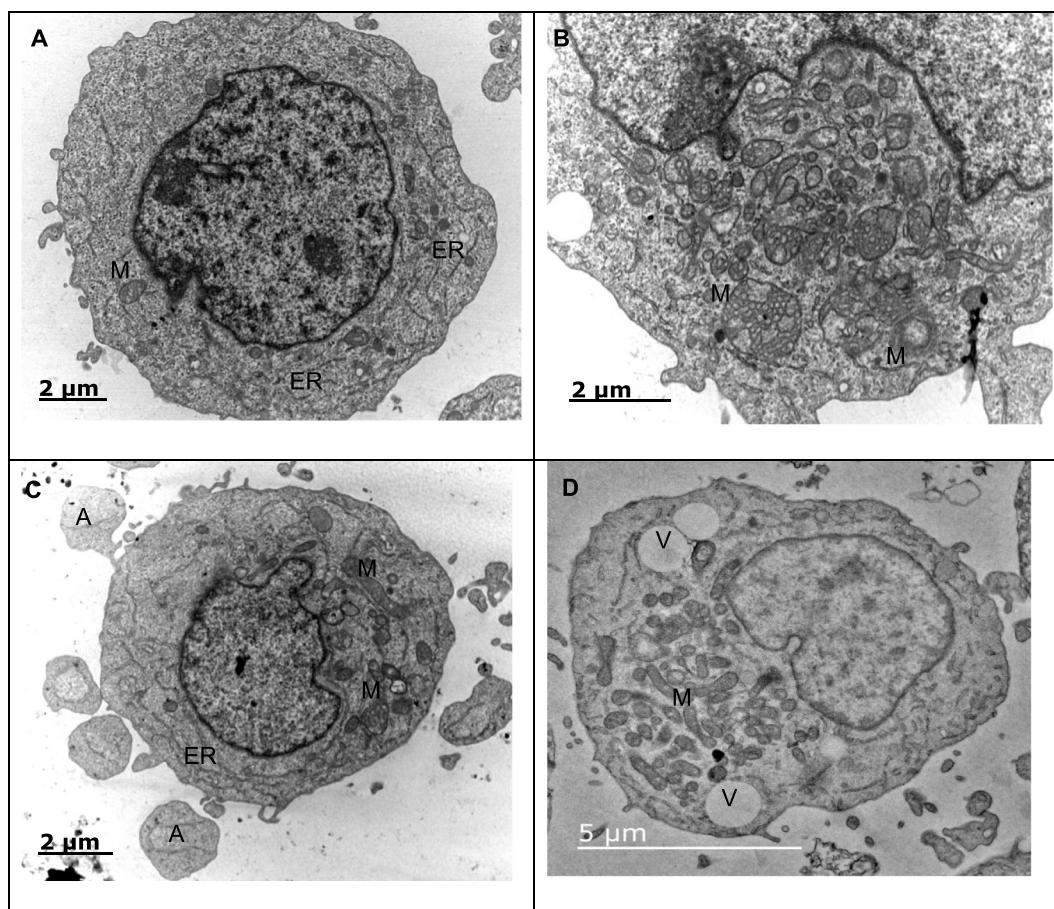


Fig. 6. Transmission Electron Microscopy of human leukemia cells. (A) Control cells, (B) U937 cell strain incubated with 11 μM of complex (3) for 4 h. Altered mitochondria [M] can be seen. (C) U937 cell line incubated for 8 h. Release of apoptotic bodies [A] can be seen at the cell periphery. Elongated endoplasmic reticulum [ER] and altered mitochondria [M] are also visible (D) U937 cell line incubated for 12 h, showing a great number of mitochondria [M] and cytoplasmic vacuoles [V].

with complex (3) (Fig. 6D), cytoplasm appears more rarefied. In some cells large vesicles and a diffuse cytoplasmic vacuolization have been observed, indicating that the cell is undergoing apoptosis, leading to inhibition of cell survival and proliferation demonstrating the cytotoxic effectiveness of complex (3) (Fig. 6D).

These data are in agreement with the loss of mitochondrial ($\Delta\Psi\text{m}$) observed by JC-1 Mitochondrial Membrane Potential Sensor (Fig. 4) and may mean that the activity of complex (3) against leukemic cell lines is mediated by an apoptotic mechanism associated with mitochondrial dysfunction. Some platinum complexes, reported in the literature, induce damage in the mitochondria in a similar way to that promoted by complex (3), causing cell death by an intrinsic pathway [41,42].

Overall, our data suggest the triggering of the apoptotic signal, highlighting the differential effect of compound (3), which due to the structure of the ligand seems to act mainly on mitochondria. Similar results were observed by our research group for copper(II) and cobalt (II) coordination compounds, respectively [19,20].

By scanning electron microscopy, untreated U937 cells show preserved rounded form and the homogeneous presence of microvilli over all the cell surface, indicating a good viability (Fig. 7A). The results of the ultrastructural analysis by SEM shown significant changes in the cell surface with intense membrane blebbing after 8 h of treatment with complex (3) at concentration of 11 μM (Fig. 7B). Some cells appear to release apoptotic bodies [star] in the medium (Fig. 7C).

After 12 h of treatment, cells present reduction of surface blebbing, probably due to release of apoptotic bodies (Fig. 7D). Few microvilli are

seen at the surface of treated cells after 12 h.

These data demonstrate that complex (3) had a significant cytotoxic effect, affected the cell morphology compared to the control, indicating ultrastructural changes characteristic of the apoptotic signal altering the dynamic properties of the plasma membrane.

The inhibitory activity of complex (3) appears to disrupt the proliferation and their invasiveness process of the U937 neoplastic cells. As a result of the treatment with complex (3) led to retraction of microvilli and filopodia, which is one way to inhibit metastasis, a feature considered fundamental to reduce the cancer malignancy [43,44].

Transmission electron microscopy (TEM) investigations are in agreement with the loss of mitochondrial potential ($\Delta\Psi\text{m}$) and indicate that the activity of the complex (3) against leukemic cell line (U937) is mediated by an apoptotic mechanism associated with mitochondrial dysfunction (intrinsic pathway).

Fig. S10 shows transmission electron microscopy (TEM) investigations for cisplatin. Ultrastructural analysis of cisplatin-treated U937 cells showed cells with alterations in the nucleus (nuclear fragmentation and chromatin condensation). In addition, the integrity of the mitochondria seems quite compromised, some seem to be enlarged and emptied. The morphology of the mitochondrial ridges was altered when compared to the cells of the control group. The microvilli of the cell membrane also decreased considerably. In addition, few vacuoles were observed in the cytoplasm in relation to cells treated with the complex (3), where they were more notable.

Ultrastructural analysis of the surface of cisplatin-treated U937 cells is presented in Fig. S11. Cells with intense membrane blebbing within

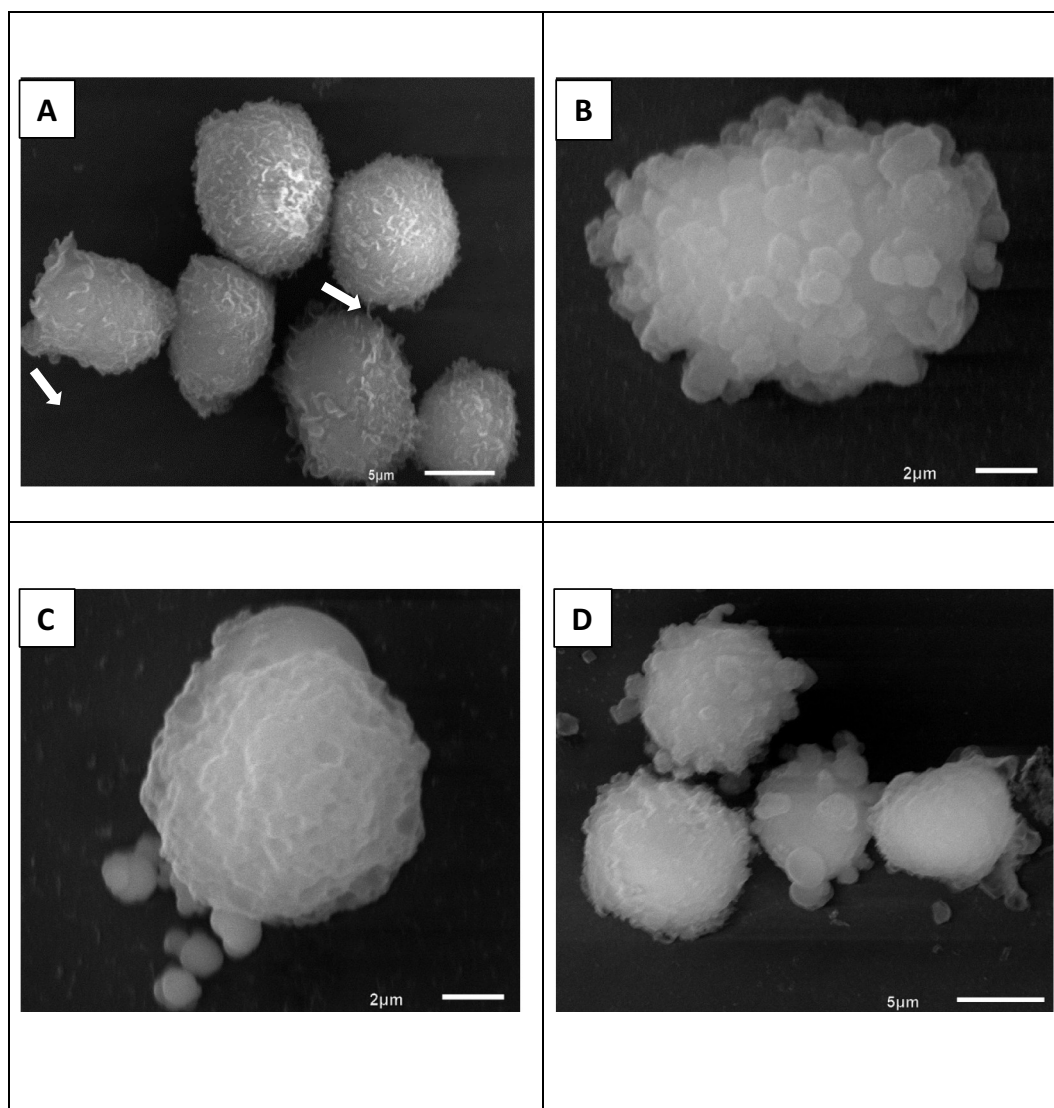


Fig. 7. Scanning Electron Microscopy of human leukemia cells (U937). (A) Control cells, showing microvilli [arrow] on the cell surface. (B) and (C) U937 cell line incubated with 11 μM of complex (3) for 8 h. The release of apoptotic bodies can be seen [star]. (D) U937 cell line incubated with 11 μM of the complex (3) for 12 h.

the first few hours of treatment are observed. In addition, the release of apoptotic bodies and the drastic reduction of cell membrane microvilli were detected mainly during the longer incubation times as the loss of its typical morphology when compared to the control group. These data emphasize the cytotoxic potential of cisplatin, and likewise demonstrate that complex (3) also affects the surface morphology of leukemic cells by inducing such changes, typical of the apoptotic process.

3.7.5. Determination of caspase activities

Considering that apoptosis may be triggered by extrinsic (via death receptor) and intrinsic (via mitochondrial) pathways, the activation of caspases 8, 9 (initiator caspases) and 3 and 6 (effector caspases) were analyzed (Fig. 8). After 3 h of incubation, all caspases were activated revealing high activity of complex (3) and suggesting that this complex may induce both apoptotic pathways (intrinsic and extrinsic). The activation of caspase 9 indicates that the apoptosis is related to damage in the mitochondria, showing agreement with TEM analyzes, which reveal alterations in the mitochondria after 4 h of incubation of U937 cells with complex (3).

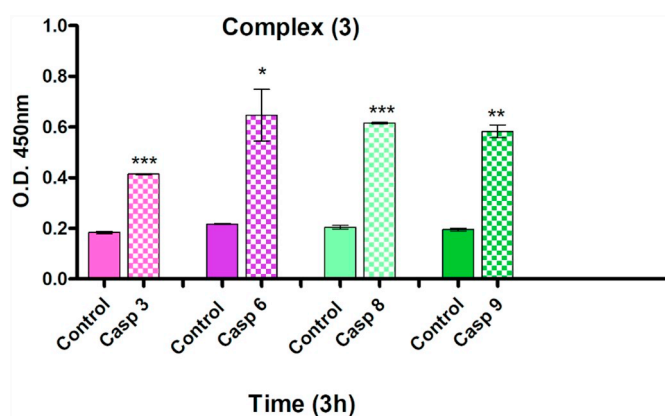


Fig. 8. Caspases 3, 6, 8 and 9 activation in U937 cells after treatment with complex (3). Cells were incubated with 22 μM of complex (3) for 3 h. Values are means \pm S. D. from two separate measurements. *P < 0.05, **P < 0.01 and ***P < 0.001 versus control.

For the copper(II) complex obtained with the same ligand and reported previously by us [19], the apoptosis signal starts from an extrinsic pathway involving the activation of caspases 4 and 8, the signal is amplified by mitochondria with the concomitant release of cytochrome *c* and the activation of caspase 9. Then, the change of the metallic centre seems to modulate the pathway apoptotic, since the complex containing Pt(II) shows activation of caspases 3 and 9 after 3 h of incubation (intrinsic pathway, *via* mitochondrial) and the complex containing Cu(II) shows the activation of caspases 4 and 8 initially, after 6 h of incubation (extrinsic pathway, *via* death receptors). Activation assays of caspases 2, 3, 4, 8 and 9, after incubation of U937 cells with cisplatin, were previously published by us [19]. These results strongly suggest that cisplatin induces apoptosis in U937 cells mainly *via* the mitochondrial pathway.

Among the substrates cleaved by the caspases, there is a component of the cytoskeleton called actin, which, when cleaved, undergoes a rearrangement, alterations in cellular form and distribution of organelles. Then, cells undergo pyknotic and there is destabilization of the plasma membrane, generating protrusions called membrane blebbing, which are considered a specific pattern of apoptosis [44,45]. As shown in this work, such characteristics can be observed in SEM micrographs (Fig. 7) in response to the action of complex (3) on U937 cells.

4. Conclusions

In this study we have presented four new Pt(II) complexes. The naphthyl group is present in the structure of complexes (3) and (4) and is related to the higher antitumoral activity presented by these complexes. Complex (3) is slightly more cytotoxic than complex (4) against Colo-205, U937 and Molt-4 and is more active than complex (4) against H460 cell line (51 ± 1 and $78 \pm 1 \mu\text{M}$, respectively) and THP1- (6 ± 1 and $20 \pm 1 \mu\text{M}$, respectively). Complex (3) presents IC_{50} values lower than cisplatin toward Colo205 (30 and $41 \mu\text{M}$, respectively), H460 (51 and $> 100 \mu\text{M}$, respectively), THP-1 (6 and $10 \mu\text{M}$, respectively) and comparable to cisplatin toward U937 (11 and $8 \mu\text{M}$, respectively) and Molt-4 (9 and $6 \mu\text{M}$, respectively) cell lines. X-ray diffraction studies were performed for complex (3) and DFT calculations indicate that, based on the known structure, all the calculated structures present the same coordination environment (N_2OCl) for the Pt centre. Then, based on DFT calculation, the better activities exhibited by complexes (3) and (4) are related to the presence of the α and β naphthyl groups, respectively.

The results presented herein show clearly the effect of isomerism on the mechanism of cell death, since complex (3) showed high apoptosis rate (98%) and complex (4) showed high necrosis rate (96%), after 24 h of treatment. Similar results were observed for complexes containing Cu(II) and Co(II) coordinated to the same ligands. This result indicates the modulation of the antitumoral activity by the insertion of the naphthyl groups, by the isomerism presented by the ligand and kind of metal center. Furthermore, the coordination of these known ligands to platinum(II) has resulted in new complexes with higher antitumoral activities than the copper and cobalt analogs. This study revealed that compound (3) promoted the activation of the initiator caspase 8 and 9 at the same time and, therefore, it is possible to conclude that it activates both intrinsic and extrinsic cell death pathways. This finding differs from that observed for the copper compound, which initially activates only the extrinsic pathway.

Acknowledgements

The authors are grateful for financial support received from CAPES (Coordenação de Aperfeiçoamento de Pessoal de Nível Superior), CNPq (Conselho Nacional de Desenvolvimento Científico e Tecnológico)-472018/2012-4 and FAPERJ (Fundação de Amparo à Pesquisa do Estado do Rio de Janeiro)-E-26/111.360/2013. Computer resources were provided by the National Facility of the Australian National

Computational Infrastructure and by the University of Queensland Research Computing Centre.

Appendix A. Supplementary data

Table S1, Relative energy for conformers for complexes (1)–(4), Cartesian coordinates for the optimized geometry for complexes (1)–(4) and Figs. S1–S9 in PDF format.

Crystallographic data (without structure factors) for the structure reported in this manuscript has been deposited with the Cambridge Crystallographic Data Centre as supplementary publication: deposition number: CCDC 1849033 for complex (3). Supplementary data to this article can be found online at <https://doi.org/10.1016/j.jinorgbio.2018.12.016>.

References

- [1] D. Wang, S.J. Lippard, *Nat. Rev. Drug Discov.* 4 (2005) 307–320.
- [2] T.C. Johnstone, G.Y. Park, S.J. Lippard, *Anticancer Res.* 34 (1) (2014) 471–476.
- [3] K. Chválová, V. Brabec, J. Kaspárkova, *Nucleic Acids Res.* 35 (6) (2007) 1812–1821.
- [4] P. Heringová, J. Kaspárkova, V. Brabec, *J. Biol. Inorg. Chem.* 14 (2009) 959–968.
- [5] N.J. Wheate, S. Walker, G.E. Craig, R. Oun, *Dalton Trans.* 39 (2010) 8113–8127.
- [6] L. Bai, C. Gao, Q. Liu, C. Yu, Z. Zhang, L. Cai, B. Yang, Y. Qian, J. Yang, X. Liao, *Eur. J. Med. Chem.* 140 (2017) 349–382.
- [7] A.I. Matesanz, I. Leitão, P. Souza, *J. Inorg. Biochem.* 125 (2013) 26–31.
- [8] A.A. Legin, S. Theiner, A. Schintmeister, S. Reipert, P. Heffeter, M.A. Jakupec, J. Mayr, H.P. Varbanov, C.R. Kowol, M. Galanski, W. Berger, M. Wagner, B.K. Keppler, *Chem. Sci.* 7 (2016) 3052–3061.
- [9] H. Chen, F. Chen, W. Hu, S. Gou, *J. Inorg. Biochem.* 180 (2018) 119–128.
- [10] L.C. Batista, F.S. de Souza, V.M. de Assis, S.H. Seabra, A.J. Bortoluzzi, M.N. Rennó, A. Horn Jr., R.A. DaMatta, C. Fernandes, *RSC Adv.* 5 (2015) 100606–100617.
- [11] L.J.H. Borges, E.S. Bull, C. Fernandes, A. Horn Jr., N.F.B. Azeredo, J.A.L.C. Resende, W.R. Freitas, E.C.Q. Carvalho, L.S. Lemos, H. Jerdy, M.M. Kanashiro, *Eur. J. Med. Chem.* 123 (2016) 128–140.
- [12] N.F.B. Azeredo, F.P. Souza, F.C. Demidoff, C.D. Netto, J.A.L.C. Resende, R.W.A. Franco, P. Colepicolo, A.M.D.C. Ferreira, C. Fernandes, *J. Mol. Struct.* 1152 (2018) 11–20.
- [13] C.A. Gomes, L.M. Lube, C. Fernandes, R.W.A. Franco, J.A.L.C. Resende, A. Horn Jr., *New J. Chem.* 41 (2017) 11498–11502.
- [14] A. Horn Jr., A. Neves, I. Vencato, V. Drago, C. Zucco, R. Werner, W. Haase, *J. Braz. Chem. Soc.* 11 (1) (2000) 7–10.
- [15] C. Fernandes, A. Horn Jr., O. Vieira-da-Motta, V.M. Assis, M.R. Rocha, L.S. Mathias, E.S. Bull, A.J. Bortoluzzi, E.V. Guimarães, J.C.A. Almeida, D.H. Russell, *J. Inorg. Biochem.* 104 (2010) 1214–1223.
- [16] A. Horn Jr., L. Fim, A.J. Bortoluzzi, B. Szpoganicz, M.S. Silva, M.A. Novak, M.B. Neto, L.S. Eberlin, R.R. Catharino, M.N. Eberlin, C. Fernandes, *J. Mol. Struct.* 797 (2006) 154–164.
- [17] A. Horn Jr., I. Vencato, A.J. Bortoluzzi, R. Hörner, R.A.N. Silva, B. Szpoganicz, V. Drago, H. Terenzi, M.C.B. Oliveira, R. Werner, W. Haase, A. Neves, *Inorg. Chim. Acta* 358 (2005) 339–351.
- [18] A. Horn Jr., I. Vencato, A.J. Bortoluzzi, V. Drago, M.A. Novak, A. Neves, *J. Braz. Chem. Soc.* 17 (8) (2006) 1584–1593.
- [19] C. Fernandes, A. Horn Jr., B.F. Lopes, E.S. Bull, N.F.B. Azeredo, M.M. Kanashiro, F.V. Borges, A.J. Bortoluzzi, B. Szpoganicz, A.B. Pires, R.W.A. Franco, J.C. de A. Almeida, L.L.F. Maciel, J.A.L.C. Resende, G. Schenk, *J. Inorg. Biochem.* 153 (2015) 68–87.
- [20] S.R. Morcelli, E.S. Bull, W.S. Terra, R.O. Moreira, F.V. Borges, M.M. Kanashiro, A.J. Bortoluzzi, L.L.F. Maciel, J.C. de A. Almeida, A. Horn Jr., C. Fernandes, *J. Inorg. Biochem.* 161 (2016) 73–82.
- [21] S.R. Morcelli, M.M. Kanashiro, D.R.S. Candela, M. Alzamora, A. Horn Jr., C. Fernandes, *Inorg. Chem. Commun.* 67 (2016) 22–24.
- [22] A. Neves, M.A. de Brito, I. Vencato, V. Drago, K. Griesar, W. Haase, Y.P. Mascarenhas, *Inorg. Chim. Acta* 214 (1993) 5–8.
- [23] A. Horn Jr., A. Neves, I. Vencato, V. Drago, C. Zucco, R. Werner, W. Haase, *J. Braz. Chem. Soc.* 11 (2007) 7–10.
- [24] Bruker, APEX3 and SAINT, Bruker AXS Inc., Madison, Wisconsin, USA, 2015.
- [25] L. Krause, R. Herbst-Irmer, G.M. Sheldrick, D. Stalke, *J. Appl. Crystallogr.* 48 (2015) 3–10.
- [26] G.M. Sheldrick, *Acta Cryst A* 71 (2015) 3–8.
- [27] G.M. Sheldrick, *Acta Cryst C* 71 (2015) 3–8.
- [28] M.J. Frisch, G.W. Trucks, H.B. Schlegel, G.E. Scuseria, M.A. Robb, J.R. Cheeseman, G. Scalmani, V. Barone, B. Mennucci, G.A. Petersson, H. Nakatsuji, M. Caricato, X. Li, H.P. Hratchian, A.F. Izmaylov, J. Bloino, G. Zheng, J.L. Sonnenberg, M. Hada, M. Ehara, K. Toyota, R. Fukuda, J. Hasegawa, M. Ishida, T. Nakajima, Y. Honda, O. Kitao, H. Nakai, T. Vreven, J.A. Montgomery Jr., J.E. Peralta, F. Ogliaro, M. Bearpark, J.J. Heyd, E. Brothers, K.N. Kudin, V.N. Staroverov, T. Keith, R. Kobayashi, J. Normand, K. Raghavachari, A. Rendell, J.C. Burant, S.S. Iyengar, J. Tomasi, M. Cossi, N. Rega, J.M. Millam, M. Klene, J.E. Knox, J.B. Cross, V. Bakken, C. Adamo, J. Jaramillo, R. Gomperts, R.E. Stratmann, O. Yazyev, A.J. Austin, R. Cammi, C. Pomelli, J.W. Ochterski, R.L. Martin, K. Morokuma,

- V.G. Zakrzewski, G.A. Voth, P. Salvador, J.J. Dannenberg, S. Dapprich, A.D. Daniels, O. Farkas, J.B. Foresman, J.V. Ortiz, J. Cioslowski, D.J. Fox, Gaussian 09, Revision D.01, Gaussian, Inc., Wallingford CT, 2013.
- [29] A.D. Becke, *J. Chem. Phys.* 98 (1993) 5648–5652.
- [30] C. Lee, W. Yang, R.G. Parr, *Phys. Rev. B* 37 (1988) 785–789.
- [31] S.H. Vosko, L. Wilk, M. Nusair, *Can. J. Phys.* 58 (1980) 1200–1211.
- [32] P.J. Stephens, F.J. Devlin, C.F. Chabalowski, M.J. Frisch, *J. Phys. Chem.* 98 (1994) 11623–11627.
- [33] P.J. Stephens, F.J. Devlin, C.S. Ashvar, C.F. Chabalowski, M.J. Frisch, *Discuss. Faraday Soc.* 99 (1994) 103–119.
- [34] A.V. Marenich, C.J. Cramer, D.G. Truhlar, *J. Phys. Chem. B* 113 (2009) 6378–6396.
- [35] C.F. Macrae, I.J. Bruno, J.A. Chisholm, P.R. Edgington, P. McCabe, E. Pidcock, L. Rodriguez-Monge, R. Taylor, J. van de Streek, P.A. Wood, *J. Appl. Crystallogr.* 41 (2) (2008) 466–470.
- [36] M.D. Hanwell, D.E. Curtis, D.C. Lonie, T. Vandermeersch, E. Zurek, G.R. Hutchison, *J. Cheminform.* 4 (2012) 17.
- [37] A.K. Rappe, C.J. Casewit, K.S. Colwell, W.A. Goddard III, W.M. Skiff, *J. Am. Chem. Soc.* 114 (25) (1992) 10024–10035.
- [38] T. Mossmann, *J. Immunol. Methods* 65 (1983) 55–63.
- [39] H.D. Flack, G. Bernardinelli, *J. Appl. Crystallogr.* 33 (2000) 1143–1148.
- [40] C. Fernandes, A. Horn Jr., O. Vieira-da-Motta, M.M. Kanashiro, M.R. Rocha, R.O. Moreira, S.R. Morcelli, B.F. Lopes, L.S. Mathias, F.V. Borges, L.J.H. Borges, W.R. Freitas, L.C. Visentin, J.C. de A. Almeida, G. Schenk, *Inorg. Chim. Acta* 416 (2014) 35–48.
- [41] S.M. Sancho-Martínez, L. Prieto-García, M. Prieto, J.M. López-Novoa, F.J. López-Hernández, *Pharmacol. Ther.* 136 (2012) 35–55.
- [42] S. Dasari, *Eur. J. Pharmacol.* 740 (2014) 364–378.
- [43] S.C. Gupta, J.H. Kim, S. Prasad, B.B. Aggarwal, *Cancer Metastasis Rev.* 29 (2010) 405–434.
- [44] S. Al-Bahlani, B. Al-Dhahli, K. Al-Adawi, A. Al-Nabhani, M. Al-Kindi, *Biomed. Res. Int.* (2017) 1–13.
- [45] M. Charpentier, S. Martin, *Cancer* 5 (2013) 1545–1565.

1 ***In vitro* and *in vivo* anti-proliferative activity and ultrastructure investigations of a**
2 **copper(II) complex toward human lung cancer cell NCI-H460**

3
4
5 Leide Laura Figueiredo Maciel ^{a,b}, William Rodrigues de Freitas ^d, Erika Soares Bull ^e, Christiane
6 Fernandes Horn ^c, Adolfo Horn Jr ^c, Milton Masahiko Kanashiro ^{b*}, João Carlos Aquino de
7 Almeida ^{a*}

8
9
10 ^a *Laboratório de Fisiologia e Bioquímica de Microrganismos, Universidade Estadual do Norte*
11 *Fluminense Darcy Ribeiro, 28013-602, Campos dos Goytacazes/RJ, Brazil*

12 ^b *Laboratório de Biologia do Reconhecer, Universidade Estadual do Norte Fluminense, 28013-*
13 *602, Campos dos Goytacazes/RJ, Brazil*

14 ^c *Laboratório de Ciências Químicas, Universidade Estadual do Norte Fluminense, 28013-602,*
15 *Campos dos Goytacazes/RJ, Brazil*

16 ^d *Universidade Federal do Sul da Bahia, Teixeira de Freitas/BA Brazil*

17 ^e *Instituto Federal Fluminense Campus Centro, Campos dos Goytacazes/RJ, Brazil*

18
19
20
21
22
23
24
25
26
27
28
29 *To whom correspondence should be addressed: Phone: +55 22 2739-7126; +55 22 99999 1638.

30 E-mail: kmilton@uenf.br; jalmeidaa@gmail.com

1 **Summary**

2

3 This study evaluated the *in vitro* and *in vivo* anti-proliferative potential of complex (2)
4 [Cu(L1)Cl]Cl.2H₂O, where L1= 1-[2-hydroxybenzyl(2-pyridylmethyl)amino]-3-(1-naphthyloxy)-
5 2-propanol on lung carcinoma cell NCI-H460 and compare with the inhibitory effect of cisplatin.
6 Cell viability determined by the MTT assay demonstrated that the complex (2) has an anti-
7 proliferative effect against three human cancer lines: NCI-H460 (lung cancer), COLO 205
8 (colon), and MOLT-4 (leukemia). Complex (2) exhibits higher activity against the NCI-H460
9 cell, with an IC₅₀ value lower than cisplatin (26.5 ± 1.1 μM and 203 ± 1.2 μM) respectively. Cell
10 death by apoptosis was investigated by flow cytometer analysis of sub-G1 populations in the cell
11 cycle and Annexin V/PI assay. Nuclear and mitochondria morphology were investigated by
12 transmission electron microscopy and by double staining Hoechst/MitoTracker fluorescence for
13 nucleus and mitochondria, respectively. Changes on the cell surface and ultrastructure were
14 detected by scanning and transmission electron microscopy. Our work revealed that complex (2)
15 induced changes associated with apoptosis, such as plasma membrane *blebbing* and a lower
16 microvilli amount; fragmentation and condensation of chromatin, alterations in mitochondria, and
17 enlargement of the endoplasmic reticulum (ER) were also detected. Mitochondrial function of
18 NCI-H460 cells evaluated by JC-1 probes showed high loss of mitochondrial membrane potential
19 when treated with complex (2). Moreover, caspase-12 was measured and showed an expressive
20 activation level, which is related to ER stress. This complex demonstrated antineoplastic potential
21 in the *in vivo* treatment of cancerous lesions of NCI-H460 cells by 48 % inhibition of tumor
22 growth compared with the control group. Based on the present results, it is possible to suggest
23 that complex (2) inhibits the *in vitro* and *in vivo* growth of lung carcinoma cell NCI-H460,
24 opening up prospects for new research for clinical application.

25

26 Keywords: Copper(II) complex. Apoptosis. Morphology. NCI-H460 lung cancer cell

27

28

29

30

31

32

1 **Introduction**

2 Cisplatin (*cis*-diamminedichloroplatinum(II)) is a powerful chemotherapeutic agent and
3 was the first platinum containing coordination complex used in oncology therapy. In 1978 its
4 efficacy in treatment of cancer patients was established and approved for use by the FDA [1, 2].
5 Cisplatin is clinically proven to treat numerous types of human cancers and has contributed to
6 increase life expectative for patients with lung, bladder, head and neck, testicular and ovarian
7 cancer, and is also used to treat other cancers, including carcinomas, germ cell tumors,
8 lymphomas and sarcomas, making it one of the most clinically successful antineoplastic drugs [1,
9 3]. In general, cisplatin mechanism of action is related to their ability to induce DNA damage by
10 cross-linking inter and intra-filament of DNA interfering with its repair, transcription and
11 replication mechanism, these events in turn, result in apoptosis cell death [1, 4].

12 Apoptosis is considered the main mechanism of cell death induced by most cancer
13 therapeutic agents. This process is accompanied by several morphological changes like rounding-
14 up of the cell, retraction of pseudopods, reduction of cellular volume (pyknosis), chromatin
15 condensation, nuclear fragmentation (karyorrhexis), classically little or no ultrastructural
16 modifications of cytoplasmic organelles, plasma membrane *blebbing* (but maintenance of its
17 integrity until the final stages of the process), and engulfment by resident phagocytes (*in vivo*)
18 causing minimal damage/inflammation to surrounding tissues [5, 6]. Death by apoptosis can be
19 triggered by the extrinsic (death receptor) and intrinsic (mitochondrial) pathways. Activation of
20 death receptor results in binding of the adapter protein TRADD and recruitment of the FADD and
21 RIP proteins followed by the dimerization of the death effector domain and then FADD
22 associates with pro-caspase-8. Death inducing signaling complex (DISC) is formed and induces
23 activation of pro-caspase-8. Then, activated caspase 8 triggers the execution phase of apoptosis
24 by activating the downstream effector caspases 3, 6 and 7 [7, 8]. The mitochondrial pathway of
25 cell death can be activated by a variety of stimuli such as radiation, chemotherapeutics, free
26 radicals, viral infections, and serum/growth factor withdrawal. It is well-established that these
27 stimuli induce the loss of mitochondrial transmembrane potential ($\Delta\Psi_m$) followed by the release
28 of pro-apoptotic proteins such as cytochrome c. This process is well controlled by BCL-2 protein
29 family. Cytochrome c interacts with APAF1 in conjunction with dATP, these proteins form
30 apoptosome that recruits and activates caspase 9, leading to the activation of executioner caspases
31 3, 6 and 7 and the death response [7, 8].

32

1 Based on high antineoplastic activity of cisplatin associated with its severe side effects
2 such as nephrotoxicity [9], hepatotoxicity, cardiotoxicity [10], ototoxicity, myelosuppression and
3 a high percentage of cancer cell resistance to treatment [1], a considerable research has been
4 devoted to development of new metallodrugs candidates, which are capable of interacting with
5 DNA or other molecular targets such as proteins and enzymes that induce cellular death [11] but
6 less severe side effects. The discovery of the cytotoxic activity of complexes with other metals
7 besides platinum, including iron [12], gallium [13], copper [14, 15], cobalt [16], palladium [4],
8 ruthenium [17] and gold complexes [18], has expanded the arsenal of metallic ions that have been
9 studied for this purpose.

10 Our group has synthesized a number of coordination complexes including iron(III)
11 complexes [12], copper(II) [15, 19], cobalt(II) [16] and platinum(II) [20] and their biological
12 activity was tested on several neoplastic cell lines. In 2015 we reported the synthesis,
13 characterization of two complexes having copper(II) as metal nuclei, and cytotoxic activity
14 toward two human leukemia cell lines (THP-1 and U937) was evaluated [19]. These complexes
15 exhibited a high anti-proliferative effect on both cell lines, whereas complex (2) exhibited higher
16 activity than cisplatin against the U937 cell line (8.20 μM vs 16.2 μM). We also demonstrated
17 that complex (2) induce apoptosis by activating the intrinsic pathway of cell death. The toxicity
18 of complex (2) determined *in vivo* in C57BL/6 mice (LD_{50} of 55 mg/kg) [19] when compared to
19 cisplatin (LD_{50} of 6.6 mg/kg) [21] the complex (2) showed 8.3 times less toxic than the standard
20 metallodrug. As the alpha isomer was the most active compound, we decided to investigate the
21 inhibitory effects of this compound on NCI-H460 lung carcinoma cells and the underlying
22 mechanisms of cell death induced by the complex (2) on this highly metastatic cancer cell. The *in*
23 *vivo* treatment of BALB/c *nude* mice bearing cancerous lesions of NCI-H460 cells, complex (2)
24 resulted in 48 % inhibition of tumor growth when compared with the control group. Based on our
25 results, it is possible to suggest that complex (2) inhibits the *in vitro* and *in vivo* growth of lung
26 carcinoma cell NCI-H460, opening up prospects for new research for clinical application.

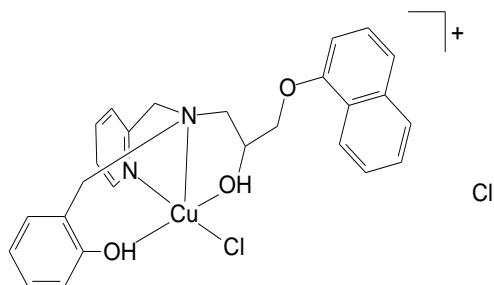
27 28 **Materials and methods**

29 **Synthesis of copper(II) complex - complex (2)**

30 The ligand (L1) and its respective copper complex $[\text{Cu}(\text{L}1)\text{Cl}] \text{Cl} \cdot 2\text{H}_2\text{O}$, where L1= 1-[2-
31 hydroxybenzyl(2-pyridylmethyl)amino]-3-(1-naphthoxy)-2-propanol (Fig. 1) were synthesized
32 as described previously [19]. For *in vitro* studies, this complex was dissolved in dimethyl

1 sulfoxide (DMSO) and DMEM-F12 medium (Gibco, BRL) and stored at $-20\text{ }^{\circ}\text{C}$.

2



3

4

5 **Fig. 1** Chemical complex (2) in solution [19].

6

7 **Cell culture**

8 Non-small cell lung cancer (NCI-H460), acute lymphoblastic leukemia (MOLT-4), and
9 human colon adenocarcinoma (COLO 205) cell lines were obtained from the American Type
10 Culture Collection (ATCC) USA, cultured routinely in DMEM-F12 medium (Gibco, BRL)
11 supplemented with 10 % fetal bovine serum (FBS) and gentamycin (20 mg/mL, Gibco, BRL) at
12 37°C in a humidified atmosphere containing 5 % CO_2 (Forma, Thermo Scientific, USA). When
13 the cells reached 70–80 % confluence, they were trypsinized, harvested and split into 3 new
14 culture flask with fresh media.

15

16 **Analysis of cell viability by MTT assay**

17 Cells at concentration of 2×10^6 cells/mL were seeded in 96 multiwell plates with a
18 volume of 100 μL per well, treated with 100 μL of different concentrations (0-400 μM) of the
19 ligand or complex (2) followed by incubation at 37°C for 36 h. DMSO (0.02 %) was used as the
20 solvent control and cisplatin (Sigma-Aldrich) was used as positive control. Cell viability was
21 measured by MTT (3-(4,5-dimethylthiazol-2-yl)-2,5-diphenyl tetrazolium bromide) colorimetric
22 microassay as described by Mosmann [22]. Volume of 20 μL of MTT stock solution (5 mg/mL)
23 were added to each well and incubated at $37\text{ }^{\circ}\text{C}$ for more 4 h. The MTT-formazan produced by
24 viable cells was dissolved in an isopropanol-HCl solution. The optical density (OD) values were
25 measured by spectrophotometry at 570 nm using a Microplate Reader (EpochTM, BioTek®
26 Instruments, Inc.). The values of IC_{50} were obtained from dose-response curves using GraphPad
27 Prism 5.0. The IC_{50} was defined as the concentration of the compound required to reduce the

1 viability of treated cells to 50 % in comparison to untreated control cells. All the experiment was
2 carried out in triplicate.

3

4 **Measurement of annexin V and propidium iodide staining**

5 NCI-H460 cells were seeded at 1×10^6 cells/mL per well in a 12 well plate and treated
6 with 1X and 2X IC_{50} of complex (2) and cisplatin for 24 h. Apoptosis was detected using an
7 Annexin V-FITC Apoptosis Detection Kit (Sigma-Aldrich). Briefly, after incubation, cells were
8 washed twice with phosphate buffered saline (PBS), and incubated in 500 μ L of binding buffer
9 (100 mM HEPES/NaOH, pH 7.5, 1.4 M NaCl and 25 mM $CaCl_2$). To each sample 5 μ L of
10 Annexin V-FITC and 10 μ L of propidium iodide (PI) were added. Samples were incubated at
11 room temperature for 10 min protected from light and immediately submitted to flow cytometer
12 (FACS Calibur-BD Sciences) analyses. All analyses were performed by recording 10,000 events.

13

14 **Cell cycle analysis by flow cytometer**

15 NCI-H460 cells were seeded and treated with complex (2) and cisplatin. After incubation,
16 the cells were fixed in ethanol 70 % at 4 °C for 30 min. Cells were centrifuged (1000 x g for 5
17 min) and re-suspended in 500 μ L of PI staining solution (50 μ g/mL PI, 1 mg/mL RNase and
18 0.2 % Triton X-100) for 30 min protected from the light. The DNA content was measured by a
19 flow cytometer and cell cycle distribution was analyzed by WinMDI version 2.9 software. The
20 proportions of cells in G_0/G_1 , S, and G_2/M phases were represented as DNA histograms.
21 Apoptotic cells with hypodiploid DNA content were measured by quantifying the sub- G_1 peak in
22 the cell cycle pattern. All analyses were performed by recording 10,000 events.

23

24 **Analysis of mitochondrial membrane potential ($\Delta\Psi_m$) using JC-1 stain**

25 NCI-H460 cells were seeded and treated with complex (2) and cisplatin. After treatment
26 cell suspension was centrifuged (400 x g, for 10 min, at room temperature) and stained with JC-1
27 (5,5',6,6'-tetrachloro 1,1',3,3' tetraethylbenzimidazolylcarbocyanine iodide) dye (25 μ g/mL) and
28 incubated at 37 °C in 5 % CO_2 for 15 min. The cells were washed twice with fresh medium and
29 immediately submitted to flow cytometry analysis. All data was analyzed by WinMDI version 2.9
30 software. Red fluorescence is emitted when JC-1 accumulates in healthy cell mitochondria
31 forming JC-1 aggregates, showing normal mitochondrial membrane potential ($\Delta\Psi_m$) and is
32 detectable in the FL2 channel. In apoptotic cells JC-1 emits green fluoresce due to the JC-1

1 monomeric form caused by loss of $\Delta\Psi_m$, which is detectable in the FL1 channel. All analyses
2 were performed by recording 10,000 events.

3 4 **Determination of caspase-12 activity**

5 Caspase-12 activity was determined using the specific substrate FITC-ATAD-FMK,
6 following the protocols of the CaspGLOWTM Fluorescein Caspase-12 Staining Kit Assay
7 (BioVision). NCI-H460 cells were seeded according to methodology previously described and
8 treated with the complex (2) and cisplatin for 18 h. After incubation, aliquots of 300 μ L of cell
9 suspension were transferred to microcentrifuge tubes and 1 μ L of FITC-ATAD-FMK was added,
10 the tubes were incubated for 40 min at 37 °C with 5 % CO₂. The cells were centrifuged at 400 x g
11 for 10 min. The supernatant was removed and the pellet was washed twice with the supplied
12 wash buffer. The samples were kept on ice until data acquisition by a flow cytometry and
13 analyzed by WinMDI version 2.9 software. All analyses were performed by recording 10,000
14 events.

15 16 **Fluorescence assay**

17 NCI-H460 cells were seeded on coverslips in a 24 well plate at final concentration of 1 x
18 10⁶ cells/mL per well, and treated with 2X IC₅₀ of complex (2) and cisplatin for 12 h. After
19 incubation, the cells were centrifuged at 400 x g for 5 min at room temperature. The cells were
20 then incubated with 1 μ g/mL Hoechst 33342 nuclear stain and 100 nM MitoTracker CMXRos
21 (Invitrogen, Molecular Probes) at 37 °C for 45 minutes, washed twice with PBS, and re-
22 suspended in fresh DMEM-F12 medium. Nuclear and mitochondrial morphology of the cells
23 were examined and images were taken at 400 X with fluorescence microscopy (Axioplan – Carl
24 Zeiss microscope).

25 26 **Electron microscopy analysis**

27 NCI-H460 cells 1 x 10⁶ cells/mL were seeded in a 25 cm² culture flask, 5 mL per flask
28 and treated with 2X IC₅₀ of complex (2) and cisplatin for 4, 8 and 12 h at 37 °C. After incubation,
29 the cells were centrifuged at 400 x g for 10 min, washed three times with PBS, pH 7.2, and fixed
30 for 2 h in 2.5 % glutaraldehyde, 0.1 M sodium cacodylate buffer, post-fixed for 20 min in a 1:1
31 solution of osmium tetroxide (1 %) and potassium ferricyanide (0.8 %). **Transmission electron**
32 **microscopy (TEM):** cells were dehydrated sequentially in a graded series of acetone (50 –

1 100 %) and embedded in Epoxy resin (Poly/Bed 812®). The resin-embedded cells were placed in
2 a silicon mold well at 60 °C for 48 h for polymerization. The obtained blocks were sectioned and
3 ultrathin sections (70 nm thick) were taken using an ultramicrotome Reichert Ultracut S,
4 collected on copper grids (400 mesh), stained with uranyl acetate and lead citrate, and observed
5 on JEOL-1400 Plus TEM (Japan) at 120 kV. **Scanning electron microscopy (SEM)**: post-fixed
6 cells were dropped onto poly-L-lysine (Sigma-Aldrich) pre-coated coverslips, dehydrated
7 sequentially in a graded series of ethanol (50 – 100 %) and critical-point dried (Bal-Tec CPD 030
8 Critical Point Dryer) with CO₂. The samples were mounted on a stub with adhesive tape, coated
9 with 40 to 60 nm of Gold/Palladium (Sputter Coater SDC 050) and analyzed on ZEISS EVO 40
10 XVP MEV (Germany) at 15 kV.

11

12 **Lethal dose determination in mice**

13 Female BALB/*c nude* mice, 6-8 weeks old, bred in the Animal House of the university
14 were housed in polypropylene cages with capacity for six animals, in a controlled environment
15 (12 h dark/light cycle), and were fed commercial standard food and water *ad libitum*. Studies
16 were approved by the Animal Ethics Use Committee of the Universidade Estadual do Norte
17 Fluminense Darcy Ribeiro under protocol number CEUA 349. In order to determine the lethal
18 dose of complex (2), male and female BALB/*c nude* mice, between 18 g and 25 g were separated
19 into groups of four animals. The complex (2) dissolved in ultrapure water (40, 50, 80, 100
20 mg.kg⁻¹) was injected into the peritoneal cavity with insulin syringes (Nipro Medical Corporation
21 do Brasil). The animals were observed closely for at least 4 h post injection and at 24 h intervals
22 for 15 days thereafter. Median lethal dose (LD₅₀), a dose required to kill half the inoculated
23 animal was determined.

24

25 ***In vivo* tumor growth inhibition**

26 To induce tumor nodules, Balb/*c nude* mice (23 ± 2 g of body weight) were injected with
27 0.1mL of NCI-H460 (5 x 10⁶ cells/mL) via subcutaneous route on the back of the animals. After
28 5 or 7 days pos-inoculation when the tumor nodules were apparent (± 3mm) mice were randomly
29 divided into three groups (six per group) and the treatment was started. One group was treated
30 with 25 mg/kg of complex (2) another group with 3.3 mg/kg of cisplatin via intra-peritoneal
31 route, corresponding to 50 % of the LD₅₀ of the both compounds. Non-treated control group was
32 injected with PBS + DMSO (v/v = 16 %). The treatment was performed by 3 doses of the

1 compounds at one week of intervals. Tumor sizes were measured every three days during the
2 treatment period using a caliper, and the tumor volume was calculated using the formula
3 $V(\text{mm}^3) = Ax^2/2$, where $V(\text{mm}^3)$ is the tumor volume in mm^3 , A = length, and B = width of the
4 tumors. At the end of treatment the animals were euthanized, photographed and the subcutaneous
5 lesions excised, weighted, and fixed in 10 % neutral buffered formalin for histological analysis.

6 7 **Statistical analysis**

8 For analysis of cell viability, the mean and standard error were evaluated from nonlinear
9 regression (curve fit) of the cytotoxicity curves using Prism 5.0 (GraphPad software). Tumor
10 volumes between different treatment groups were compared using one-way ANOVA followed by
11 Tukey adjustments to correct for multiple comparisons using Prism 5.0. Significant difference
12 was taken as * $p < 0.05$, ** $p < 0.01$, and *** $p < 0.001$.

13 14 **Results**

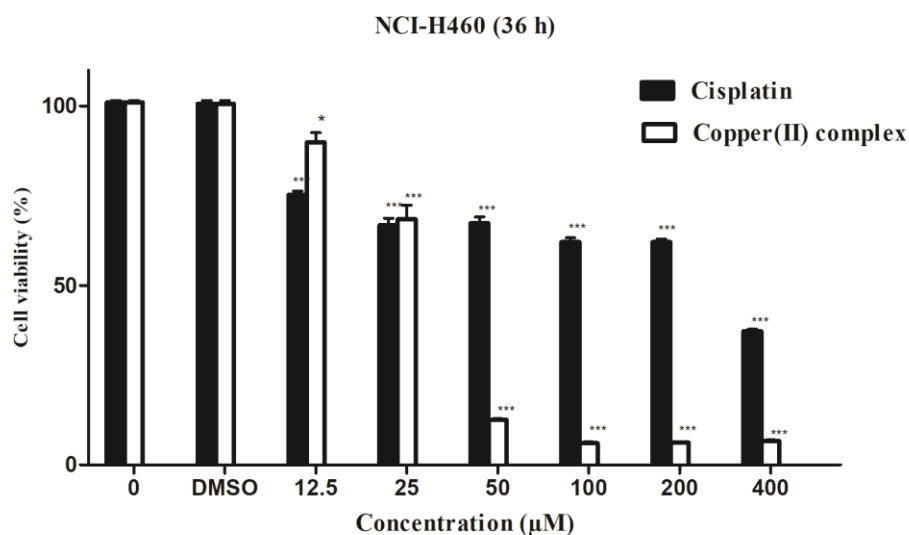
15 **Complex (2) induces cytotoxicity on neoplastic cells**

16 The screening of the anti-proliferative activity of new biologically active compounds is
17 essential in cancer research regarding the development of new antitumor drugs. Thus, the *in vitro*
18 cytotoxicity of ligand L1, metallic salt, complex (2), and cisplatin (control) were evaluated
19 against three human cancer cell lines, NCI-H460, COLO 205, and MOLT-4 by MTT assay.
20 Complex (2) showed a significant inhibitory effect on the growth of the neoplastic cell lines NCI-
21 H460, COLO 205 and MOLT-4, with IC_{50} of $26.5 \pm 1.1 \mu\text{M}$, $27 \pm 1.2 \mu\text{M}$, and $35.6 \pm 1.1 \mu\text{M}$,
22 respectively (Table 1). In contrast, $\text{CuCl}_2 \cdot 2\text{H}_2\text{O}$ and the free ligand L1 treatments at highest
23 concentrations $100 \mu\text{M}$ did not affect the viability of any of the cell lines tested (Table 1).
24 Interestingly complex (2) showed close to seven times more cytotoxicity than cisplatin to the
25 NCI-H460 tumor cell line, with an IC_{50} of $26.5 \pm 1.1 \mu\text{M}$ against $203 \pm 1.2 \mu\text{M}$, respectively.
26 Figure 2 shows the dose-response-curve data comparison of cytotoxic activity of complex (2) and
27 cisplatin, and a striking difference of cytotoxic activity between them can be seen. Based on this
28 data, the NCI-H460 cell line was chosen for additional studies of the underlying cell death
29 mechanism and *in vivo* evaluation of antineoplastic activity of complex (2).

1 **Table 1.** Determination of IC₅₀ values of complex (2) toward neoplastic cell lines

Compounds	IC ₅₀ (μM)		
	COLO 205	NCI-H460	MOLT-4
Complex (2)	35.6 ± 1.1	26.5 ± 1.1	27 ± 1.2
L1	> 100	> 100	> 100
CuCl ₂ ·2H ₂ O	> 100	> 100	> 100
Cisplatin	46.7 ± 1.1	203 ± 1.2	21.4 ± 1.0

2 IC₅₀ - compound concentration that is required to induce 50 % of cell cytotoxicity; data are expressed as mean ± SD
 3 of three independent experiments, each in triplicate.

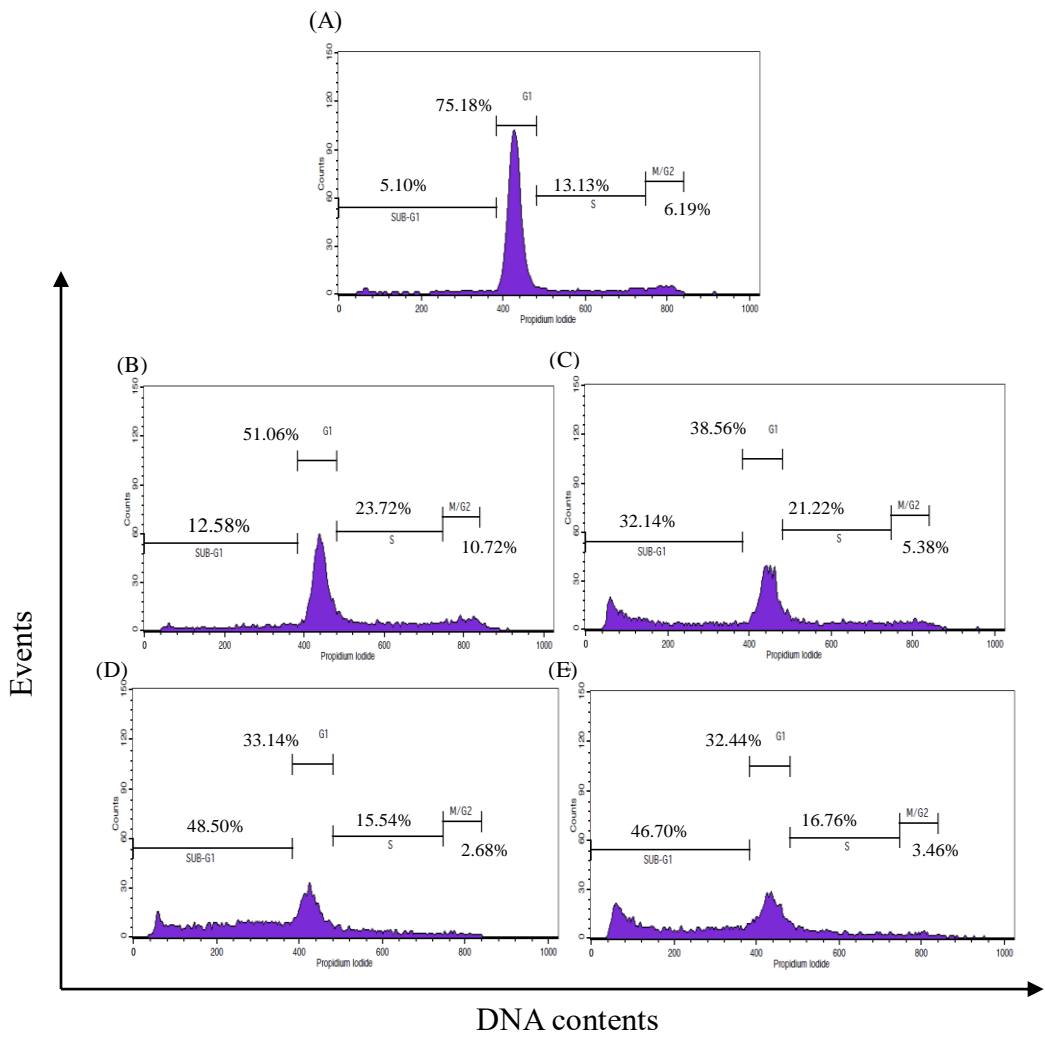


4
 5 **Fig. 2** Viability of NCI-H460 cells after treatment with complex (2) and cisplatin. The cells were treated with
 6 increasing concentrations of the complexes up to 400 μM for 36 h of exposure. Dose-response curves were obtained
 7 by MTT assay. Each data point represents means ± S.D. (n = 3). *P < 0.05, **P < 0.01 and ***P < 0.001 in relation
 8 to control

10 Lung carcinoma cells undergo apoptosis cell death when treated with complex (2)

11 The induction of apoptosis is a major goal in the development of antitumor drugs and it is
 12 considered the most important target of many cancer treatment strategies. We evaluated apoptosis
 13 by measuring the cell DNA content by flow cytometry after the treatment of the NCI-H460 cells
 14 with complex (2) and stained with PI. Flow cytometry allows the identification and quantification
 15 of low DNA content cells that appear in the sub-G1 region of the histogram. As shown in Figs.
 16 3a, 3b and 3c the population of cells in the sub-G1 region changed from 5 % in untreated control

1 cells to 13 % and to 32 % after treatment with complex (2), for 24 h at 1X and 2X IC_{50} ,
 2 respectively. After incubation with the 2X IC_{50} of cisplatin concentrations, the NCI-H460 cell
 3 population identified at the sub-G1 region presented similar levels at around 47 % (Fig. 3d, 3e).
 4 These results suggest that NCI-H460 treatment with complex (2) induces cell death by apoptosis.
 5 To confirm that complex (2) induces apoptosis cell death when incubated with lung cancer cells,
 6 we evaluated the exposition of phosphatidylserine after NCI-H460 treatment with the compound.
 7

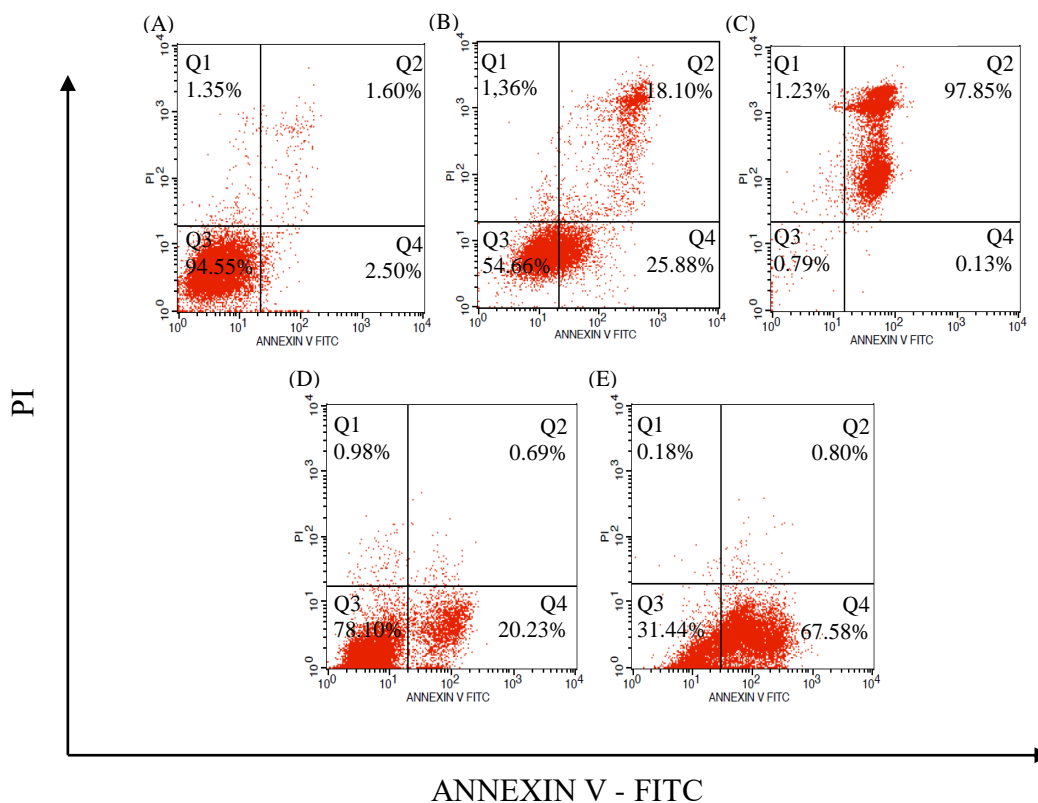


8
 9
 10
 11
 12
 13
 14
 15
 16

Fig. 3 Cell cycle analysis by flow cytometry of NCI-H460 cells after 24 h of incubation. Cells with hypodiploid DNA content were measured by the sub-G1 fraction in the cell cycle pattern. Each experiment per sample was determined by recording 10,000 events. (A) Control cells. (B, C) Cells treated with 1X and 2X IC_{50} of complex (2). (D, E) Cells treated with 1X and 2X IC_{50} of cisplatin

1 Annexin V/PI labeling of exposed phosphatidylserine in viable cells was used to
 2 determine the involvement of apoptosis and necrosis in the cytotoxicity of the copper(II) complex
 3 and cisplatin treatment. Lung cancer cells treated with 1X and 2X IC₅₀ of complex (2) for 24 h of
 4 incubation showed 44 % and 97.85 % of cells in apoptosis (Fig. 4b, 4c), respectively. Cisplatin
 5 positive control was able to promote 20 % and 67 % of apoptosis on NCI-H460 treated with 1X
 6 and 2X IC₅₀ of the drug (Fig. 4d and 4e), respectively. Untreated control cells showed 94.55 % of
 7 viability (Fig. 4a). Taking together the results of sub-G1 cell population analysis and
 8 phosphatidylserine exposition confirm that NCI-H460 cells undergo apoptosis when submitted to
 9 treatment with complex (2), which is consistent with the MTT assay.

10



11
 12
 13
 14
 15
 16
 17
 18
 19
 20

Fig. 4 The Annexin V/PI assay by flow cytometry of NCI-H460 cells after 24 h of incubation. (A) Control cells. (B, C) Cells treated with 1X and 2X IC₅₀ of complex (2). (D, E) Cells treated with 1X and 2X IC₅₀ of cisplatin. The data are presented in the diagrams depicting annexin V/FITC vs PI staining. The percentage of cells in each quadrant is presented: necrotic cells (Q1), late apoptotic cells (Q2), living cells (Q3) and early apoptotic cells (Q4)

1 **Apoptosis induced by complex (2) on NCI-H460 involves mitochondrial dysfunction.**

2 It is well known that cisplatin induces apoptosis by the intrinsic pathway and it is also
3 known that the mitochondrial pathway is commonly activated by most anti-cancer
4 chemotherapeutics. We carried out mitochondria integrity evaluation by fluorescence microscopy
5 using Hoechst/MitoTracker double staining for nucleus and mitochondria, respectively [23]. Fig.
6 5a shows the untreated control of the NCI-H460 indicated viable cells with organized cellular
7 structure, the nucleus appears homogeneous in blue, and a thin red layer in the periphery of the
8 cells corresponds to the mitochondria. Morphological changes were seen in cells after 12 h of
9 incubation with 2X IC₅₀ of complex (2) and cisplatin. Fluorescence patterns revealed typical
10 morphological changes of apoptosis in NCI-H460 cells after treatment with complex (2), such as
11 condensation of chromatin or bright blue fragments of DNA and red fluorescence dispersed in the
12 cytoplasm, evidencing that the complex affected the function of mitochondria (Fig. 5b). While
13 the treatment with cisplatin, DNA fragmentation and binucleation have been evidenced, although
14 the mitochondria appear to be less affected, compared to the control (Fig. 5c).

15

16 **Complex (2) induces decrease of cell microvilli, mitochondria and endoplasmic reticulum**
17 **alterations on lung carcinoma cell line.**

18 The influence of complex (2) on the ultrastructural level of NCI-H460 cell line after
19 treatment with 2X IC₅₀ of complex (2) and with cisplatin for 4, 8 and 12 h of incubation was
20 investigated by SEM (Fig. 6) and TEM (Fig. 7). Analysis by SEM all cells of the untreated
21 control group presented well defined morphology, with innumerable uniform microvilli on cell
22 surfaces (Fig. 6a, 6b). In the first 4 h of treatment, complex (2) was able to induce a rapid
23 response in lung carcinoma cells, forming cell membrane specializations represented in various
24 patterns including formation of cytoplasmic invaginations and decrease of microvilli in the
25 membrane (Fig. 6c). In 8 h of treatment more drastic changes were observed on the cell surface
26 associated with the apoptotic process, such as intense membrane *blebbing* and formation of
27 apoptotic bodies (Fig. 6e). After 12 h of treatment, the cells underwent profound modifications in
28 shape when compared to the control group, losing their typical surface morphology and almost
29 total absence of microvilli (Fig. 6g). In contrast, treatment with cisplatin induced more subtle
30 changes and the most significant results appear only in the longer incubation time (Fig. 6h),
31 indicative that the complex (2) induced cytotoxic activity more rapidly when compared to
32 cisplatin.

1
2
3
4
5
6
7
8
9
10
11
12
13
14
15
16

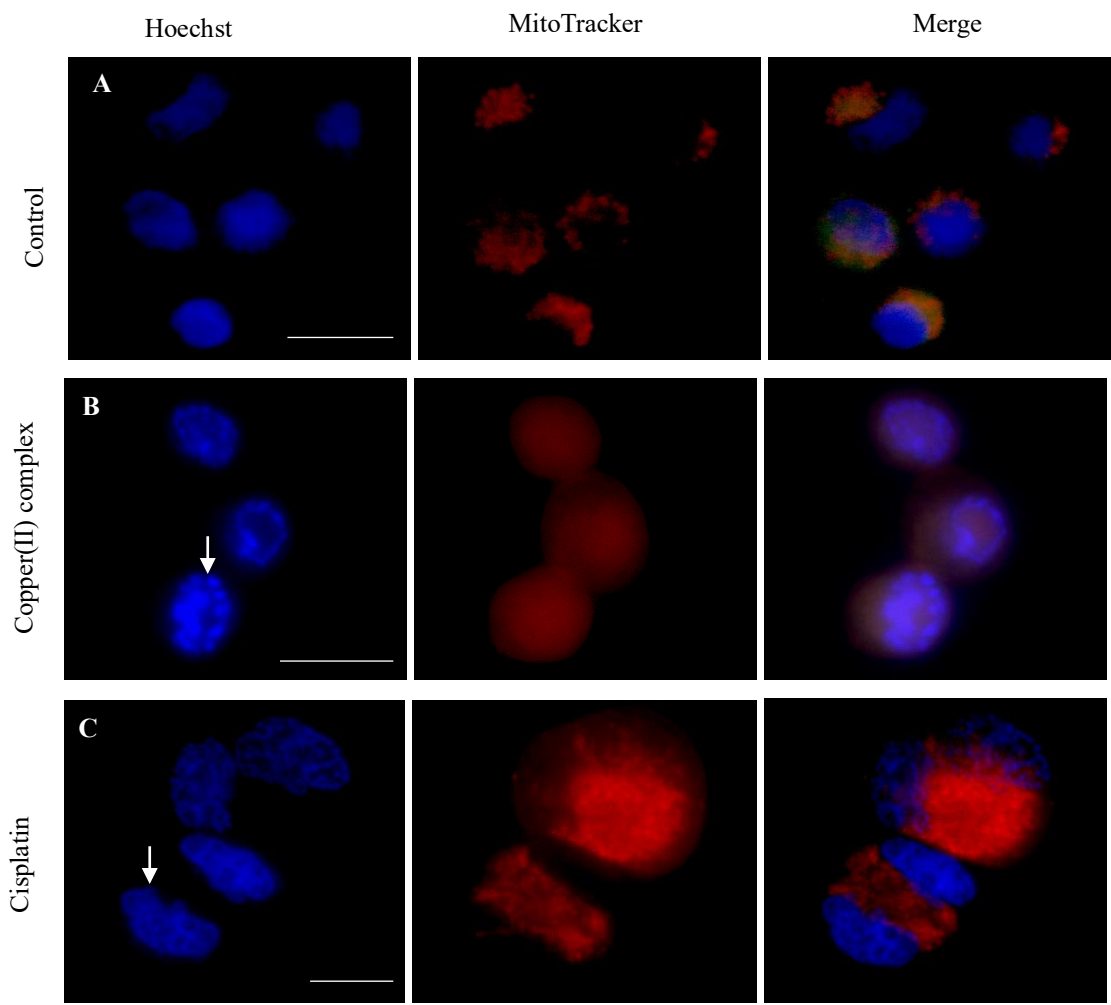


Fig. 5 Morphological analysis of NCI-H460 cells double stained with Hoechst/MitoTracker examined under a fluorescence microscope after 12 h of incubation. (A) Control cells. (B) Cells treated with 2X IC₅₀ of complex (2). (C) Cells treated with 2X IC₅₀ of cisplatin. Chromatin condensation and nuclear fragmentation are indicated by the white arrow. Magnification 400x

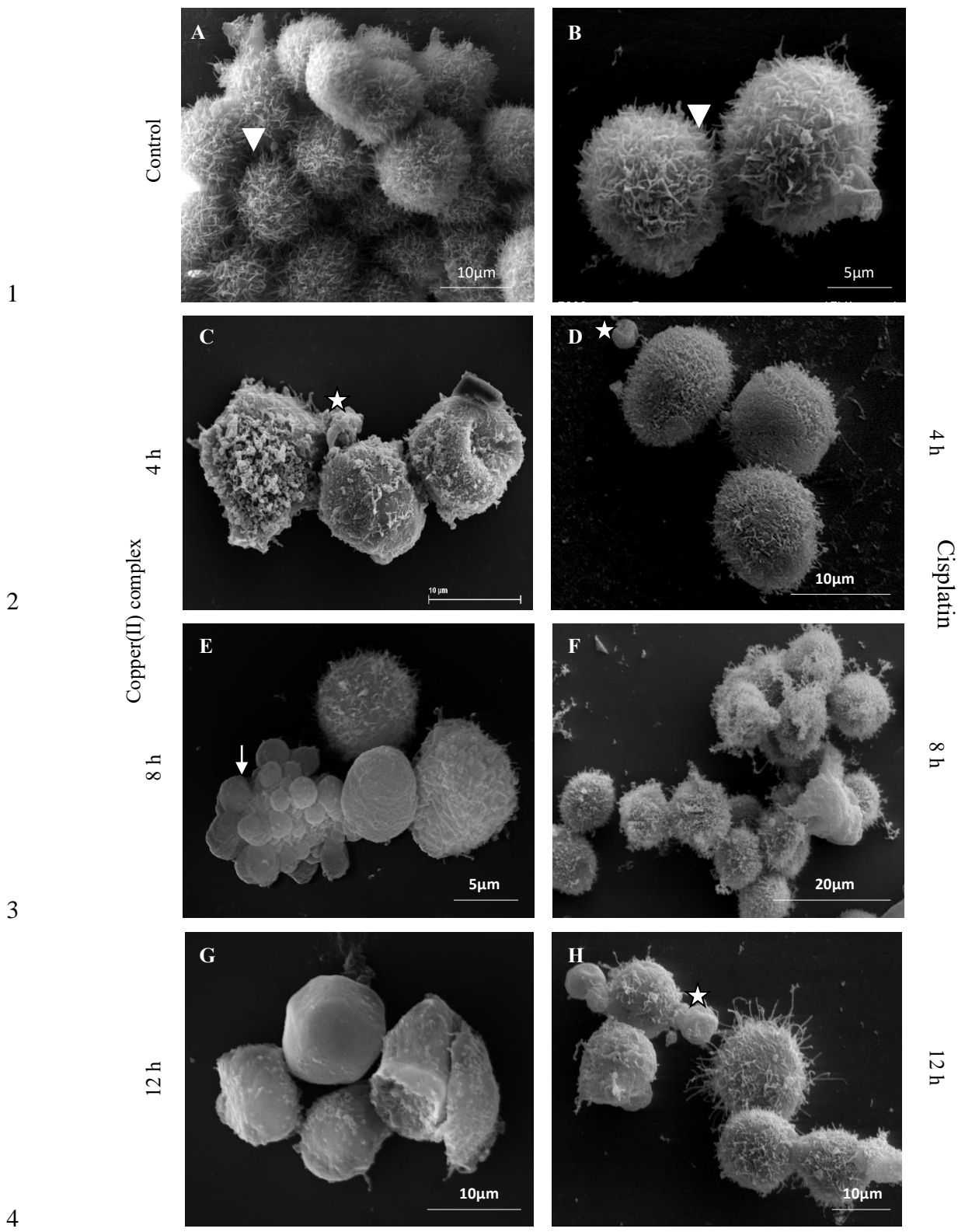


Fig. 6 Morphological analysis of NCI-H460 cells treated with 2X IC₅₀ of copper complex and cisplatin after 4, 8 and 12 h of incubation by SEM. (A, B) Control cells. (C, E, G) Cells treated with complex (2) after 4, 8 and 12 h of

1 incubation. (D, F, H) Cells treated with cisplatin after 4, 8 and 12 h of incubation. Cells with intense membrane
2 *blebbing* [white arrow]. The release of apoptotic bodies can be seen [star]. Numerous microvilli are shown
3 [arrowhead] on the cell surface
4

5 TEM analysis shows that NCI-H460 cells from the untreated control group presented
6 many microvilli throughout the cell surface (Fig. 7a black arrow), which is consistent with the
7 SEM micrographs (Fig. 6a, 6b). Organelles such as mitochondria and ER appeared in large
8 numbers homogeneously distributed throughout the cytoplasm, as well as nuclear chromatin
9 indicating good cell status (Fig. 7a, 7b). On the complex (2) treated cells, cytoplasmic
10 vacuolization was evident, as well as segregation of the chromatin in the periphery of the nucleus,
11 as shown in Fig. 7c. Damage of cell morphology was dependent on time, with drastic changes
12 after 8 h of incubation. As presented in Fig. 7e, the mitochondrial matrix is rarefied, becoming
13 less colored in the image, with some appearing with an empty matrix (indicated by white arrows),
14 at the same time the cytoplasm became progressively more vacuolated, accompanied by
15 chromatin margination and compaction towards in the nuclear periphery, fragmentation of DNA,
16 and ER enlargement. In addition, the number of microvilli on the cell surface decreases
17 considerably (Fig. 7e, 7g) as well as decreased cell density compared with an untreated control
18 group (not shown). However, the plasma membrane remained intact during these morphological
19 changes. NCI-H460 cells treated with cisplatin showed mainly changes in nuclear morphology,
20 increased condensation of the genetic material (star) and the emergence of large electron lucent
21 vacuoles (V). The presence of a network of tubular elements in the cytoplasm (arrowhead) was
22 also observed in the longer incubation time (Fig. 7f, 7h), although less pronounced when
23 compared to treatment with complex (2). This sequence of ultra-structural changes in the
24 cytoplasmic content are in agreement with our finding that complex (2) induces apoptosis in lung
25 carcinoma cells with compromising mitochondrial function and indicates the involvement of ER
26 stress.

27

1
2
3
4
5
6
7

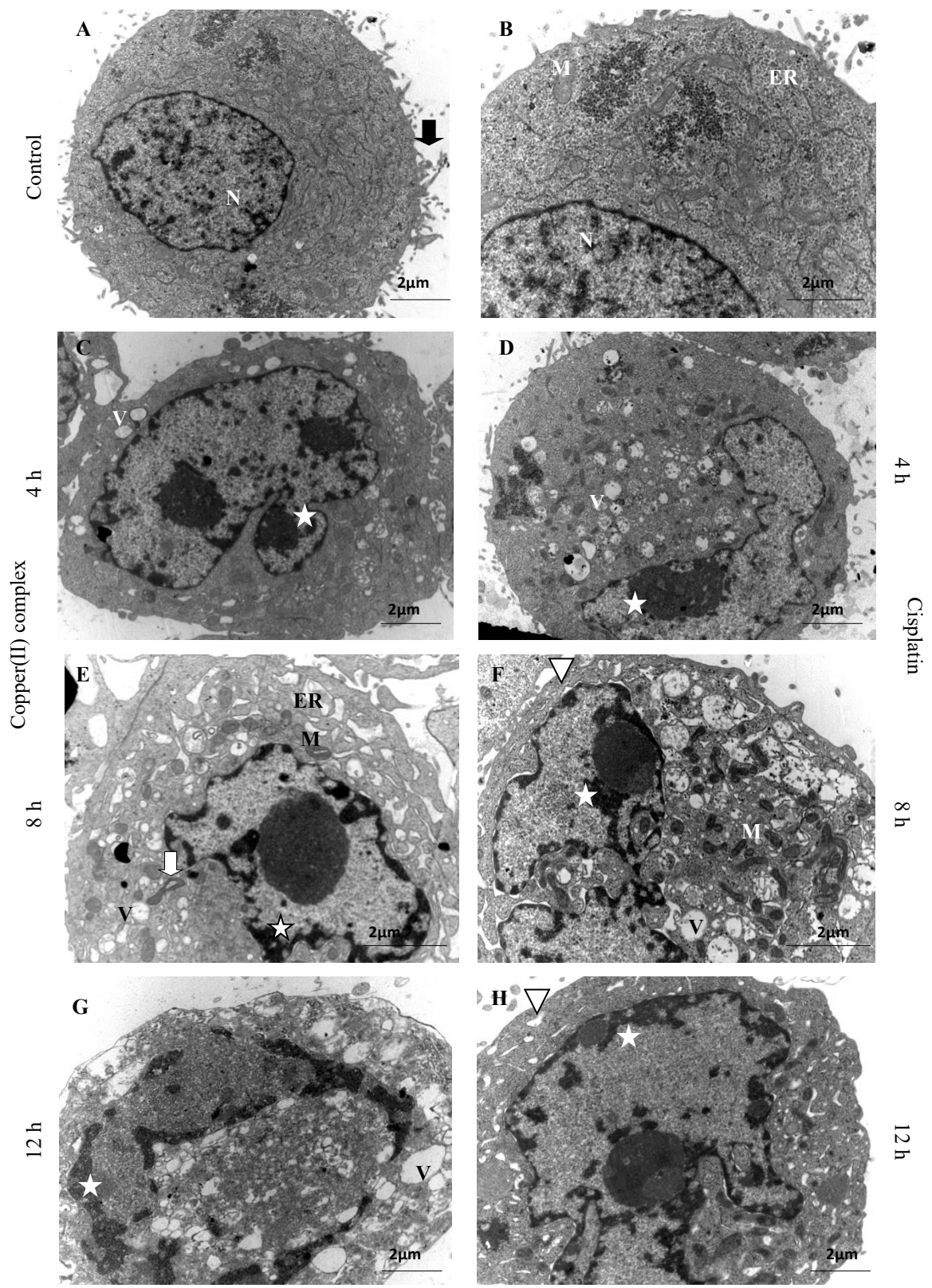


Fig. 7 Ultrastructural analysis of NCI-H460 cells treated with 2X IC₅₀ of copper complex and cisplatin after 4, 8 and 12 h

1 12 h of incubation by TEM. (A, B) Control cells. (C, E, G) Cells treated with complex (2) after 4, 8 and 12 h of
2 incubation. (D, F, H) Cells treated with cisplatin after 4, 8 and 12 h of incubation. Microvilli [arrow] on the cell
3 surface; [M] Mitochondria; [ER] Endoplasmic Reticulum; [V] Vacuoles and [N] Nucleus. Chromatin condensation is
4 indicated by the star

5

6 **NCI-H460 cell line treatment with complex (2) results in decrease of mitochondrial**
7 **membrane potential and endoplasmic reticulum stress with caspase-12 release to cytoplasm**

8 Mitochondrial membrane potential ($\Delta\Psi_m$) plays different roles in a cell and the loss of
9 $\Delta\Psi_m$ is an important parameter to evaluate non-functional mitochondria and its involvement in
10 apoptotic cell death [24] defining the intrinsic pathway. This pathway is the response to several
11 kinds of cell insult that lead to an increase in mitochondrial membrane permeability followed by
12 the release of pro-apoptotic molecules into the cytoplasm [8]. As presented in Fig. 8a, untreated
13 control cells showed high red fluorescence result of aggregated form of JC-1 stain. After
14 treatment with complex (2), for 24 h with 1X and 2X IC_{50} , the monomeric form of JC-1 stain
15 emitting green fluorescence was observed in 69 % and 84 % of treated cells, respectively (Fig.
16 8b, 8c), indicating that the $\Delta\Psi_m$ had collapsed. After treatment with cisplatin with 1X and 2X
17 IC_{50} cells emitting green fluorescence was observed in 24 % and 50 % respectively (Fig. 8d, 8e).
18 Comparing both compounds cooper(II) complex shows more effectiveness than the
19 chemotherapeutic cisplatin to induce NCI-H460 cells death. These data are very consistent with
20 mitochondrial alterations shown by the MitoTracker probe analysis (Fig. 5b) and TEM
21 ultrastructure evaluation (Fig. 7e) after NCI-H460 cells treatment with complex (2). Altogether
22 our data show that complex (2) induces the intrinsic pathway of apoptosis with involvement of
23 mitochondrial dysfunction.

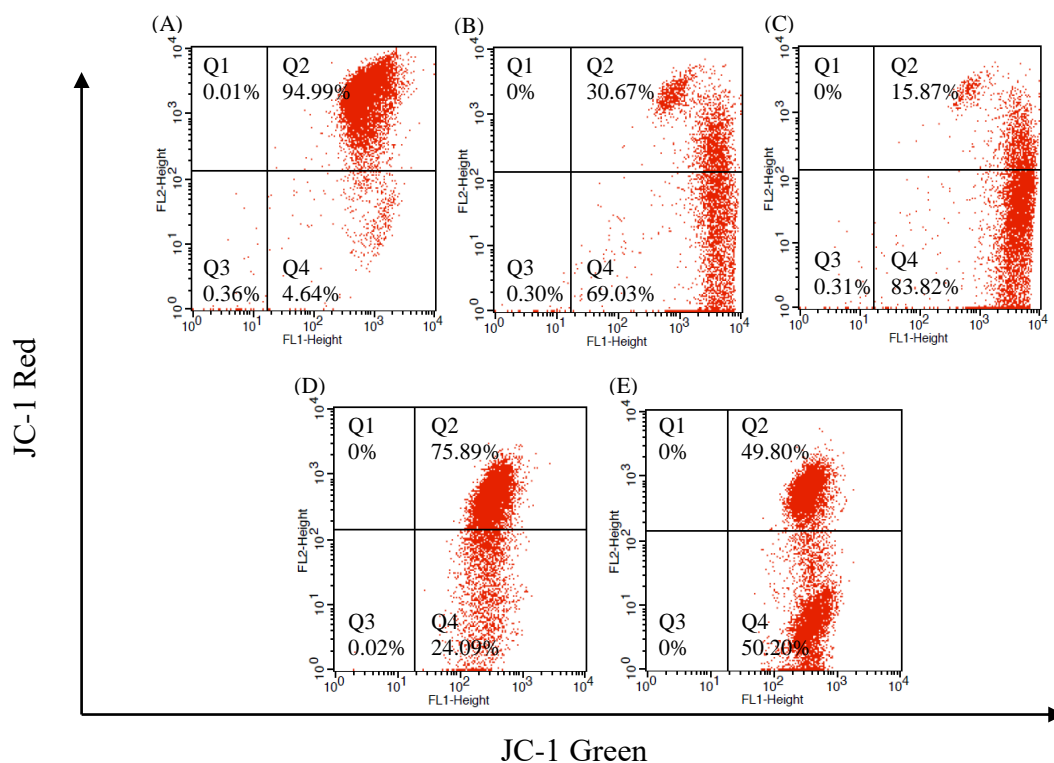
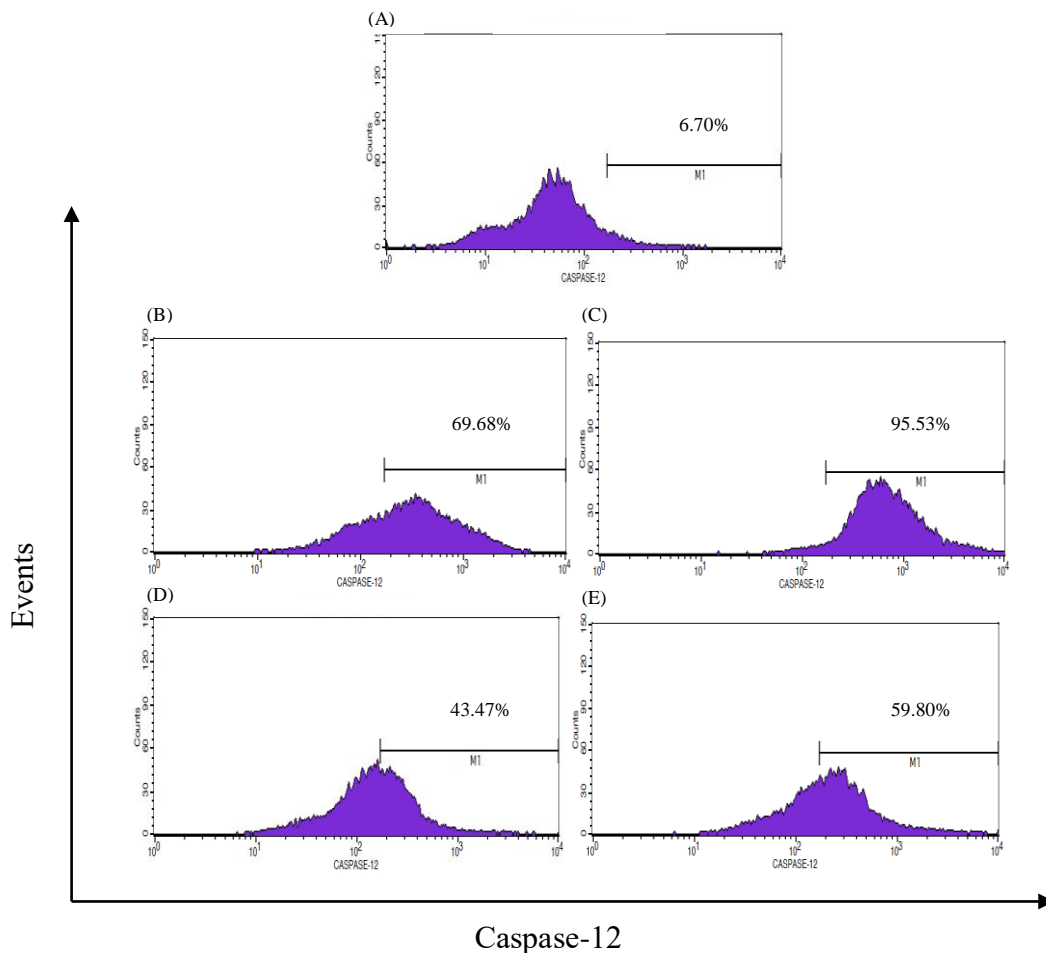


Fig. 8 Mitochondrial membrane potential assay probed by JC-1 staining and flow cytometry analysis. NCI-H460 cells were incubated with complex (2) for 24 h, stained by JC-1 and analyzed by flow cytometry. (A) Control cells. (B, C) Cells treated with 1X and 2X IC₅₀ of complex (2). (D, E) Cells treated with 1X and 2X IC₅₀ of cisplatin

To confirm whether complex (2) induces ER stress on NCI-H460 cells we evaluated the caspase-12 release [25, 26] after cell treatment with the compound. NCI-H460 cells were analyzed by flow cytometry after treatment with 1X and 2X IC₅₀ of complex (2) and cisplatin for 18 h of incubation. Untreated control cells incubated with Z-VAD-FMK (specific caspase-12 substrate) presented about 7% of caspase-12 activation (Fig. 9a) as expected. Cooper(II) complex treated cells Figs. 9b and 9c showed an increase activation of caspases-12 in a dose-dependent manner reaching 69.7% and 95.5% for both concentration used. Cells treated with two different concentration of cisplatin 43.5% and 59.8% of cells showed activated caspases-12 (Fig. 9d, 9e). Our data show that complex (2) has high potential to activate caspase-12 in the lung cancer cells compared with cisplatin, which result in critical events leading to apoptosis. Taking together our *in vitro* results show that complex (2) induces mitochondrial dysfunction and ER stress, driving NCI-H460 cells to apoptosis by the intrinsic pathway.

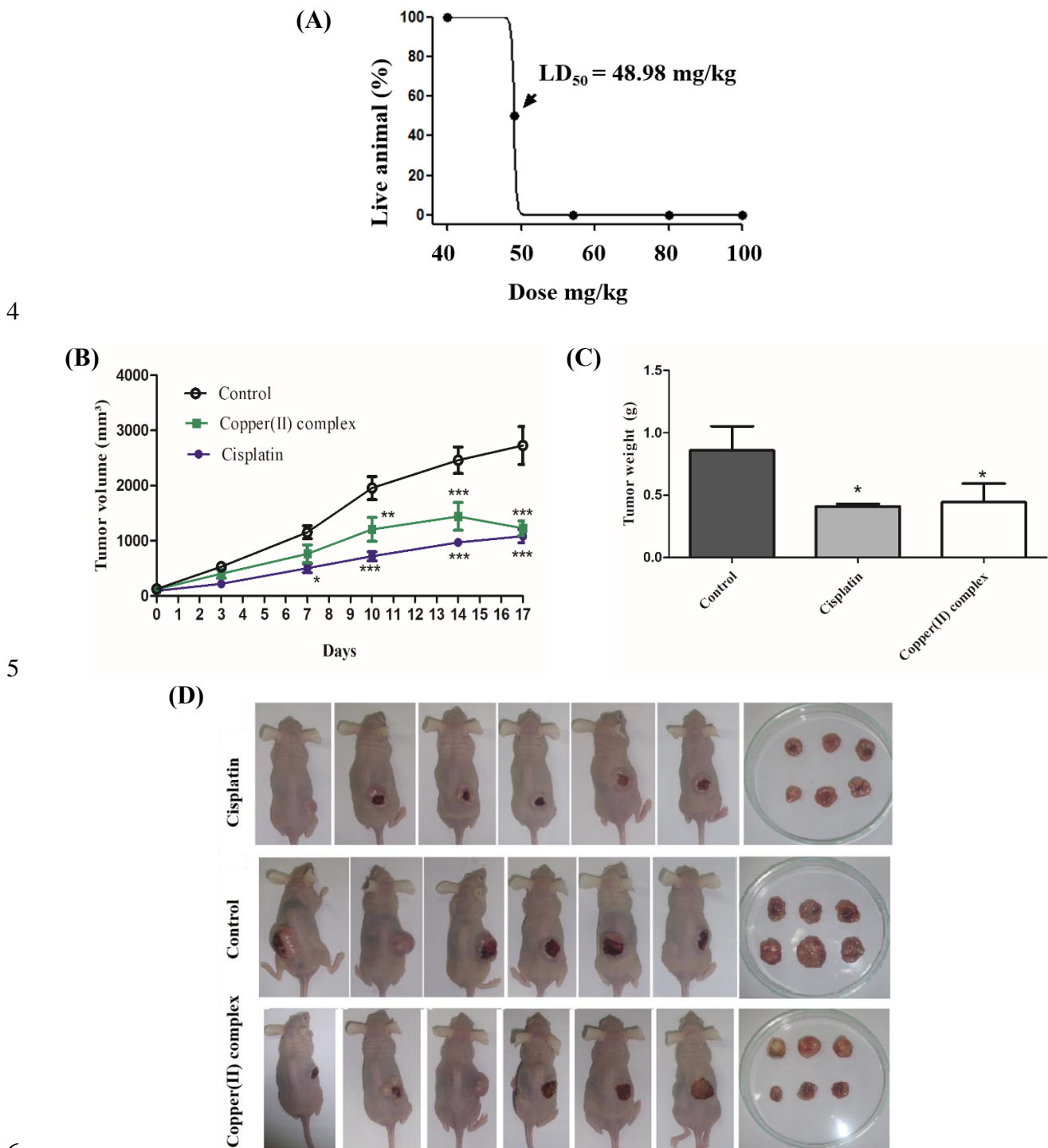


1
2
3
4 **Fig. 9** The activation of caspases-12 by flow cytometry analysis in NCI-H460 cells after 18 h of incubation. (A)
5 Control cells. (B, C) Cells treated with 1X and 2X IC₅₀ of complex (2). (D, E) Cells treated with 1X and 2X IC₅₀ of
6 cisplatin. Results are expressed as relative fluorescent intensities (from left to right)

7
8 **Complex (2) and cisplatin reduce tumor growth in murine model of lung cancer**

9 We start *in vivo* experiments by determining the lethal dose (LD₅₀) of complex (2) in
10 BALB/c *nude* mice. Groups of four animals were injected intra-peritoneally with complex (2) in
11 different concentrations ranging from 40 to 100 mg/kg, and the animal survival was monitored
12 for up to 15 days (Fig. 10a); LD₅₀ was defined at 48.98 mg/kg. BALB/c *nude* mice bearing
13 human lung cancer cells were treated with 50 % of DL₅₀ of each compound, as follows: 25 mg/kg
14 of complex (2) and 3.3 mg/kg of cisplatin [21] in three doses with intervals of seven days.
15 Treatment with the compounds was found to significantly reduce the growth of tumor nodules
16 (Fig. 10b). As shown in Figs. 10c and 10d, cisplatin presented slightly better results under the
17 same experimental conditions, reducing tumor weight by 52 % versus 48 % in treatment with

1 complex (2) when compared to the non-treated control group. Our *in vivo* results are in
 2 agreement with the *in vitro* data showing that complex (2) is cytotoxic to the NCI-H460 lung
 3 cancer cell line.



7 **Fig. 10** Evaluation of tumor growth inhibition by complex (2) in a BALB/c *nude* murine model. A) Lethal dose
 8 determination. LD₅₀ was calculated using Probit analysis. B) and C) Evaluation of tumor growth inhibition. Balb/c

1 *nude* mice bearing NCI-H460 tumor nodules were treated ip with 50% of DL₅₀ of cisplatin or complex (2) in three
2 dose with one week of intervals. D) Images of excised tumors of euthanized mice. Statistical analyses: One-way
3 ANOVA with Tukey multiple comparison test. Significant difference was taken as *p < 0.05, **p < 0.01 and ***p
4 < 0.001 comparing the treated and control groups

6 **Discussion**

7 Inorganic chemistry uses in medicine have been described for many centuries [7, 37].
8 However, only after the clinical success of cisplatin in the 1970s the consolidation of inorganic
9 medicinal chemistry was established [7]. At that time the cytotoxic properties of cisplatin was
10 proven and it was considered one of the most potent drugs used against numerous kinds of
11 cancers. Although Pt-based therapies have been largely used in cancer treatment, two major
12 limitations are commonly observed: the side effects and the high percentage of resistance against
13 the drug [27]. In this sense, copper complexes have attracted considerable attention in anticancer
14 therapy since this metal has shown promising results *in vitro* and in preclinical models
15 attenuating various mechanisms of tumor progression including growth, angiogenesis, and
16 metastasis [28]. Likewise, in this work we investigated the anti-proliferative effects of complex
17 (2) on non-small cell lung carcinoma *in vitro* and *in vivo* assay.

18 Complex (2) showed cytotoxic activity against all tested lines, but the conventional
19 copper salt and the ligand L1 did not affect the viability of any of the cells, showing that the α -
20 naphthol group coordinating with the respective copper ion effectively improved the cytotoxic
21 activity of the compound in agreement to ours previous work [19]. We also reported in this work
22 that cooper(II) complex was cytotoxic against two leukemic cell lines (U937 and THP-1) and less
23 cytotoxic to normal peripheral blood mononuclear cells (PBMC), indicating the selectivity of our
24 compound. When we tested the cooper(II) complex on non-small cell lung cancer NCI-H460 cell
25 line, we observed the IC₅₀ of 26.5 μ M in contrast to cisplatin 203 μ M, demonstrating that
26 cooper(II) complex was more effective than cisplatin the standard chemotherapeutic. Supporting
27 our results, several authors have shown the effective cytotoxicity of the different complexes (2)
28 against breast adenocarcinoma (MCF-7 and MDA-MB-231), lung carcinoma (A549 and NCI-
29 H460) and human gastric cancer (MGC80-3) cell lines [14, 29, 30].

30 The induction of apoptosis is a major goal in the development of antitumor drugs and it
31 is considered the most important target of many cancer treatment strategies [31]. Recent studies
32 have demonstrated that anticancer activity of metal compounds such as copper(II) compounds via

1 intercalative mode, tends to recognize, bind and cause DNA damage to cancer cells, driving them
2 to cell death by apoptosis [32, 33]. In this context, the analysis of the cell cycle performed with
3 NCI-H460 cells treated with copper (II) complex at a higher concentration tested for 24 h showed
4 that 32.14 % occur in the sub-G1 peak, while for cisplatin 46.70 % was observed in the same
5 region of the histogram (Fig. 3). The sub-G1 region of the histogram shows cells with reduced
6 DNA content due to fragmentation caused by the action of endonucleases that are activated in the
7 late stages of apoptosis [34]. Our data show DNA damage in lung cancer cells treated with
8 complex (2), suggesting that cytotoxicity induced by complex (2) results in cell death by
9 apoptosis. Our results are in agreement with previous studies carried out with copper(II),
10 cobalt(II), and platinum(II) complexes obtained with the same ligand in U937 cells. The
11 population of cells that loss DNA content after treatment with these complexes increases
12 significantly when compared to the control cells [16, 19, 20]. Apoptosis is also characterized by
13 exposure of phosphatidylserine on the outside of apoptotic cells, which acts as a signal that
14 triggers removal of the dying cell by phagocytosis [35]. In order to confirm the apoptosis on NCI-
15 H460 cells treated with complex (2), we used annexin V to identify and to quantify the
16 phosphatidylserine exposition on the cell surface by flow cytometry analysis. Our results show
17 that after treatment the percentage of early and late apoptotic cells reaches 97.98 % and 68.38 %
18 for complex (2) and cisplatin respectively (Fig. 4). These data confirm that complex (2) induces
19 apoptosis in NCI-H460 in a dose-dependent manner and is, therefore, worthy of further
20 investigation.

21 It is well established that apoptosis is triggered by two main pathways of intrinsic
22 (mitochondrial) and extrinsic (death receptor) involvement. And the mitochondrial pathway is
23 commonly activated by several anticancer chemotherapeutics. We carried out mitochondria
24 integrity evaluation by fluorescence microscopy using Hoechst/MitoTracker double staining for
25 nucleus and mitochondria respectively [23]. In the control group, living cells (control) with usual
26 nucleus morphology are observed. Nevertheless, the cells treated with copper(II) complex and
27 with cisplatin showed morphological changes which show the apoptosis highlights such as
28 chromatin condensation and nuclear fragmentation, as well as mitochondrial disruption also
29 being evident (Fig. 5). The obtained results corroborate with the apoptosis observed from DNA
30 cleavage by sub-G1 (Fig. 3) and Annexin V/PI (Fig. 4) cell cycle assay. Additionally, the results
31 indicate that the intrinsic pathway of apoptosis was induced by complex (2) with involvement of
32 mitochondrial dysfunction.

1 In order to investigate more deeply the mechanism by which copper (II) complex
2 induces cytotoxicity in the NCI-H460 cell line we performed ultrastructural analysis by SEM and
3 TEM of 4, 8 and 12 h of treatment. Apoptotic cell death is an active and organized process,
4 regulated by caspases that cleave critical proteins leading to morphological and biochemical
5 changes including cell shrinkage, loss of membrane lipid asymmetry, microvilli retraction,
6 formation of membrane *blebbing*, fragmentation and condensation of chromatin, swelling of
7 some organelles such as mitochondria and ER, and formation of apoptotic bodies without
8 compromising adjacent tissues [31]. SEM micrographs illustrated specific surface morphology of
9 NCI-H460 cells, showing the morphological organization, such as the presence of numerous
10 microvilli (cytoplasmic projections) and phyllopodia of these cells (Fig. 6a, 6b), usually
11 associated with their invasive capacity [36]. This aspect was also observed even with less
12 alterations in cisplatin treated cells, whereas complex (2) treated cells presented significant
13 morphological changes in the membrane structure with an irregular surface and several pores.
14 Prolonged treatment resembled distinct apoptotic features such as shrinkage, membrane blebs,
15 and narrowing of phyllopodia with blunt microvilli. These data reveal that complex (2) has a
16 more potent effect compared to cisplatin, altering the membrane cell surface morphology. The
17 TEM analyses of lung cancer cells treated with complex (2) revealed significant damage to the
18 cellular morphology when compared to the untreated control, showing altered mitochondria, and
19 some having an empty matrix. In addition, there is evidence of ER dilatation, again suggesting
20 the possible participation of this organelle in the apoptotic process. In some cells a diffuse
21 cytoplasmic vacuolization was observed, representing cell stress due to the cytotoxic effect of the
22 compound (Fig. 7e, 7g). Taken together, these data and those presented above show
23 mitochondrial impairment, these data are in good agreement with the morphological analysis by
24 fluorescence microscopy against NCI-H460 cells, demonstrating the effectiveness of complex (2)
25 in affecting their morphology. As depicted in micrographs, NCI-H460 cells treated with complex
26 (2) displayed ultra-structural changes such as plasma membrane *blebbing* and decrease of
27 microvilli (Fig. 6c, 6e and 6g), condensation of the chromatin, cell nucleus fragmentation, and
28 vacuolization in times equal or greater than 8 h (Fig. 7c, 7e and 7g), which are typical
29 characteristics of the apoptotic process. Cancer cells possess a broad strategy of invasion and
30 metastasis, and one of the main characteristics of the spread of neoplastic cells is presented by the
31 high number of phyllopodia, which are protrusive filamentous actin and signaling proteins which
32 play a role in cell migration and cell-cell communication, being important to enhance movement

1 and adhesion surrounding stroma [37]. In support of these data, our results shows that treatment
2 of NCI-H460 with copper(II) compound led to the retraction of microvilli and phyllopodia, which
3 is suggestive to interfere with the dynamics of the actin-tubulin system, responsible for adhesion
4 and metastasis, although further studies are needed for better understanding of the biology of
5 these cells.

6 Regulation of the mitochondrial membrane potential ($\Delta\Psi_m$) is an important event for
7 cell viability. The intrinsic pathway of apoptosis can be triggered by different stimuli and
8 mechanisms; however, they all result in the release of cytochrome c and other pro-apoptotic
9 proteins regulated by Bcl-2 family proteins. The release of cytochrome c in the mitochondrial
10 pathway is associated with opening of the mitochondrial permeability transition pore and loss of
11 $\Delta\Psi_m$ [38]. Dysregulation of $\Delta\Psi_m$ is crucial for cell death and induction of apoptosis [24, 39].
12 Several potential anticancer and chemotherapeutic metal-based compounds induce apoptosis as a
13 consequence of mitochondrial collapse [14, 16, 33]. Ours data demonstrate that complex (2) can
14 interfere in the $\Delta\Psi_m$ and are in agreement with cytotoxic activity observed by MTT assay,
15 MitoTracker probe and TEM analysis, and shows that the intrinsic pathway of apoptosis was
16 activated by the compound with the involvement of mitochondrial dysfunction. Our results are in
17 accordance with those published by Qi-Yuan Yang and co-workers showing that gastric cancer
18 cells (MGC80-3) undergo apoptosis after treatment with copper complexes, demonstrating their
19 high cytotoxic activity [29].

20 Caspases are critical mediators of the programmed cell death mechanism as they are the
21 initiators and executioners of the process and eventually lead to a common pathway the execution
22 phase of apoptosis [31]. However, ER stress can also result in cell death, when the ER is injured
23 by the disruption of calcium homeostasis, hypoxia, excess ROS or glucose starvation for
24 example, caspase-12 can be activated by pro-apoptotic factors and translocate from ER to the
25 cytosol and cleaves caspase-9. Activated caspase-9 cleaves and activates effector caspase-3
26 driving cells to apoptosis [40]. Many studies have shown that various metal complexes induce ER
27 stress, and high stress in the cytosol may compromise protein folding capacity and induce
28 apoptosis in cancer cells [41, 42]. Notably, our result shows that the complex (2) and cisplatin
29 increases the levels of activated caspase-12 in the NCI-H460 cell line when treated with the
30 compounds (Fig. 9). Based on the ours result we can conclude that cooper(II) complex induces
31 apoptosis in NCI-H460 lung cancer cell as a result of $\Delta\Psi_m$ collapses and caspase-12 releasing to
32 the cytosol from ER stress. We previously reported that this complex activates caspases-3, 4, 8

1 and 9 in the U937 line, suggesting that both the extrinsic and intrinsic pathways of apoptotic cell
2 death are triggered [19].

3 Although, there are series of reports in the literature describing copper (I,II) cytotoxic
4 activity *in vitro* only a few researches evaluating *in vivo* antitumor efficacy has been published.
5 Animal models have several advantages over *in vitro* cell cultures as tumors develop vasculature
6 and interact with the stroma; therefore, they allow evaluation of toxicity and provide
7 pharmacokinetic data of the agent [43]. In 2016, Borges and coworkers [15] reported the
8 antitumor *in vivo* studies of the antineoplastic activity of the complex [Cu(HL1)Cl₂] against
9 human leukemia THP-1 and murine melanoma B16-F10 cell lines. This complex presents LD₅₀
10 of 24 mg/kg and showed a 92 % inhibition of tumor growth in BALB/c nude bearing a THP-1
11 tumor [15]. Complex (2) showed to be less toxic (LD₅₀ 48.98 mg/Kg) than the standard drug
12 cisplatin (6.6 mg/Kg) [21], but a similar tumor growth inhibition results was observed when
13 compared to cisplatin treatment with half of LD₅₀ concentration. Our result indicates a reasonable
14 possibility to use complex (2) as a less toxic alternative to treat lung cancers.

16 **Conclusion**

17 In this study, we showed the anti-proliferative potential of the complex (2) by decreasing
18 NCI-H460 cell viability by apoptosis involving intrinsic pathway. This process is a result of
19 mitochondrial membrane potential depolarization and activation of caspase-12 associated with
20 ER stress. The complex is further able to significantly reduce the growth of tumor nodules in the
21 *in vivo* model. Thus, we speculated that this compound could be a promising therapeutic
22 candidate for the treatment of NSCLC cells, opening the prospect for further research. New
23 investigations are being carried out aiming to understand more about the anticancer activity of
24 this compound alone or in combination with other traditional chemotherapeutics.

26 **Compliance with ethical standards**

27 This work was financed in part by the Coordenação de Aperfeiçoamento de Pessoal de
28 Nível Superior - Brazil (CAPES) - Finance Code 001, CNPq (Conselho Nacional de
29 Desenvolvimento Científico e Tecnológico) and FAPERJ (Fundação de Amparo à Pesquisa do
30 Estado do Rio de Janeiro).

1 **Conflict of interest**

2 All authors declare no conflict of interests.

3 **Ethical approval Studies**

4 The studies involving the use of animals were approved by the Animal Ethics Use
5 Committee of Darcy Ribeiro North Fluminense State University (Campos dos Goytacazes, Rio de
6 Janeiro, Brazil) – protocol number CEUA 349.

7 **References**

- 8 1. Dasari S, Bernard Tchounwou P (2014) Cisplatin in cancer therapy: Molecular
9 mechanisms of action. *Eur J Pharmacol* 740:364–378.
10 <https://doi.org/10.1016/j.ejphar.2014.07.025>
- 11 2. Dilruba S, Kalayda G V. (2016) Platinum-based drugs: past, present and future. *Cancer*
12 *Chemother Pharmacol* 77:1103–1124. <https://doi.org/10.1007/s00280-016-2976-z>
- 13 3. Medici S, Peana M, Nurchi VM, et al (2015) Noble metals in medicine: Latest advances.
14 *Coord Chem Rev* 284:329–350. <https://doi.org/10.1016/j.ccr.2014.08.002>
- 15 4. Fanelli M, Formica M, Fusi V, et al (2016) New trends in platinum and palladium
16 complexes as antineoplastic agents. *Coord Chem Rev* 310:41–79.
17 <https://doi.org/10.1016/j.ccr.2015.11.004>
- 18 5. Kroemer G, Galluzzi L, Vandenabeele P, et al (2009) Classification of cell death:
19 Recommendations of the Nomenclature Committee on Cell Death 2009. *Cell Death Differ*
20 16:3–11. <https://doi.org/10.1038/cdd.2008.150>
- 21 6. Indran IR, Tufo G, Pervaiz S, Brenner C (2011) Recent advances in apoptosis,
22 mitochondria and drug resistance in cancer cells. *Biochim Biophys Acta - Bioenerg*
23 1807:735–745. <https://doi.org/10.1016/j.bbabi.2011.03.010>
- 24 7. Prokhorova EA, Zamaraev A V., Kopeina GS, et al (2015) Role of the nucleus in
25 apoptosis: Signaling and execution. *Cell Mol Life Sci* 72:4593–4612.
26 <https://doi.org/10.1007/s00018-015-2031-y>
- 27 8. Baig S, Seevasant I, Mohamad J, et al (2016) Potential of apoptotic pathway-targeted
28 cancer therapeutic research: Where do we stand. *Cell Death Dis* 7:e2058.
29 <https://doi.org/10.1038/cddis.2015.275>

- 1 9. De Jongh F, Van Veen R, Veltman S, et al (2003) Weekly high-dose cisplatin is a feasible
2 treatment option : analysis on prognostic factors for toxicity in 400 patients. *Br J Cancer*
3 88:1199–1206. <https://doi.org/10.1038/sj.bjc.6600884>
- 4 10. Al-Majed AA (2007) Carnitine deficiency provokes cisplatin-induced hepatotoxicity in
5 rats. *Basic Clin Pharmacol Toxicol* 100:145–150. [https://doi.org/10.1111/j.1742-
6 7843.2006.00024.x](https://doi.org/10.1111/j.1742-7843.2006.00024.x)
- 7 11. Lainé A-L, Passirani C (2012) Novel metal-based anticancer drugs: a new challenge in
8 drug delivery. *Curr Opin Pharmacol* 12:420–426.
9 <https://doi.org/10.1016/J.COPH.2012.04.006>
- 10 12. Horn A, Fernandes C, Parrilha GL, et al (2013) Highly efficient synthetic iron-dependent
11 nucleases activate both intrinsic and extrinsic apoptotic death pathways in leukemia cancer
12 cells. *J Inorg Biochem* 128:38–47. <https://doi.org/10.1016/j.jinorgbio.2013.07.019>
- 13 13. Fischer-Fodor E, Vălean AM, Virag P, et al (2014) Gallium phosphinoarylbisthiolato
14 complexes counteract drug resistance of cancer cells. *Metallomics* 6:833–844.
15 <https://doi.org/10.1039/c3mt00278k>
- 16 14. Dhivya R, Jaividhya P, Riyasdeen A, et al (2015) In vitro antiproliferative and apoptosis-
17 inducing properties of a mononuclear copper(II) complex with dppz ligand, in two
18 genotypically different breast cancer cell lines. *BioMetals* 28:929–945.
19 <https://doi.org/10.1007/s10534-015-9877-1>
- 20 15. Borges LJH, Bull ÉS, Fernandes C, et al (2016) In vitro and in vivo studies of the
21 antineoplastic activity of copper (II) compounds against human leukemia THP-1 and
22 murine melanoma B16-F10 cell lines. *Eur J Med Chem* 123:128–140.
23 <https://doi.org/10.1016/j.ejmech.2016.07.018>
- 24 16. Morcelli SR, Bull ÉS, Terra WS, et al (2016) Synthesis, characterization and antitumoral
25 activity of new cobalt(II)complexes: Effect of the ligand isomerism on the biological
26 activity of the complexes. *J Inorg Biochem* 161:73–82.
27 <https://doi.org/10.1016/j.jinorgbio.2016.05.003>
- 28 17. Zeng L, Gupta P, Chen Y, et al (2017) The development of anticancer ruthenium(II)
29 complexes: From single molecule compounds to nanomaterials. *Chem Soc Rev* 46:5771–
30 5804. <https://doi.org/10.1039/c7cs00195a>
- 31 18. Elie BT, Fernández-Gallardo J, Curado N, et al (2019) Bimetallic titanocene-gold
32 phosphane complexes inhibit invasion, metastasis, and angiogenesis-associated signaling

- 1 molecules in renal cancer. *Eur J Med Chem* 161:310–322.
2 <https://doi.org/10.1016/J.EJMECH.2018.10.034>
- 3 19. Fernandes C, Horn A, Lopes BF, et al (2015) Induction of apoptosis in leukemia cell lines
4 by new copper(II) complexes containing naphthyl groups via interaction with death
5 receptors. *J Inorg Biochem* 153:68–87. <https://doi.org/10.1016/j.jinorgbio.2015.09.014>
- 6 20. Moreira RO, Morcelli SR, Fernandes C, et al (2019) Modulating the antitumoral activity
7 by the design of new platinum(II) compounds: synthesis, characterization, DFT,
8 ultrastructure and mechanistic studies. *J Inorg Biochem* in press:
- 9 21. Aston WJ, Hope DE, Nowak AK, et al (2017) A systematic investigation of the maximum
10 tolerated dose of cytotoxic chemotherapy with and without supportive care in mice. *BMC*
11 *Cancer* 17:1–10. <https://doi.org/10.1186/s12885-017-3677-7>
- 12 22. Mosmann T (1983) Rapid colorimetric assay for cellular growth and survival: Application
13 to proliferation and cytotoxicity assays. *J Immunol Methods* 65:55–63.
14 [https://doi.org/10.1016/0022-1759\(83\)90303-4](https://doi.org/10.1016/0022-1759(83)90303-4)
- 15 23. Han J, Han MS, Tung CH (2013) A non-toxic fluorogenic dye for mitochondria labeling.
16 *Biochim Biophys Acta - Gen Subj* 1830:5130–5135.
17 <https://doi.org/10.1016/j.bbagen.2013.07.001>
- 18 24. Zorova LD, Popkov VA, Plotnikov EY, et al (2018) Mitochondrial membrane potential.
19 *Anal Biochem* 552:50–59. <https://doi.org/10.1016/j.ab.2017.07.009>
- 20 25. Nakagawa T, Zhu H, Morishima N, et al (2000) Caspase-12 mediates endoplasmic-
21 reticulum-specific apoptosis and cytotoxicity by amyloid- β . *Nature* 403:98–103.
22 <https://doi.org/10.1038/47513>
- 23 26. Morishima N, Nakanishi K, Takenouchi H, et al (2002) An endoplasmic reticulum stress-
24 specific caspase cascade in apoptosis. Cytochrome c-independent activation of caspase-9
25 by caspase-12. *J Biol Chem* 277:34287–34294. <https://doi.org/10.1074/jbc.M204973200>
- 26 27. Kelland L (2007) The resurgence of platinum-based cancer chemotherapy. *Nat Rev Cancer*
27 7:573–584. <https://doi.org/10.1038/nrc2167>
- 28 28. Denoyer D, Clatworthy SAS, Cater MA (2018) Copper complexes in cancer therapy. In:
29 Sigel A, Sigel H, Freisinger E, Sigel RKO (eds) *Metallo-Drugs: Development and Action*
30 *of Anticancer Agents*. De Gruyter, Berlin, Boston, pp 469–506
- 31 29. Yang Q-Y, Cao Q-Q, Qin Q-P, et al (2018) Syntheses, Crystal Structures, and Antitumor
32 Activities of Copper(II) and Nickel(II) Complexes with 2-((2-(Pyridin-2-

- 1 yl)hydrazono)methyl)quinolin-8-ol. Int J Mol Sci Artic 19:2–17.
2 <https://doi.org/10.3390/ijms19071874>
- 3 30. Rogolino D, Cavazzoni A, Gatti A, et al (2017) Anti-proliferative effects of copper(II)
4 complexes with hydroxyquinoline-thiosemicarbazone ligands. Eur J Med Chem 128:140–
5 153. <https://doi.org/10.1016/j.ejmech.2017.01.031>
- 6 31. Wong RS (2011) Apoptosis in cancer: from pathogenesis to treatment. J Exp Clin Cancer
7 Res 30:87. <https://doi.org/10.1186/1756-9966-30-87>
- 8 32. Shobha Devi C, Thulasiram B, Aerva RR, Nagababu P (2018) Recent Advances in Copper
9 Intercalators as Anticancer Agents. J Fluoresc 28:1195–1205.
10 <https://doi.org/10.1007/s10895-018-2283-7>
- 11 33. Mahendiran D, Amuthakala S, Bhuvanesh NSP, et al (2018) Copper complexes as
12 prospective anticancer agents: *in vitro* and *in vivo* evaluation, selective targeting of cancer
13 cells by DNA damage and S phase arrest. RSC Adv 8:16973–16990.
14 <https://doi.org/10.1039/C8RA00954F>
- 15 34. Nunez R (2001) DNA measurement and cell cycle analysis by flow cytometry. Curr Issues
16 Mol Biol 3:67–70. <https://doi.org/https://doi.org/10.21775/cimb.003.037>
- 17 35. Crowley LC, Marfell BJ, Scott AP, et al (2016) Dead cert: Measuring cell death. Cold
18 Spring Harb Protoc 2016:1064–1072. <https://doi.org/10.1101/pdb.top070318>
- 19 36. Balzer EM, Whipple RA, Thompson K, et al (2010) C-Src differentially regulates the
20 functions of microtentacles and invadopodia. Oncogene 29:6402–6408.
21 <https://doi.org/10.1038/onc.2010.360>
- 22 37. Friedl P, Wolf K (2003) Tumour-cell invasion and migration: diversity and escape
23 mechanisms. Nat Rev Cancer 3:362–374. <https://doi.org/10.1038/nrc1075>
- 24 38. Hüttemann M, Helling S, Sanderson TH, et al (2012) Regulation of mitochondrial
25 respiration and apoptosis through cell signaling: Cytochrome c oxidase and cytochrome c
26 in ischemia/reperfusion injury and inflammation. Biochim Biophys Acta - Bioenerg
27 1817:598–609. <https://doi.org/10.1016/j.bbabi.2011.07.001>
- 28 39. Perry SW, Norman JP, Barbieri J, et al (2011) Mitochondrial membrane potential probes
29 and the proton gradient: A practical usage guide. Biotechniques 50:98–115
- 30 40. Dolai S, Pal S, Yadav RK, Adak S (2011) Endoplasmic reticulum stress-induced apoptosis
31 in leishmania through Ca²⁺-dependent and caspase-independent mechanism. J Biol Chem
32 286:13638–13646. <https://doi.org/10.1074/jbc.M110.201889>

- 1 41. Al-Bahlani SM, Al-Bulushi KH, Al-Alawi ZM, et al (2017) Cisplatin Induces Apoptosis
2 Through the Endoplasmic Reticulum-mediated, Calpain 1 Pathway in Triple-negative
3 Breast Cancer Cells. Clin Breast Cancer 17:e103–e112.
4 <https://doi.org/10.1016/j.clbc.2016.12.001>
- 5 42. Zaki M, Arjmand F, Tabassum S (2016) Current and future potential of metallo drugs:
6 Revisiting DNA-binding of metal containing molecules and their diverse mechanism of
7 action. Inorganica Chim Acta 444:1–22. <https://doi.org/10.1016/j.ica.2016.01.006>
- 8 43. Santini C, Pellei M, Gandin V, et al (2014) Advances in Copper Complexes as Anticancer
9 Agents. Chem Rev 114:815–862. <https://doi.org/10.1021/cr400135x>
- 10

5. DISCUSSÃO GERAL

O câncer é uma condição patológica com crescente prevalência e incidência, apesar de todas as pesquisas e avanços conquistados, ainda é uma das preocupações mais latentes na área da saúde em nível mundial (INCA 2018).

Entre os diversos métodos para o tratamento da doença, a quimioterapia é a modalidade em maior uso. Porém, a resistência intrínseca e adquirida aos fármacos antineoplásicos, a heterogeneidade do tumor e a toxicidade sistêmica, são os maiores obstáculos para o seu sucesso clínico, impulsionando extensas pesquisas em busca de novas drogas que possam atuar de forma mais eficaz (FLOREA e BÜSSELBERG, 2011). Entre as abordagens utilizadas, está a síntese de compostos metálicos. De fato, a descoberta da cisplatina por Barnett Rosenberg na década de 1960 foi um marco na história da medicina moderna, desde então, inúmeros compostos baseados em metais foram propostos e atualmente são usados no tratamento de cânceres e outras patologias (MEDICI et al., 2015; NDAGI et al., 2017).

Neste contexto, o desenvolvimento de novos fármacos antitumorais de platina e de outros íons metálicos tem sido motivado pelas potenciais propriedades farmacológicas e anticancerígenas da cisplatina e seus análogos. Entretanto, os efeitos secundários e o percentual de resistência gerada por muitos tumores a esses compostos impulsionaram os pesquisadores ao desenvolvimento de novas estruturas químicas com menor perfil citotóxico, com o objetivo de contornar as limitações clínicas atuais (NDAGI et al., 2017).

Como já relatado anteriormente, os estudos dos processos bioquímicos e fisiológicos envolvidos nas células cancerígenas mostram que a maioria dos quimioterápicos, orgânicos ou sintéticos buscam promover a morte das células pelo mecanismo de apoptose. As complexas alterações genéticas das neoplasias que ocorrem principalmente nos centros regulatórios da apoptose e de suas vias de sinalização, têm destacado este tipo de morte celular como um alvo potencial no planejamento de novos fármacos (TAN et al., 2014). Assim, a morte celular apresenta fundamental importância para o controle da carcinogênese, uma vez que

falhas nesse processo podem promover a sobrevivência e o acúmulo de células transformadas levando à progressão do câncer, sendo de extrema importância o seu estudo, dado o seu impacto na terapêutica (FREZZA et al., 2010; TAN et al., 2014).

Portanto, fundamentando-se nestes aspectos e em estudos prévios do grupo, este trabalho visou demonstrar os efeitos antineoplásico de compostos de coordenação de platina (II) e um composto de coordenação de cobre (II), a fim de fornecer contribuições no desenvolvimento e melhoramento no *design* de novos possíveis metalofármacos.

Nos resultados apresentados no capítulo I, foi relatada a síntese, caracterização e a avaliação da atividade biológica de quatro novos complexos de platina (II) [Pt (HL1) Cl] .H₂O (1), [Pt (HL2) Cl] .H₂O (2), [Pt (HL3) Cl] .H₂O (3) e [Pt (HL4) Cl] .H₂O (4), contra as seguintes linhagens neoplásicas humanas, de leucemia (THP-1, U937, MOLT-4), colorretal (COLO 205) e carcinoma pulmonar (NCI-H460). O *screening* inicial da atividade citotóxica dos complexos foram avaliadas através do ensaio de viabilidade celular utilizando MTT (brometo de 3-(4,5-17 dimetiliazol-2-il)-2,5-difeniltretazólio). Os complexos (3) e (4) são isômeros e apresentam o grupo α e β – naftol na estrutura de seus ligantes, respectivamente. Esses compostos foram os mais ativos, exibindo menores valores de IC₅₀ para todas as linhagens investigadas, conforme mostrado na tabela 5. No ensaio do tipo de morte celular realizado pelo teste de dupla marcação com anexina V/PI induzidos pelos respectivos compostos, foi demonstrado que o complexo (3) promove morte celular por apoptose enquanto o complexo (4) apresentou alta taxa de necrose na linhagem leucêmica U937 (figura 3), demonstrando o efeito da isomeria na atividade biológica. Na avaliação do ciclo celular, averiguou alteração no perfil em relação a controle não tratado, a população de células na região do sub-G1 no histograma, aumentou consideravelmente após o tratamento com complexo (3), resultando em mudança de 7,38 para 61,38%, evidenciando a clivagem do DNA nos estágios mais tardios da apoptose (figura 5). Já na análise do potencial de membrana mitocondrial ($\Delta\Psi_m$), evidenciou que o complexo (3) induziu a redução do potencial de ação da membrana mitocondrial em 96,30% na linhagem testada, mostrando que o tratamento com complexo (3) gera danos na mitocôndria e sugere o envolvimento da via intrínseca de apoptose (figura 4). Na análise ultraestrutural por microscopia eletrônica de transmissão (MET) e

microscopia eletrônica de varredura (MEV) foi possível identificar o potencial tempo-dependente do efeito do complexo 3 sobre a linhagem U937, incluindo alterações tanto na superfície celular como *blebbing* de membrana, quanto alterações em organelas como mitocôndrias e núcleo, uma vacuolização no citoplasma também foi evidente com posterior liberação de corpos apoptóticos, conforme apresentado nas figuras 6 e 7. Além disso, a ativação das caspases 3, 6, 8 e 9 confirmam a indução de morte celular por apoptose e que ambas as vias extrínseca e intrínseca são disparadas nesse processo (figura 8).

Segundo Denoyer e colaboradores (2018), os complexos de cobre têm atraído considerável atenção na terapia anticâncer, uma vez que este metal tem demonstrado resultados promissores frente a diferentes linhagens neoplásicas *in vitro* e em modelos pré-clínicos, inibindo vários mecanismos da progressão tumoral incluindo crescimento, angiogênese e metástase.

Neste sentido, no capítulo II deste trabalho, investigou-se o efeito do tratamento do complexo de coordenação de cobre (II) [Cu(L1)Cl] Cl.2H₂O (figura 1) e da cisplatina sobre a linhagem celular de câncer de pulmão humano NCI-H460 *in vitro* e *in vivo*. O complexo de cobre e seu respectivo ligante [1-{2-hidroxibenzil(2-piridilmetil)amino}-3-(1-naftiloxi)-2-propanol] (L1), foram sintetizados como descrito anteriormente por Fernandes e colaboradores (2015).

O complexo de cobre (II) apresentou IC₅₀ de 26,52 contra 203 µM para cisplatina, demonstrando seu significativo potencial citotóxico em baixas concentrações para a linhagem NCI-H460. Os mecanismos subjacentes à sua atuação farmacológica foram verificados por diferentes ensaios experimentais. O teste de coloração de anexina V/PI, mostraram que após o tratamento a porcentagem de células apoptóticas precoces e tardias chegou a 97,98% para o complexo cobre e de 68,38% para a cisplatina, respectivamente (figura 4). Análise do ciclo celular (Sub-G1), demonstrou que após 24 horas de tratamento com o complexo de cobre, 32,14% das células encontravam-se no pico sub-G1, enquanto que para a cisplatina foi observado 46,70% na mesma região do histograma (figura 3). Na avaliação do potencial de membrana mitocondrial ($\Delta\Psi_m$), verificou-se que após tratamento com 2X IC₅₀, o complexo de cobre foi mais ativo do que a cisplatina, capaz de reduzir o $\Delta\Psi_m$ em quase 85%, enquanto a cisplatina nas mesmas

condições reduziu em apenas 50,20% (figura 8), indicando que a citotoxicidade induzida pelo complexo de cobre (II) resulta em disfunção desta organela. Já a ativação de caspase 12, que está relacionada com o estresse do retículo endoplasmático, evidenciou que após o tratamento com o complexo e com a cisplatina, houve um aumento na atividade de caspase 12 de aproximadamente 96% e de 60%, respectivamente, sugerindo a participação desta organela na amplificação do sinal apoptótico (figura 9).

Alterações morfológicas e ultraestruturais foram detectadas por microscopia de fluorescência, MEV e MET sobre a linhagem NCI-H460, após tratamento com o complexo de cobre, reforçando o desencadeamento de morte celular por apoptose, uma vez que, diversas estruturas celulares apresentaram alterações fenotípicas características deste processo incluindo *blebbing* de membrana, diminuição das microvilosidades na superfície celular, fragmentação de DNA, além de alteração nas mitocôndrias e no retículo endoplasmático (figuras 5, 6 e 7).

Baseado nessa premissa e pelo fato dos resultados apresentados anteriormente, ou que já foram previamente publicados pelo grupo sugerirem a ativação da morte celular por apoptose (FERNANDES et al., 2015; MORCELLI et al., 2016), é possível afirmar que estes complexos metálicos parecem atuar de maneira semelhante, permitindo inferir que o sinal apoptótico disparado por eles, induzem alterações funcionais e ultraestruturais dose e tempo-dependentes, demonstrando que compostos desta natureza são eficazes tanto em neoplasias sanguíneas quanto em tumores sólidos, confirmando seu amplo espectro de atuação.

Além da capacidade indutora de apoptose *in vitro*, o potencial antitumoral do complexo de cobre (II) também foi averiguado em modelo murino *in vivo* no tratamento de lesões cancerígenas de células de câncer de pulmão NCI-H460. Os tumores do grupo tratado com o complexo de cobre apresentaram uma redução de aproximadamente 48% do volume tumoral, significativamente menor do que os tumores do grupo controle, demonstrando notável atuação próxima dos valores da cisplatina, que reduziu o volume tumoral em 52% (figura 10 – capítulo II). As análises imuno-histoquímicas das lesões tumorais confirmaram que o tratamento com o complexo de cobre também induziu morte celular *in situ*, identificada através das marcações para TUNEL. Esse teste baseia-se na marcação direta do DNA

nuclear danificado (LOO, 2011), sugerindo que este composto é capaz de induzir *in vivo* a morte de células de câncer de pulmão humano da linhagem NCI-H460 (dados não mostrados). Portanto, os resultados obtidos neste trabalho, ratificam a substancial atividade farmacológica dos compostos baseados em metais, em especial os de platina (II) e o de cobre (II).

Em 2015, Fernandes e colaboradores demonstraram a atividade citotóxica de quatro complexos de coordenação de cobre. O complexo contendo o grupo α -naftol em seu ligante apresentou maior atividade do que a cisplatina frente as linhagens leucêmicas U937 (8,2 vs 16,25 μ M) e valores muito próximos na linhagem THP-1 (11,3 vs 11,84 μ M), respectivamente. Além disso, no ensaio *in vivo*, foi determinada a DL₅₀ (dose letal mediana que mata 50% do grupo de animais) do complexo de cobre usando camundongos C57BL/6, apresentando DL₅₀ de 55 mg/kg contra 14,5 mg/kg de cisplatina, demonstrando que esse composto é quase quatro vezes menos tóxico do que o fármaco padrão. O mecanismo de morte celular evidenciou que o sinal de apoptose desencadeado pelo complexo parte inicialmente da via extrínseca envolvendo a ativação de caspase 8, posteriormente é amplificado pela mitocôndria, uma vez que houve redução do potencial de membrana mitocondrial em aproximadamente 87%, com a liberação concomitante do citocromo c e ativação da caspase 9, além disso, alterações no DNA e nas mitocôndrias também foram detectadas, mediante análise de microscopia de fluorescência e microscopia eletrônica de transmissão (MET).

Morcelli e colaboradores (2016), relataram a síntese e a atividade citotóxica de três novos compostos de cobalto (II), frente às linhagens leucêmicas (U937, THP-1, MOLT-4), carcinoma colorretal (COLO 205) e carcinoma de pulmão (NCI-H460). Novamente, é observada a mesma relação descrita anteriormente, pois dentre os complexos testados, o que contém o grupo α -naftol em sua estruturação foi o mais ativo e exibiu valores de IC₅₀ inferiores aos da cisplatina para as linhagens COLO 205 (90 vs 196 μ M) e NCI-H460 (147 vs 197 μ M), respectivamente. Além disso, o complexo demonstrou não afetar a viabilidade das células normais (PBMC), exibindo valores de IC₅₀ de >400 μ M. A investigação do tipo de morte celular induzido pelo complexo de cobalto, sugere que a atividade citotóxica contra a linhagem leucêmica U937 é mediada por via apoptótica, associada à disfunção mitocondrial, uma vez

que, a ação do potencial de membrana mitocondrial foi reduzida em aproximadamente 98%, seguido de análise por MET que apoiam essa hipótese.

É interessante ressaltar que os resultados observados para os complexos sintetizados pelo grupo com centros metálicos de Cu (II), Co (II) e Pt (II), os que apresentaram derivados do grupamento naftol retrataram a mesma tendência de atividade, o que nos leva a acreditar que a inserção deste grupo na estruturação racional dos complexos seja o modulador de sua alta bioatividade com os sistemas biológicos, uma vez que os sais inorgânicos e os ligantes isolados utilizados nas sínteses dos complexos, demonstraram pouca ou nenhuma atividade na redução da viabilidade celular das linhagens testadas, sugerindo que a citotoxicidade dos complexos contra as células neoplásicas é dependente do íon metálico e isomerismo apresentado pelo ligante ao qual ele está coordenado.

Para o complexo de platina (3) e para o complexo de cobre (II) estudados nos capítulos I e II, respectivamente, os valores de IC₅₀ variaram de 6 até 51 µM em diferentes linhagens neoplásicas (tabela 5 – capítulo I; tabela 1 – capítulo II). Refletindo a relevância do potencial farmacológico de cada composto e inferindo diretamente no grau de sensibilidade de cada linhagem celular, uma vez que a complexidade morfológica e fisiológica, além das inúmeras alterações genéticas que ocorrem entre os diferentes tipos de câncer, revele um padrão de resposta à citotoxicidade induzida por eles (ROSAS et al., 2013; WANG et al., 2018).

O advento da cisplatina levou ao desenvolvimento de milhares de outros compostos baseado neste metal, incluindo complexos de platina (IV), multinucleares, de geometria *trans* ou monofuncionais, alguns dos quais já estão sendo submetidos a ensaios clínicos para diagnóstico e tratamento, na busca de compostos metálicos alternativos com propriedades anticancerígenas e farmacocinéticas melhoradas, bem como na estruturação de análogos que possam ser administrados por via oral ou formulações lipossomais, por exemplo (WHEATE et al., 2010; DILRUBA e KALAYDA, 2016; NDAGI et al., 2017).

Embora a transplatina *trans*-[Pt(NH₃)₂Cl₂] não tenha alcançado o mesmo sucesso clínico do seu isômero, estudos vêm demonstrando a atividade promissora de derivados de platina com geometria *trans*, uma vez, que podem interagir de forma diferenciada com o DNA, além de exibir elevada atividade antitumoral em cânceres

refratários à cisplatina (ARIS e FARRELL, 2009; DILRUBA e KALAYDA, 2016). Skander e colaboradores (2010) relataram a atividade antineoplásica de uma série de complexos *trans*-configurados de Pt (II) mono e bimetálicos estruturados com um grupamento de aminas aromáticas, o complexo mononuclear (NHC) exibiu elevada citotoxicidade, induziu a translocação de fatores pró-apoptóticos e ativação de caspase 12 em linhagem de leucemia (CEM) e carcinoma pulmonar (NCI-H460). Além disso, foi eficiente contra linhagens resistentes à cisplatina, incluindo câncer de ovário (A2780 e SK-OV-3), câncer de pulmão (DDP) e linfoma (CH1).

Vários compostos metálicos vêm apresentando potencial atividade em contornar a resistência às drogas e aos efeitos colaterais da cisplatina e seus análogos, demonstrando impressionante espectro de atuação para vários tipos de tumor, assim como mecanismos de ação distintos dos atuais fármacos baseados em platina, por exemplo, complexos que interagem com proteínas intra e extracelulares, com metaloenzimas ou que visem as mitocôndrias e retículo endoplasmático, são promissores por predispor as células cancerígenas à morte celular (WANG e GUO, 2008; LOVEJOY e LIPPARD, 2009; FEI CHIN et al., 2011; FISCHER-FODOR et al., 2014; YANG et al., 2016; IRACE et al., 2017; WANG et al., 2018). As mitocôndrias são os produtores de energia das células, como tal, são vitais para a geração de ATP, o que torna o metabolismo mitocondrial um alvo potencial para a terapia do câncer (ZOROVA et al., 2018), como no exemplo mostrado a seguir.

Dois complexos de platina (II) estruturados com derivados de quinolina foram investigados recentemente por Wang e colaboradores (2018). O complexo Mon-Pt-2 exibiu maior atividade inibitória contra hepatocarcinoma (BEL-7404 e HepG-2), câncer de ovário (SK-OV-3), câncer colorretal (HCT116), câncer de pulmão (A549) e apresentou menor toxicidade contra células hepáticas normais HL-7702 quando comparado com a cisplatina. Os resultados apontaram que o complexo Mon-Pt-2 por sua função lipofílica se acumula principalmente nas mitocôndrias, no qual iniciou uma série de eventos associados à disfunção desta organela, incluindo depleção de ATP, perda do $\Delta\Psi_m$, liberação significativa de EROs e a inibição de TrxR induziram uma aparente resposta de estresse de RE, bem como a aumento da expressão de proteínas relacionadas com a autofagia, sugerindo que o complexo

Mon-Pt-2 pode induzir simultaneamente tanto apoptose dependente da via intrínseca como autofagia em células de carcinoma de pulmão A549.

Neste sentido, conforme apresentado nos capítulos I e II deste trabalho, tanto o complexo de platina (3) quanto o de cobre (II) demonstraram a substancial capacidade de reduzir o potencial de ação da membrana mitocondrial em 96,30% (figura 4) e em aproximadamente 85% (figura 8) em linhagem de leucemia U937 e carcinoma de pulmão NCI-H460, respectivamente. O complexo de platina ativou as caspases 3, 6, 8 e 9 já nas primeiras horas de tratamento, permitindo inferir o sinal apoptótico induzido por ele. Já o complexo de cobre induziu 95,93% de ativação de caspase 12, além disso, foi previamente relatado a liberação de citocromo c do espaço intermembranar após colapso mitocondrial quando células leucêmicas foram tratadas com este complexo (FERNANDES et al., 2015). Apoiando esses dados, alterações ultraestruturais nas células U937 e NCI-H460 tratadas com ambos os complexos foram detectadas por MET, sugerindo que essas organelas possam ser possíveis alvos no disparo da maquinaria apoptótica. Nossos resultados são coerentes com fato da citotoxicidade de vários complexos metálicos, serem mediados pela capacidade de alterar as funções mitocondriais (INDRAN et al., 2011; ZHANG et al., 2017).

O estudo das propriedades farmacológicas *in vitro* e a avaliação do potencial de eficácia clínica desses novos protótipos *in vivo* em modelos animais, é um passo essencial para desenvolvimento de novos candidatos a metalofármacos, não à toa, pesquisadores em todo o mundo tem buscado substâncias com propriedades anticâncer que promovam a morte celular (TAN et al., 2014).

Os compostos de coordenação de cobre estão em crescente desenvolvimento na pesquisa de novos agentes anticâncer. Investigações com esse metal tornaram-se atraentes, principalmente porque apresentam propriedades adequadas para aplicações biológicas, uma vez que o cobre 2+ é um oligoelemento crucial para a maioria dos organismos vivos, importante para a função de várias enzimas que envolvem reações de oxi-redução. São inúmeros os exemplos na literatura de ligantes complexados ao cobre, gerando compostos com elevada atividade contra diversos tipos de linhagens neoplásicas, tanto *in vitro* quanto *in vivo* (TAN et al., 2014; DENOYER et al., 2015; NDAGI et al., 2017; XIE et al., 2018).

Recentemente Yang e colaboradores (2018), relataram o perfil citotóxico de dois complexos, um estruturado com o cobre (II), $[\text{Cu}(\text{L})\text{Cl}_2] \cdot 2$ (1) e o outro com níquel (II) $[\text{Ni}(\text{L})\text{Cl}_2]\text{CH}_2\text{Cl}_2$ (2). O complexo de cobre (1) foi o mais ativo e exibiu atividade inibitória mais alta do que a cisplatina contra células de cânceres de ovário (SK-OV-3), estômago (MGC80-3) e cervical (HeLa) com valores de IC_{50} de $3,69 \pm 0,16$, $2,60 \pm 0,17$ e $3,62 \pm 0,12$ μM , respectivamente. A avaliação do ciclo celular sugere que complexo (1) causa a permanência das células MGC80-3 na fase S, o que levou à regulação negativa de proteínas relacionadas como a Ciclina A, Ciclina B e p53. Além disso, observou-se que a relação entre as concentrações das proteínas bcl-2 e BAX foi diminuída, ocorrendo perda do potencial de membrana mitocondrial, com consequente liberação de citocromo c, aumento de EROs e nos níveis de Ca^{2+} intracelular, além de ativação das caspases 3 e 9, sugerindo o desencadeamento da via intrínseca de apoptose em células MGC80-3.

Em outro estudo, Borges e colaboradores (2016) analisaram a atuação farmacológica de um composto de cobre (II) $[\text{Cu}(\text{HBPA})\text{Cl}_2]$, contendo uma piridina em seu ligante frente às linhagens leucêmicas (THP-1, U937, HL60, MOLT-4, JURKAT), colorretal (COLO 205) e de melanoma metastático murino B16F10. O complexo exibiu melhor atividade inibitória contra células THP-1 e B16F10 com valores de IC_{50} de $23,70 \pm 1,12$ e $21,11 \pm 1,17$ μM , respectivamente. O composto induziu altas taxas de apoptose na linhagem THP-1 que foi determinada por monitoramento do ciclo celular, onde 81,34% das células encontravam-se no pico sub-G1 e pela análise de exposição da fosfatidilserina, marcadas por anexina V-FITC/PI, sendo observado em 92% da população celular. Além disso, observou-se liberação do citocromo c para o citoplasma, ativação de caspases 3, 6, 8 e 9, sugerindo que ambas as vias de apoptose são ativadas. Nos estudos *in vivo* em modelos murinos, o complexo apresentou uma inibição significativa de 92% e 87% do crescimento tumoral no desenvolvimento das lesões de células THP-1 e B16F10, respectivamente.

Desse modo, em concordância com os relatos da literatura, neste trabalho averiguamos que ambos os complexos de platina (3) e de cobre (II) induzem aumento no índice apoptótico das linhagens U937 e NCI-H460, respectivamente. Por exemplo, no ensaio monitorado pelo teste de coloração de anexina V/PI, que

após o tratamento com os complexos a porcentagem de células apoptóticas foram de quase 100% (figura 3 - capítulo I e figura 4 - capítulo II). Já a citometria de fluxo permite a identificação e quantificação de células com baixo conteúdo de DNA que aparecem na região sub-G1 do ciclo celular, neste ensaio foi demonstrado alteração no perfil em relação ao controle não tratado, a população de células na região sub-G1 no histograma aumentou consideravelmente de 7,38 para 61,38% (figura 5 – capítulo 1) para o complexo de platina (3) e de 5,10% para 32,14% (figura 3 – capítulo II) para o complexo de cobre. Os dados aqui descritos, sugere ainda a possível interação dos complexos com a molécula de DNA, o que levaria a ativação de uma cascata de sinalização, como externalização de fosfatidilserina, ativação de caspases, desencadeando morte celular via apoptose.

Além disso, avaliamos *in vivo* o potencial antineoplásico do complexo de cobre (II) em modelo murino de células de carcinoma pulmonar NCI-H460, no qual foi observada menor toxicidade aguda do que a cisplatina e redução significativa de 48% no volume tumoral (figura 10 – capítulo II). Nossos dados demonstram que complexos desta natureza podem exercer uma atividade anticâncer eficazmente, corroborando com alguns trabalhos que também ratificaram resultados semelhantes (LIU et al., 2016; MAHENDIRAN et al., 2018).

A descoberta da atividade citotóxica de complexos com outros metais além da platina e do cobre, como ferro, paládio, ouro, ósmio, irídio, zinco, gálio, cobalto, rutênio e titânio, também tem ampliado o leque de íons metálicos que vêm sendo estudados para este fim (DEO et al., 2016; MEDICI et al., 2015; NDAGI et al., 2017). Por exemplo, complexos de rutênio tem sido objeto de extensiva pesquisa, devido a sua atuação farmacológica promissora, apresentando baixa toxicidade para células normais, propriedades antimetastáticas (inibição de metaloproteínas), além de proporcionarem forte interação com o DNA e com proteínas intra e extracelulares (ZENG et al., 2017).

O composto de rutênio (II) denominado NAMI-A em triagem clínica de fase II, tem apresentado excelentes resultados *in vivo*, exibindo eficácia contra processos de metástases de cânceres de pulmão, colorretal e ovário e, atualmente, está sendo testado para o uso como uma terapia de segunda linha contra câncer de pulmão de

células não pequenas em combinação com o fármaco Gemcitabina (TRONDL et al., 2014; ZENG et al., 2017).

O gálio (III) é um dos íons metálicos que também está em crescente investigação. O composto de gálio (III) KP46 está atualmente em testes clínicos de fase II, como um composto administrável por via oral para o tratamento de uma variedade de neoplasias, incluindo melanoma, ovário, mama, cólon, pulmão e bexiga e de câncer ovariano e de cólon resistentes à cisplatina. O mecanismo de ação de alguns compostos com este metal pode estar relacionado a sua interação com ácidos nucleicos, modulação da expressão de proteínas relacionadas ao ciclo celular, inibição de proteossoma e aos seus efeitos anti-mitóticos (CHITAMBAR, 2012; FISCHER-FODOR et al., 2014; TAN et al., 2014; ELLAHIOUI et al., 2017).

Acredita-se que a baixa toxicidade sistêmica apresentada pelos complexos contendo esses dois metais brevemente relatados, seja atribuída à habilidade que estes elementos têm em mimetizar o ferro (II e III) na ligação a certas biomoléculas, incluindo a transferrina e a albumina, proteínas responsáveis entre outras funções, pela solubilização e transporte de ferro. Como resultado dessas propriedades, complexos de rutênio e gálio poderiam seguir uma via bioquímica análoga, o que levaria ao bloqueio de ciclos biológicos em processos críticos dependentes de ferro (FISCHER-FODOR et al., 2014).

Todo este contexto ressalta a necessidade de pesquisas para o desenvolvimento de novas alternativas terapêuticas, principalmente estudos visando a busca de novos fármacos que possam combater neoplasias. Embasados nos relatos apresentados, os complexos metálicos, destacam-se neste cenário e constituem-se como grande promessa para os próximos anos. A versatilidade sintética dos ligantes permite a obtenção de um amplo espectro de compostos bioativos, especialmente como potenciais antitumorais, portanto, desvendar os mecanismos de ação desses novos compostos é um grande desafio a ser conquistado pela química inorgânica medicinal (TAN et al., 2014; LIANG et al., 2017; NDAGI et al., 2017).

Assim, a abordagem sobre a investigação anticâncer dos complexos de platina (3) e de cobre (II) mostrou resultados consistentes de citotoxicidade. Neste trabalho, evidenciamos a inibição da proliferação celular nas células de leucemia

U937 e carcinoma pulmonar NCI-H460, revelada pela alta taxa de apoptose induzida pelos complexos de platina e de cobre, respectivamente. Embasado nos relatos da literatura e na atuação farmacológica *in vitro*, o potencial de membrana mitocondrial foi substancialmente reduzido após tratamento com ambos os complexos, apoiando nossa hipótese de que a disfunção mitocondrial está envolvida na promoção da morte celular. Além disso, a ativação das caspases 3, 6 8 e 9 promovida pelo complexo de platina (3) confirmaram a indução de morte celular por apoptose e que ambas as vias extrínseca e intrínseca são disparadas nesse processo. Para o complexo de cobre (II) houve ainda a ativação da caspase 12 que foi notavelmente aumentada em células NCI-H460, sugerindo a participação do retículo endoplasmático na amplificação do sinal apoptótico. Corroborando com os ensaios quantitativos, alterações morfológicas e ultraestruturais detectadas neste trabalho amparam nossos achados, uma vez que a ativação das caspases executoras têm efeito sobre o citoesqueleto e proteínas citoplasmáticas que clivam substratos específicos contribuindo para as alterações morfológicas fenotípicas da apoptose, incluindo retração de filopódios, *blebbing* de membrana, fragmentação de DNA, vacuolização e liberação de corpos apoptóticos (Wong et al., 2011). Finalmente, investigamos o potencial terapêutico *in vivo* do complexo de cobre em modelo murino de câncer, demonstrando que assim como a cisplatina, o complexo de cobre reduziu significativamente o volume tumoral.

Diante dessas observações, é possível sugerir que os compostos investigados apresentam perfil farmacológico promissor, e demonstram potencial de novos protótipos de metalofármacos, dignos de mais investigações para o tratamento de um amplo espectro de neoplasias.

Por fim, este trabalho ratifica o crescente interesse na medicina pelo desenvolvimento racional de novos compostos baseados em metal, uma vez que possuem a capacidade de coordenar diferentes ligantes, permitindo a funcionalização de grupos que podem ser moldados para alvos moleculares definidos, buscando superar os grandes desafios associados ao tratamento oncológico com a cisplatina e seus análogos, na tentativa de desenvolver fármacos com menor toxicidade para as células sadias, maior biodisponibilidade e seletividade para células neoplásicas (BENTOUHAMI et al., 2017). Entretanto, estudos

multidisciplinares futuros serão necessários para melhor explorar as suas propriedades farmacológicas em cada via de sinalização, acerca dos mecanismos envolvidos e relação estrutura-atividade.

6. CONCLUSÃO

Com base nos nossos resultados podemos concluir que:

- ✓ O isomerismo pode interferir no mecanismo de morte celular, uma vez que o complexo (3) de platina apresentou alta taxa de apoptose (98%) e o complexo (4) apresentou alta taxa de necrose (96%), após 24 horas de tratamento em células da linhagem leucêmica U937.
- ✓ O complexo (3) de platina ativa tanto a via extrínseca quanto intrínseca de morte celular apoptótica em células U937.
- ✓ O composto de cobre (II) induz morte celular por apoptose na linhagem de carcinoma de pulmão NCI-H460 com comprometimento mitocondrial e estresse do retículo endoplasmático.
- ✓ Nos modelos murinos de carcinoma pulmonar de células NCI-H460, o complexo de cobre (II) foi eficaz no tratamento das lesões, reduzindo em 48% o crescimento tumoral em comparação com o grupo controle.
- ✓ Diante destes resultados, acredita-se que o composto (3) de platina e o composto de cobre (II) são promissores em virtude de suas substanciais atuações farmacológicas. Nos estudos *in vivo*, é consistente a hipótese de que o composto de cobre apresenta relevante índice terapêutico para ação antineoplásica e se mostra como um candidato em potencial para um futuro metalofármaco.

7. PERSPECTIVAS

Justifica-se, como perspectivas, que ensaios adicionais devem ser realizados para o aprofundamento dos estudos de mecanismos de ação dos compostos e melhor avaliar a eficácia destas moléculas *in vitro* e *in vivo*, com inclusão de novas linhagens que apresentam hoje alta incidência e taxa de mortalidade, além de se investigar a potencialização de seus efeitos farmacológicos quando combinados a diferentes quimioterápicos, podendo ser exploradas possibilidade de novas doses e atuação sinérgica nas células, almejando alcançar maior resposta a cada aplicação, atenuando o risco de resistência e da alta toxicidade dos medicamentos convencionais.

Vale mencionar que outros estudos com o composto de coordenação de platina, tem apresentado resultados promissores em uma linhagem de carcinoma de mama altamente metastática MDA-MB-231, onde foi inferido que a apoptose é o tipo de morte celular induzido pelo complexo, os ensaios foram realizados por meio das técnicas de marcação com anexina V, análise do ciclo celular (Sub-G1), potencial de membrana mitocondrial e atividades de caspases averiguados por citometria de fluxo, além de microscopia eletrônica de rotina. Pretendemos ainda, realizar técnicas de tomografia e de microanálise, a fim de demonstrar alterações ultraestruturais nas organelas afetadas e o acúmulo intracelular do composto no intuito de melhor elucidar os mecanismos envolvidos no processo de morte celular e citotoxicidade.

Nos ensaios *in vivo*, o complexo de platina demonstrou ser menos tóxico do que a cisplatina e quanto à sua eficácia antineoplásica, exibiu notória capacidade de inibição do crescimento de lesões cancerígenas de células MDA-MB-231 em modelos murinos. Os dados obtidos estão em fase de conclusão e em breve serão submetidos para publicação descrevendo tais achados.

8. REFERÊNCIAS BIBLIOGRÁFICAS

ALBERTS, B. et al. *Molecular Biology of the cell*. 5. ed. **Garland Science**, 2010. 1392p.

AL-BAHLANI, S. M. et al. Cisplatin Induces Apoptosis Through the Endoplasmic Reticulum-mediated, Calpain 1 Pathway in Triple-negative Breast Cancer Cells. **Clinical breast cancer**, v. 17, n. 3, p. 103–112, 2017.

ALMEIDA, V. L. et al. Câncer e agentes antineoplásicos ciclo-celular específicos e ciclo-celular não específicos que interagem com o DNA: uma introdução. **Química Nova**, v. 28, n. 1, p. 118–129, 2005.

AMERICAN CANCER SOCIETY. Treating Advanced Cancer. Disponível em: <https://www.cancer.org/treatment/understanding-your-diagnosis/advanced-cancer/treatment.html>. Acesso: Agosto 2019.

ARIS, S. M.; FARRELL, N. P. Towards Antitumor Active *trans*-Platinum Compounds. **European Journal of Inorganic Chemistry**, v. 2009, n. 10, p. 1293–1302, 2009.

BARBOSA, I. R. et al. Cancer mortality in Brazil: Temporal trends and predictions for the year 2030. **Medicine (United States)**, v. 94, n. 16, p. 1–6, 2015.

BARRY, N. P. E.; SADLER, P. J. Exploration of the medical periodic table: Towards new targets. **Chemical Communications**, v. 49, n. 45, p. 5106–5131, 2013.

BENTOUHAMI, E. et al. Medicinal chemistry Progress in Copper Complexes as Anticancer Agents. **Med Chem**, v. 7, n. 5, p. 875, 2017.

BHATTACHARJEE, A.; CHAKRABORTY, K.; SHUKLA, A. Cellular copper homeostasis: Current concepts on its interplay with glutathione homeostasis and its implication in physiology and human diseases. **Metallomics**, v. 9, n. 10, p. 1376–1388, 2017.

BORGES, F.V. (2013) Síntese, caracterização e avaliação da atividade antineoplásica de complexos de cobre e zinco frente a células leucêmicas e melanômicas. Tese (Doutorado em Ciências Naturais), programa de Pós-Graduação em Ciências Naturais, Universidade Estadual do Norte Fluminense Darcy Ribeiro, Campos dos Goytacazes-RJ.

BORGES, L. J. H. et al. In vitro and in vivo studies of the antineoplastic activity of copper (II) compounds against human leukemia THP-1 and murine melanoma B16-F10 cell lines. **European Journal of Medicinal Chemistry**, v. 123, p. 128–140, 2016.

BORNER, C. The Bcl-2 protein family: sensors and checkpoints for life-or-death decisions. **Molecular immunology**, v. 39, n. 11, p. 615–47, 2003.

BOULSOURANI, Z. et al. Synthesis, structure elucidation and biological evaluation of triple bridged dinuclear copper(II) complexes as anticancer and antioxidant/anti-inflammatory agents. **Materials Science and Engineering C**, v. 76, p. 1026–1040, 2017.

BRABEC, V.; HRABINA, O.; KASPARKOVA, J. Cytotoxic platinum coordination compounds. DNA binding agents. **Coordination Chemistry Reviews**, v. 351, p. 2–31, 2017.

BULL, E. S. (2008). Síntese, Caracterização e Avaliação das Atividades de Nuclease e Antitumoral de Compostos de Coordenação de Cobre. Dissertação (Mestrado) - Programa de Pós-Graduação em Ciências Naturais, Universidade Estadual do Norte Fluminense Darcy Ribeiro, Campos dos Goytacazes-RJ

BULL, E. S. (2016). Síntese, caracterização e avaliação da atividade citotóxica de compostos de coordenação de cobre(II) e gálio (III). Tese (Doutorado) - Programa de Pós-Graduação em Ciências Naturais, Universidade Estadual do Norte Fluminense Darcy Ribeiro, Campos dos Goytacazes-RJ

CAI, L. et al. Telodendrimer nanocarrier for co-delivery of paclitaxel and cisplatin: A synergistic combination nanotherapy for ovarian cancer treatment. **Biomaterials**, v. 37, p. 456–468, 2015.

CAO, J. Y.; DIXON, S. J. Mechanisms of ferroptosis. **Cellular and Molecular Life Sciences**, v. 73, n. 11–12, p. 2195–2209, 2016.

CHEN, H. et al. Effective platinum(IV) prodrugs conjugated with lonidamine as a functional group working on the mitochondria. **Journal of Inorganic Biochemistry**, v. 180, p. 119–128, 2018.

CHEN, W. et al. Autophagy: a double-edged sword for neuronal survival after cerebral ischemia. **Neural regeneration research**, v. 9, n. 12, p. 1210–6, 2014.

CHITAMBAR, C. R. Gallium-containing anticancer compounds. **Future Medicinal Chemistry**, v. 4, n. 10, p. 1257–1272, 2012.

CHOU, T.-C. Theoretical Basis, Experimental Design, and Computerized Simulation of Synergism and Antagonism in Drug Combination Studies. **Pharmacological Reviews**, v. 58, n. 3, p. 621–681, 2006.

CROCE, C. M. Oncogenes and Cancer. **New England Journal of Medicine**, v. 358, n. 5, p. 502–511, 2008.

DASARI, S.; BERNARD TCHOUNWOU, P. Cisplatin in cancer therapy: Molecular mechanisms of action. **European Journal of Pharmacology**, v. 740, p. 364–378, 2014.

DENOYER, D. et al. Targeting copper in cancer therapy: 'Copper That Cancer'. **Metallomics**, v. 7, n. 11, p. 1459–1476, 2015.

DENOYER, D.; CLATWORTHY, S. A. S.; CATER, M. A. Copper complexes in cancer therapy. In: SIGEL, A. et al. (Eds.). . **Metallo-Drugs: Development and Action of Anticancer Agents**. Berlin, Boston: De Gruyter, 2018. v. 18p. 469–506.

DEO, K. M. et al. Transition Metal Intercalators as Anticancer Agents-Recent Advances. **International journal of molecular sciences**, v. 17, n. 11, p. 1–17, 2016.

DHIVYA, R. et al. In vitro antiproliferative and apoptosis-inducing properties of a mononuclear copper(II) complex with dppz ligand, in two genotypically different breast cancer cell lines. **BioMetals**, v. 28, n. 5, p. 929–945, 2015.

DILRUBA, S.; KALAYDA, G. V. Platinum-based drugs: past, present and future. **Cancer Chemotherapy and Pharmacology**, v. 77, n. 6, p. 1103–1124, 2016.

DIXON, M.; NEEDHAM, D. M. Biochemical Research on Chemical Warfare Agents. **Nature**, v. 158, n. 4013, p. 432–438, 1946.

DJOKO, K. Y. et al. Antimicrobial effects of copper(II) bis(thiosemicarbazonato) complexes provide new insight into their biochemical mode of action. **Metallomics : integrated biometal science**, v. 6, n. 4, p. 854–63, 2014.

ELIE, B. T. et al. Bimetallic titanocene-gold phosphane complexes inhibit invasion, metastasis, and angiogenesis-associated signaling molecules in renal cancer. **European Journal of Medicinal Chemistry**, v. 161, p. 310–322, 2019.

ELLAHIOUI, Y.; PRASHAR, S.; GÓMEZ-RUIZ, S. Anticancer Applications and Recent Investigations of Metallodrugs Based on Gallium, Tin and Titanium. **Inorganics**, v. 5, n. 1, p. 4, 2017.

ELMORE, S. Apoptosis: a review of programmed cell death. **Toxicologic pathology**, v. 35, n. 4, p. 495–516, 2007.

FEI CHIN, C. et al. Anticancer Platinum (IV) Prodrugs with Novel Modes of Activity. **Current Topics in Medicinal Chemistry**, v. 11, n. 21, p. 2602–2612, 2011.

FERNANDES, C. et al. Induction of apoptosis in leukemia cell lines by new copper (II) complexes containing naphthyl groups via interaction with death receptors ☆. **Journal of Inorganic Biochemistry**, v. 153, p. 68–87, 2015.

FISCHER-FODOR, E. et al. Gallium phosphinoarylthiolato complexes counteract drug resistance of cancer cells. **Metallomics**, v. 6, n. 4, p. 833–844, 2014.

FLOREA, A.-M.; BÜSSELBERG, D. Cisplatin as an Anti-Tumor Drug: Cellular Mechanisms of Activity, Drug Resistance and Induced Side Effects. **Cancers**, v. 3, n. 4, p. 1351–1371, 2011.

FREITAS, W.R. (2014). Efeitos Antineoplásicos In Vitro Da Caulibugulona A e In Vivo Do Complexo De Coordenação De Cobre [Cu(L1)Cl]Cl.2H₂O. Tese (Doutorado) - Programa de Pós-Graduação em Biociências Biotecnologia, Universidade Estadual do Norte Fluminense Darcy Ribeiro, Campos dos Goytacazes, RJ

FREZZA, M. et al. Novel Metals and Metal Complexes as Platforms for Cancer Therapy. **Current Pharmaceutical Design**, v. 16, n. 16, p. 1813–1825, 2010.

GALLUZZI, L. et al. Molecular definitions of cell death subroutines: recommendations of the Nomenclature Committee on Cell Death 2012. **Cell death and differentiation**, v. 19, n. 1, p. 107–20, 2012.

GALLUZZI, L. et al. Essential versus accessory aspects of cell death: Recommendations of the NCCD 2015. **Cell Death and Differentiation**, v. 22, n. 1, p. 58–73, 2015.

GARCÍA, V. M. N. et al. Antifungal activities of nine traditional Mexican medicinal plants. **Journal of Ethnopharmacology**, v. 87, n. 1, p. 85–88, 2003.

GLICK, D.; BARTH, S.; MACLEOD, K. F. Autophagy: cellular and molecular mechanisms. **The Journal of pathology**, v. 221, n. 1, p. 3–12, 2010.

GOLSTEIN, P.; KROEMER, G. Cell death by necrosis: towards a molecular definition. **Trends in Biochemical Sciences**, v. 32, n. 1, p. 37–43, 2007.

GONZALEZ, V. M. et al. Is cisplatin-induced cell death always produced by apoptosis? **Molecular pharmacology**, v. 59, n. 4, p. 657–663, 2001.

GROSSI, I. et al. Biological Function of MicroRNA193a-3p in Health and Disease. **International Journal of Genomics**, v. 2017, p. 1–13, 2017.

GUDISEVA et al. Molecular biology of head and neck cancer. **Journal of Dr. NTR University of Health Sciences**, v. 6, n. 1, p. 1, 2017.

GUICHARD, N. et al. Antineoplastic drugs and their analysis: A state of the art review. **Analyst**, v. 142, n. 13, p. 2273–2321, 2017.

GUIMARÃES, E.G. (2019). Avaliação *in vitro* da atividade antineoplásica da associação entre um composto de coordenação de cobre e o fármaco cisplatina. Dissertação (Mestrado) - Programa de Pós-Graduação em Biociências Biotecnologia, Universidade Estadual do Norte Fluminense Darcy Ribeiro, Campos dos Goytacazes, RJ.

HANAHAN, D.; WEINBERG, R. A. Hallmarks of cancer: the next generation. **Cell**, v. 144, n. 5, p. 646–74, 2011.

HONG, E. et al. Elevated pressure enhanced TRAIL-induced apoptosis in hepatocellular carcinoma cells via ERK1/2-inactivation. **Cellular and Molecular Biology Letters**, v. 20, n. 4, p. 535–48, 2015.

HORN, A. et al. Highly efficient synthetic iron-dependent nucleases activate both intrinsic and extrinsic apoptotic death pathways in leukemia cancer cells. **Journal of Inorganic Biochemistry**, v. 128, p. 38–47, 2013.

HUANG, R. Z. et al. Synthesis and biological evaluation of terminal functionalized thiourea-containing dipeptides as antitumor agents. **RSC Advances**, v. 7, n. 15, p. 8866–8878, 2017.

INCA - Instituto Nacional de Câncer José Alencar Gomes da Silva (2018). Estimativa 2018: Incidência de Câncer no Brasil. Disponível em: <<https://www.inca.gov.br/publicacoes/livros/estimativa-2018-incidencia-de-cancer-no-brasil>>. Acesso 2019

INDRAN, I. R. et al. Recent advances in apoptosis, mitochondria and drug resistance in cancer cells. **Biochimica et Biophysica Acta - Bioenergetics**, v. 1807, n. 6, p. 735–745, 2011.

IORIO, M. V.; CROCE, C. M. microRNA involvement in human cancer. **Carcinogenesis**, v. 33, n. 6, p. 1126–1133, 2012.

IRACE, C. et al. Antiproliferative effects of ruthenium-based nucleolipidic nanoaggregates in human models of breast cancer in vitro: Insights into their mode of action. **Scientific Reports**, v. 7, n. 1, p. 45236, 2017.

JIANG, P.; MIZUSHIMA, N. Autophagy and human diseases. **Cell Research**, v. 24, n. 1, p. 69–79, 2014.

JOHANSEN, T.; LAMARK, T. Selective autophagy mediated by autophagic adapter proteins. **Autophagy**, v. 7, n. 3, p. 279–96, 2011.

KAJIYAMA, H. et al. The expression of Mdm2 on Helicobacter pylori infected intestinal metaplasia and gastric cancer. **Journal of Clinical Biochemistry and Nutrition**, v. 60, n. 1, p. 33–38, 2017.

KANDUC, D. et al. Cell death: apoptosis versus necrosis (review). **International journal of oncology**, v. 21, n. 1, p. 165–70, 2002.

KAO, S. TE et al. A Chinese herbal decoction, modified Yi Guan Jian, induces apoptosis in hepatic stellate cells through an ROS-mediated mitochondrial/caspase pathway. **Evidence-based Complementary and Alternative Medicine**, v. 2011, p. 459531, 2011.

KHAN, R. et al. Design, Synthesis, and Biological Evaluation of Benzimidazole-Derived Biocompatible Copper(II) and Zinc(II) Complexes as Anticancer Chemotherapeutics. **International Journal of Molecular Sciences**, v. 19, n. 5, p. 1492, 2018.

KHORDADMEHR, M. et al. A comprehensive review on miR-451: A promising cancer biomarker with therapeutic potential. **Journal of Cellular Physiology**, p. 1-16, 2019.

KOSTOVA, I. Platinum Complexes as Anticancer Agents. **Recent Patents on Anti-Cancer Drug Discovery**, v. 1, n. 1, p. 1–22, 2006.

KROEMER, G. et al. Classification of cell death: Recommendations of the Nomenclature Committee on Cell Death 2009. **Cell Death and Differentiation**, v. 16, n. 1, p. 3-11, 2009.

KUMAR, V., ABBAS, A. K., FAUSTO, N. Robbins and Cotran pathologic basis of disease. 9.ed. Philadelphia: Elsevier Saunders, 2014. 1393p.

LAINÉ, A.-L.; PASSIRANI, C. Novel metal-based anticancer drugs: a new challenge in drug delivery. **Current Opinion in Pharmacology**, v. 12, n. 4, p. 420–426, 2012.

LEVINE, B.; KROEMER, G. Autophagy in the pathogenesis of disease. **Cell**, v. 132, n. 1, p. 27–42, 2008.

LIANG, J. X. et al. Recent development of transition metal complexes with in vivo antitumor activity. **Journal of Inorganic Biochemistry**, v. 177, n. March, p. 276–286, 2017.

LIU, X. et al. Targeting ALDH1A1 by disulfiram/copper complex inhibits non-small cell

lung cancer recurrence driven by ALDH-positive cancer stem cells. **Oncotarget**, v. 7, n. 36, p. 58516–58530, 2016.

LOO, D. T. In Situ Detection of Apoptosis by the TUNEL Assay: An Overview of Techniques. **Methods in molecular biology (Clifton, N.J.)**, v. 682, p. 3–13, 2011.

LOPES, B.F. (2012) Síntese, Caracterização e Avaliação da Atividade Antineoplásica de Compostos de Coordenação de Cobre: Influência do Naftol e da Cumarina na Atividade Biológica. Tese (Doutorado) - Programa de Pós-Graduação em Ciências Naturais, Universidade Estadual do Norte Fluminense Darcy Ribeiro, Campos dos Goytacazes-RJ.

LOVEJOY, K. S.; LIPPARD, S. J. Non-traditional platinum compounds for improved accumulation, oral bioavailability, and tumor targeting. **Dalton Transactions**, n. 48, p. 10651–10659, 2009.

MA Z. Y. et al. Activities of a novel Schiff Base copper (II) complex on growth inhibition and apoptosis induction toward MCF-7 human breast cancer cells via mitochondrial pathway. **Journal of Inorganic Biochemistry**, v. 117, n. 2, p. 1-9, 2012.

MAHENDIRAN, D. et al. Copper complexes as prospective anticancer agents: *in vitro* and *in vivo* evaluation, selective targeting of cancer cells by DNA damage and S phase arrest. **RSC Advances**, v. 8, n. 30, p. 16973–16990, 2018.

MARÍN-MEDINA, A. et al. Investigation on the self-association of an inorganic coordination compound with biological activity (Casiopeína III-ia) in aqueous solution. **Chemistry Central Journal**, v. 10, n. 1, p. 65, 2016.

MARZANO, C. et al. Copper Complexes as Anticancer Agents. **Anti-Cancer Agents in Medicinal Chemistry**, v. 9, n. 2, p. 185–211, 2009.

MEDICI, S. et al. Noble metals in medicine: Latest advances. **Coordination Chemistry Reviews**, v. 284, n. December, p. 329–350, 2015.

MORCELLI, S. R. et al. Synthesis, characterization and antitumoral activity of new cobalt(II) complexes: Effect of the ligand isomerism on the biological activity of the complexes. **Journal of Inorganic Biochemistry**, v. 161, p. 73–82, 2016.

MOREIRA, R. O. et al. Modulating the antitumoral activity by the design of new platinum(II) compounds: Synthesis, characterization, DFT, ultrastructure and mechanistic studies. **Journal of Inorganic Biochemistry**, v. 194, p. 200–213, 2019.

MUHAMMAD, N.; GUO, Z. Metal-based anticancer chemotherapeutic agents. **Current Opinion in Chemical Biology**, v. 19, n. 1, p. 144–153, 2014.

NDAGI, U.; MHLONGO, N.; SOLIMAN, M. E. Metal complexes in cancer therapy – An update from drug design perspective. **Drug Design, Development and Therapy**, v. 11, p. 599-616, 2017.

NEVES, A. P.; VARGAS, M. D. Complexos de Platina (II) na Terapia do Câncer. **Revista Virtual de Química**, v. 3, n. 3, p. 196–209, 2011.

OKADA, H.; MAK, T. W. Pathways of apoptotic and non-apoptotic death in tumour cells. **Nature Reviews Cancer**, v. 4, n. 8, p. 592–603, 2004.

PASETTO, L. M. et al. The development of platinum compounds and their possible combination. **Critical Reviews in Oncology/Hematology**, v. 60, n. 1, p. 59–75, 2006.

PEIXOTO, M. S.; DE OLIVEIRA GALVÃO, M. F.; BATISTUZZO DE MEDEIROS, S. R. Cell death pathways of particulate matter toxicity. **Chemosphere**, v. 188, p. 32–48, 2017.

PORTES, J. A. et al. In vitro treatment of *Toxoplasma gondii* with copper(II) complexes induces apoptosis-like and cellular division alterations. **Veterinary Parasitology**, v. 245, p. 141–152, 2017.

PORTUGAL, J.; BATALLER, M.; MANSILLA, S. Cell Death Pathways in Response to Antitumor Therapy. **Tumori Journal**, v. 95, n. 4, p. 409–421, 2009.

ROSAS, M. S. L. et al. Incidência do câncer no Brasil e o potencial uso dos derivados de isatinas na cancerologia experimental. **Revista Virtual de Química**, v. 5, n. 2, p. 243–265, 2013.

ROSENBERG, B.; VAN CAMP, L.; KRIGAS, T. Inhibition of Cell Division in *Escherichia coli* by Electrolysis Products from a Platinum Electrode. **Nature**, v. 205, n. 4972, p. 698–699, 1965.

ROSENBERG, B.; VANCAMP, L. The successful regression of large solid sarcoma 180 tumors by platinum compounds. **Cancer research**, v. 30, n. 6, p. 1799–802, 1970.

SANTINI, C. et al. Advances in Copper Complexes as Anticancer Agents. **Chemical Reviews**, v. 114, n. 1, p. 815–862, 2014.

SCHWIETERT, C. W.; MCCUE, J. P. Coordination compounds in medicinal

chemistry. **Coordination Chemistry Reviews**, v. 184, n. 1, p. 67–89, 1999.

SERMENT-GUERRERO, J. et al. Genotoxic assessment of the copper chelated compounds Casiopeinas: Clues about their mechanisms of action. **Journal of Inorganic Biochemistry**, v. 166, p. 68–75, 2017.

SIEBER, O. M.; HEINIMANN, K.; TOMLINSON, I. P. M. Genomic instability - The engine of tumorigenesis? **Nature Reviews Cancer**, v. 3, n. 9, p. 701–708, 2003.

SIEGEL, R. et al. Cancer statistics, 2014. **CA: A Cancer Journal for Clinicians**, v. 64, n. 1, p. 9–29, 2014.

SKANDER, M. et al. N-heterocyclic carbene-amine Pt(II) complexes, a new chemical space for the development of platinum-based anticancer drugs. **Journal of Medicinal Chemistry**, v. 53, n. 5, p. 2146-2154, 2010.

SWANTON, C. et al. Chromosomal instability determines taxane response. **Proceedings of the National Academy of Sciences**, v. 106, n. 21, p. 8671–8676, 2009.

TAN, C.-P. et al. Metallomics insights into the programmed cell death induced by metal-based anticancer compounds. **Metallomics**, v. 6, n. 5, p. 953–1098, 2014.

TRONDL, R. et al. NKP-1339, the first ruthenium-based anticancer drug on the edge to clinical application. **Chemical Science**, v. 5, n. 8, p. 2925-2932, 2014.

VOGELSTEIN, B.; KINZLER, K. W. Cancer genes and the pathways they control. **Nature Medicine**, v. 10, n. 8, p. 789–799, 2004.

VOLTAGGIO, L. et al. Current concepts in the diagnosis and pathobiology of intraepithelial neoplasia: A review by organ system. **CA: A Cancer Journal for Clinicians**, v. 66, n. 5, p. 408–436, 2016.

WANG, F. Y. et al. Mitochondria-targeted platinum(II) complexes induce apoptosis-dependent autophagic cell death mediated by ER-stress in A549 cancer cells. **European Journal of Medicinal Chemistry**, v. 155, p. 639–650, 2018.

WANG, X.; GUO, Z. Towards the rational design of platinum(II) and gold(III) complexes as antitumour agents. **Dalton Transactions**, n. 12, p. 1521–1532, 2008.

WHEATE, N. J. et al. The status of platinum anticancer drugs in the clinic and in clinical trials. **Dalton Transactions**, v. 39, n. 35, p. 8113, 2010.

WHO - World Health Organization (2019). Cancer. Disponível em:

<<http://www.who.int/cancer/en/index.html>>. Acesso 2019.

WONG, R. S. Apoptosis in cancer: from pathogenesis to treatment. **Journal of Experimental & Clinical Cancer Research**, v. 30, n. 1, p. 87, 2011.

XIE, F.; CAI, H.; PENG, F. Anti-prostate cancer activity of 8-hydroxyquinoline-2-carboxaldehyde-thiosemicarbazide copper complexes in vivo by bioluminescence imaging. **Journal of Biological Inorganic Chemistry**, v. 23, n. 6, p. 949–956, 2018.

XU, B. et al. Disulfiram/copper selectively eradicates AML leukemia stem cells in vitro and in vivo by simultaneous induction of ROS-JNK and inhibition of NF- κ B and Nrf2. **Cell death & disease**, v. 8, n. 5, p. 1–12, 2017.

YANG, Q. Y. et al. Syntheses, crystal structures, and antitumor activities of copper(II) and nickel(II) complexes with 2-((2-(Pyridin-2-yl)hydrazono)methyl)quinolin-8-ol. **International Journal of Molecular Sciences**, v. 19, n. 7, 2018.

YANG, Y. et al. Disulfiram chelated with copper promotes apoptosis in human breast cancer cells by impairing the mitochondria functions. **Scanning**, v. 38, n. 6, p. 825–836, 2016.

ZENG, L. et al. The development of anticancer ruthenium(II) complexes: From single molecule compounds to nanomaterials. **Chemical Society Reviews**, v. 46, n. 19, p. 5771–5804, 2017.

ZHANG, Z. et al. Novel copper complexes as potential proteasome inhibitors for cancer treatment (Review). **Molecular Medicine Reports**, v. 15, n. 1, p. 3–11, 2017.

ZIEGLER, U.; GROSCURTH, P. Morphological Features of Cell Death. **Physiology**, v. 19, n. 3, p. 124–128, 2004.

ZOROVA, L. D. et al. Mitochondrial membrane potential. **Analytical Biochemistry**, v. 552, p. 50–59, 2018.

